DEVELOPMENT OF STIMULI-RESPONSIVE POLYMERIC HYDROGELS AND THEIR APPLICATIONS

A thesis submitted
in partial fulfillment of the requirements for the degree of

Doctor of Philosophy

By

Monalisha Boruah

Registration No. 040 of 2010

School of Sciences
Department of Chemical Sciences
Tezpur University
Napaam, Tezpur - 784028
Assam, India

November 2014

Dedicated

To

Maa and Papa

Development of stimuli-responsive polymeric hydrogels and their applications

ABSTRACT

The present thesis deals with synthesis, characterization and evaluation of pH and electro-responsive swelling behaviour, actuation and drug release behaviour of some of the composite and nanocomposite hydrogels. A considerable effort has been devoted to enhance their pH and electro-responsive behaviour by the incorporation of different fillers such as polyaniline, graphite, organically modified montmorillonite clay (OMMT) and multiwall carbon nanotubes (MWCNTs). The influence of various parameters on swelling behaviour and *in vitro* biocompatibility of the prepared hydrogels have been determined. The actuation and drug release behaviour under the application of an electric field have been determined and reported. Moreover, the effects of fillers and nanofillers on mechanical strength and conductivity of the hydrogels have also been reported. The contents of the thesis have been compiled into six chapters.

Chapter 1 deals with the general introduction on gels, hydrogels and stimuli-responsive polymeric hydrogels, their synthesis, characterizations, properties, importance, history and various fields of applications. A brief review on classification of different hydrogels according to preparation methods, ionic charges, nature of the crosslinked junctions, crystallinity and various environmental responses has been described in this chapter. The applications of hydrogels in actuator and controlled drug delivery systems have been outlined. The chapter also focuses the scopes and objectives along with the plans of work of the present investigation.

Chapter 2 reports the synthesis and characterization of two sets of pH and electro-responsive composites based on poly(acrylamide-*co*-acrylic acid)/polyaniline and poly(acrylamide-*co*-acrylic acid)/graphite. The composite hydrogels are characterized by FT-IR, UV-Visible, XRD and SEM analysis. The tensile strengths of the both sets of

hydrogels are determined by using a universal testing machine. The influence of various parameters on swelling and electrical properties of the composite hydrogels is evaluated. The *in vitro* biocompatibility of the composite hydrogels is tested by hemolytic potentiality test. Also, the bending behaviours of the both sets of composite hydrogels under the application of an external electric field have been determined by a home-made apparatus.

Chapter 3 describes the synthesis of electric field responsive poly (vinyl alcohol)-*g*-polyacrylic acid/OMMT nanocomposite hydrogels and evaluation of their swelling kinetics. The prepared nanocomposite hydrogels are characterized by FT-IR, XRD, SEM and TG analysis. The various network parameters such as average molecular weight between crosslinks (M_c), crosslinking density (ρ), and mesh size (ξ) are evaluated and the effect of these parameters on swelling behaviour is also determined. Finally, the bending behaviour of the nanocomposite hydrogels under an external electric field has also been measured.

Chapter 4 deals with the synthesis of pH-responsive, biocompatible carboxymethylcellulose-*g*-poly(acrylic acid)/OMMT nanocomposite hydrogels for *in vitro* release of vitamin B_{12}. The nanocomposite hydrogels are characterized by using techniques such as FTIR, SEM and XRD analysis. The mechanical strength of the nanocomposite hydrogels is determined by dynamic mechanical analysis (DMA). The effects of various parameters on the swelling behaviour of the hydrogels have been studied and the *in vitro* biocompatibility has been determined by hemolytic potentiality test. The pH-responsive release of vitamin B_{12} has been studied during different time periods using a UV-visible spectrophotometer and reported.

Chapter 5 reports the study of electric field assisted drug release from pH and electro-responsive Gelatin-*g*-poly(acrylic acid)/MWCNTs nanocomposite hydrogels. The nanocomposite hydrogels are characterized by FTIR, SEM and XRD analysis. The effects of pH, MWCNT-COOH content and applied electric field on swelling behaviour of the hydrogels are determined. The pulsatile release of vitamin B_{12} under the applied electric field is evaluated and the influence of ionic strength of the release media and MWCNT-

COOH content has been determined. The drug release behaviour is also studied by using response surface methodology.

Chapter 6, the last chapter of the thesis includes the concluding remarks, highlights of the findings and future scopes of the present investigation. The synthesized composite and nanocomposite hydrogels possess improved stimuli-responsive behaviour than the native gel in all the cases. The hemolytic potentiality test reveals that, all the prepared hydrogels are biocompatible in nature. The observed behaviour suggests the possible applications of the composite and nanocomposite hydrogels as artificial muscle, sensors, switches and electric current modulated drug delivery systems etc.

DECLARATION BY THE CANDIDATE

The thesis entitled *"Development of stimuli-responsive polymeric hydrogels and their applications"* is being submitted to the Tezpur University in partial fulfillment for the award of the degree of Doctor of Philosophy in ***Chemical Sciences*** is a record of bonafide research work accomplished by me under the supervision of Prof. S. K. Dolui.

All helps received from various sources have been duly acknowledged. No part of this thesis has been submitted elsewhere for award of any other degree.

Monalisha Boruah

Date: 27.11.2014

Monalisha Boruah

Place: Tezpur

Department of Chemical Sciences

Tezpur University

TEZPUR UNIVERSITY

(A Central University by an Act of Parliament)

DISTRICT: SONITPUR:: ASSAM:: INDIA

Napaam, Tezpur-784028

Fax: 03712-267006 Ph: 03712-267004 *Email : adm@agnigarh.tezu.ernet.in*

CERTIFICATE OF THE PRINCIPAL SUPERVISOR

This is to certify that the thesis entitled "*Development of stimuli-responsive polymeric hydrogels and their applications*" submitted to the School of *Sciences*, Tezpur University in partial fulfillment for the award of the degree of Doctor of Philosophy in ***Chemical Sciences*** is a record of research work carried out by ***Ms. Monalisha Boruah*** under my supervision and guidance.

All help received by her from various sources have been duly acknowledged. No part of this thesis has been submitted elsewhere for award of any other degree.

Date: 27.11.14

Place: Tezpur

S. K. Dolui
Professor
School of Sciences
Department of Chemical Science
Tezpur University

TEZPUR UNIVERSITY

(A Central University by an Act of Parliament)

DISTRICT: SONITPUR:: ASSAM:: INDIA

Napaam, Tezpur-784028

Fax: 03712-267006 Ph: 03712-267004 ***Email : adm@agnigarh.tezu.ernet.in***

CERTIFICATE OF THE EXTERNAL EXAMINER AND ODEC

This is to certify that the thesis entitled "*Development of stimuli-responsive polymeric hydrogels and their applications*" submitted by ***Ms. Monalisha Boruah*** to Tezpur University in the **Department of Chemical Sciences** under the school of **Sciences** in partial fulfillment of the requirement for the award of the degree of Doctor of Philosophy in **Chemical Sciences** has been examined by us on 17.6.15 and found to be satisfactory.

Signature of:

Principal Supervisor

17/6/15

External Examiner

Date: 17.6.15

Preface

Hydrogels are three-dimensional (3D) macromolecular networks composed of crosslinked hydrophilic polymer chains which can absorb upto thousands of times their dry weight of water or biological fluids Stimuli-responsive (smart or intelligent) hydrogels are the polymeric networks which change their equilibrium swelling with the change of the surrounding environment such as pH, ionic strength, temperature, pressure, light, electric, magnetic, sound etc Due to the fascinating properties of the stimuli-responsive hydrogels, they provide platform for creating novel smart materials for a wide range of applications especially in the biomedical field As a result, hydrogels are commonly used in clinical practice and experimental medicine for a wide range of applications, including controlled drug delivery, tissue engineering, wound dressing, actuators, sensors etc

The present thesis deals with synthesis, characterization and evaluation of pH and electro-responsive swelling behaviour, actuation and drug release behaviour of some of the composite and nanocomposite hydrogels An effort has been devoted to enhance their pH and electro-responsive behaviour by the incorporation of different fillers such as polyaniline, graphite, organically modified montmorillonite clay (OMMT) and multiwall carbon nanotubes (MWCNTs) The contents of the thesis have been compiled into six chapters Chapter 1 deals with the general introduction of hydrogels Chapter 2 deals with the synthesis of two sets of pH and electro-responsive composites based on poly(acrylamide-co-acrylic acid)/polyaniline and poly(acrylamide-co-acrylic acid)/graphite The bending behaviours of the composite hydrogels under the application of an external electric field have been determined Chapter 3 describes the synthesis of electric field responsive poly (vinyl alcohol)-g-polyacrylic acid/OMMT nanocomposite hydrogels The network parameters such as average molecular weight between crosslinks (M_c), crosslinking density (ρ), and mesh size (ξ) are evaluated Chapter 4 describes the synthesis of pH-responsive, biocompatible carboxymethylcellulose-g-poly(acrylic acid)/OMMT nanocomposite hydrogels for in vitro release of vitamin B_{12}. Chapter 5 reports the study of electric field assisted drug release from pH and electro-responsive Gelatin-g-poly(acrylic acid)/MWCNTs nanocomposite hydrogels Chapter 5 reports the study of electric field assisted drug release from pH and electro-responsive Gelatin-g-poly(acrylic acid)/MWCNTs nanocomposite hydrogels Chapter 6, the last chapter of the thesis deals with the conclusion and future scope of the thesis The major findings of the thesis are reported in this chapter

We hope that this study contributes a little knowledge to the rapidly advancing field of 'smart hydrogels' and also opens up the possibilities of further research on the subject

This research was carried out in the Department of Chemical Sciences, Tezpur University with financial assistance from DRDO and CSIR under sponsored research scheme

Monalisha Boruah

Acknowledgement

This PhD thesis is the fruit of a few years of ardent learning and research experience. Words cannot express how grateful I am to all those who played a significant role during my PhD years and without whom this thesis would not have been possible.

At first, I would like to thank to almighty for giving me encouragement to complete this step.

I would like to express my sincere thanks to my respected supervisor, Prof. S. K. Dolui for his inspiring guidance, endless patience and work of freedom and giving me the opportunity to work in his laboratory. It would have not been possible for me to bring out this thesis without his help, fatherly care and constant encouragement throughout the research work. Words are not enough to thank him for all the concern he has shown and all the support he has rendered to ensure my personal well-being.

I am grateful to Dr. R. K. Dutta and Dr. A. J. Thakur Sir for their suggestions and discussions. I am grateful to all the faculty members of Department of Chemical Sciences for their help and suggestions.

I would like to acknowledge the sophisticated instrument facilities received from Dept. of Chemical Sciences and other Departments of Tezpur University.

I am particularly thankful to technical staff, for arranging instrumental and laboratory facilities throughout the study. Special thanks also go to office staff, Chemical Sciences Department. They are always there for the students.

I am truly thankful to my lab mates and friends Binod da, Lakhya da, Isha da, Amar da, Shyamalima, Pronob, Dhaneswar, Momina, Bhaskar, Bikash and Kiran, for their aspiring guidance, invaluably constructive criticism and friendly advice during my work. It has been a great adventure. I will remember forever for their friendship and help.

I am also thankful to all my friends and seniors especially Barnali ba, Nilima ba, Hasnahana ba, Rasna ba, Sikha ba, Parthana ba, Bondita ba, Nib, Priyanka, Sanjeev da, Ujjal, Iftikar, Ajay, Pinki ba, Nirmali, Sangeeta, Minoti, Nibedita, Medha, Neelam da, for their support and help. Thank you very much for being my wonderful friend.

I am grateful to Mrs. Sutapa Dolui for her motherly care, kindness and encouragement and Swapnil for his brotherly affection and support.

I am thankful to library staff and administrative staff of TU for cooperation and DRDO for financial support in the form Junior Research Fellowship (Grant No. ERIP/ER/1103999M/01/1441).I would also like to thank CSIR for financial support in the form Senior Research Fellowship (Grant No. 09/796/(0045)/2013/EMRI).

I feel deepest sense of gratitude to my parents for their blessing, love and affection. I would like to express my respect and gratitude to all my late Koka, my Aita, Tun, Mun, Bablu and Pankaj, for their constant encouragement, inspiration and support throughout my studies to fulfill my dream.

Finally, I thank the authorities of Tezpur University for granting me the permission to do this work.

Monalisha Boruah

Contents

List of Tables

List of Figures

Abbreviations used in the thesis

AAc	Acrylic acid
AMF	Alternating magnetic fields
ANOVA	Analysis of variance
APS	Ammonium persulphate
CCD	Central composite design
CMC	Carboxymethylcellulose
CNT	Carbon nanotube
CP	Conducting polymers
CTAB	Cetyltrimethyl ammonium bromide
DC	Direct current
DDW	Double distilled water
DMA	Dynamic mechanical analysis
DMSO	Dimethyl sulfoxide
EBA	Effective bending angle
EGDMA	Ethylene glycol dimethylacrylate
FTIR	Fourier transform infrared spectroscopy
KPS	Potassium persulfate
LCST	Lower critical solution temperature
LCV	Lower critical voltage
LMOGs	Low molecular-mass organic gelators
MBA	Methylene bis-acrylamide
MEC	Mechano-electro-chemical

MMT	Montmorillonite
MPa	Mega Pascal
$\overline{M}_c$	Number average molecular weight between the crosslinks
$\overline{M}_n$	Number average molecular weight
$\overline{M}_w$	Weight average molecular weight
MRI	Magnetic resonance imaging
MWCNT-COOH	Acid functionalized multiwall carbon nanotube
NBF	Nano Bio-Fusion
NIPA	N-isopropylacrylamide
NMP	N-methyl pyrrolidone
NMR	Nuclear magnetic resonance
OMMT	Organically modified montmorillonite
PAAm	Polyacrylamide
PAAc	Poly(acrylic acid)
PANI	Polyaniline
PDEAAm	Poly(N, N-diethylacrylamide)
PDEAEM	Poly(N,N′-diethylaminoethyl methacrylate)
PEG	Poly(ethylene glycol)
PHEMA	Poly(hydroxyethyl methacrylate)
P-NIPAm	Poly(N-isopropylacrylamide)
PVA	Poly(vinyl alcohol)
RBC	Red blood cell
SAH	Superabsorbent hydrogel
SEM	Scanning Electron Microscopy

SWCNT	Single-walled carbon nanotube
TEM	Transmission Electron Microscopy
TEMED	N,N,N′,N′-tetramethylethylenediamine
TGA	Thermogravimetric analysis
UCST	Upper critical solution temperature
UV	Ultra violet
XRD	X-ray diffraction
μm	micro meter
Å	Angstrom

CHAPTER 1

Introduction

1.1 Introduction

Materials are so important in the development of civilization that we associate 'Ages' with them. In the Stone Age, people used only natural materials, like stone, clay, skins, and wood. Undoubtedly materials represent one of the most important preconditions of the quality of life of human society.[1,2] For the past few decades, advancements in material science have driven economic, social and scientific progress and profoundly shape our everyday lives. Polymeric products have become so useful and so integral to the modern world that it is difficult to imagine life without them. In the 20th century, polymer science gave birth to multiple fascinating materials that completely changed our way of life. From car tyres and plastic bottles to contact eye lenses, paints etc. we are so used to polymers, it can be said that we now live in a polymer age.[3]

Natural polymers such as cellulose, starch, proteins, lignin, shellac, amber, wool, silk and natural rubber etc. have been used for centuries.[4] However, these compounds are not always found to be suitable for specific use. So, in order to compensate for the unsuitability and inconvenience of natural polymers, synthetic polymers have been developed by using petroleum based raw materials. The first synthetic polymer was produced in 1909, called Bakelite which could be moulded at a high temperature and it would retain its shape once cooled. But it wasn't until the World War I that significant changes took place in the polymer industry. Polymers have become essential materials for almost every industry as adhesives, building materials, paper, cloths, fibers, coatings, plastics, cosmetics etc. Now-a-days, researchers have focused on developing synthetic routes toward well-defined speciality polymers.

In the last few years, we have observed a remarkable migration of interest and activity from the traditional hard materials towards soft materials, such as biomaterials, self-assembly materials, complex fluids and polymer gels. These soft materials will probably never replace hard ones, but their study has led to significant advances in many applications for mankind. Polymeric hydrogels are unique materials in the sense that no other class of materials can be made to respond to so many different stimuli as polymeric

hydrogels. In the last few years, these gels have become of major interest as novel intelligent materials. Different kinds of such gels have been developed and studied with regard to their application to several biomedical and industrial fields, for example, controlled drug delivery systems, musclelike soft linear actuators, biomimetic energy-transducing devices and separation techniques etc.

1.2 Gels of polymers

The utilization of 'gel' in human society date back to 3000 years ago, where ancient Egyptians used 'a fat-based hair gel' when they were embalmed. Recently, McCreesh et al. from the University of Manchester (UK), revealed in a study that both men and women of ancient Egyptians were found to style their hair with 'a fat based gel' to keep their identity during the embalming process. They have examined hair samples of 15 mummies from the Kellis 1 cemetery, Dakhleh Oasis, Egypt and stated that the hair was styled and perfectly curled by using that gel.[5] An art, representing the application of the 'hair gel' is shown in the **Fig 1.1**.

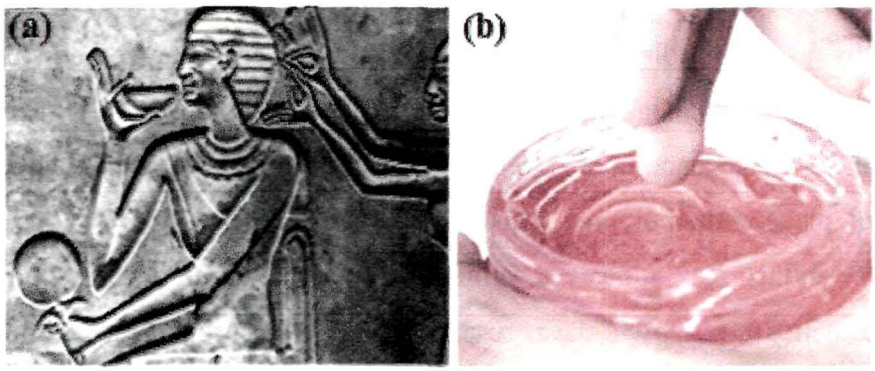

Fig 1.1 Representation of: (a) use of 'hair gel' in ancient days and (b) a modern 'hair gel'.

Gels of polymers are the materials of extreme importance to modern human society also. They are of great significance in the food industry, industries of photographic materials, man-made fibres and many other branches of technology as well as to living organisms. A 'gel' is a polymer solvent system, with a network of sufficiently stable bonds which are not destroyed by thermal motion.[6] Polymeric gels can be categorized into two major classes: thermo-reversible gels and permanent gels.[7] A thermo-reversible gel

passes over to the solution due to a change in temperature and the crosslink in a network become weaker and may be destroyed by thermal motion, which is known as gel melting. But a permanent gel consists of solvent-logged covalently bonded polymer networks. They are insoluble and can swell upto a considerable extent when kept in a solvent. Permanent gels can be classified according to the nature of the swelling agent. When the swelling agent is water, the gel is termed as 'hydrogel'. Similarly, when the swelling agent is an organic solvent, mineral oil or vegetable oil, the gel is coined to be organogel. A xerogel is a solid formed from a gel by drying with unhindered shrinkage.[8] Hydrogels can be defined as, a crosslinked network of hydrophilic polymers which possess the ability to absorb large amounts of water and swell.[9] A hydrogel exhibits swelling in aqueous media for the same reasons that an analogous linear polymer dissolves in water to form an ordinary polymer solution. Thus, the feature central to the functioning of a hydrogel is its inherent crosslinking.

There are plenty of natural gels which are present in nature. For example, Aloe vera leaves are filled with a gel containing vitamins like A, B_1, B_2, B_3, B_6, B_{12}, C and E and folic acid. This plant is considered to be a miracle plant because of its numerous curative and healing benefits. Carrageenans are a family of linear sulphated polysaccharides that are extracted from red edible seaweeds. They are widely used in the food industry for their gelling, thickening and stabilizing properties. Carrageenan based gel is found to be effective against HIV infection also.

Xanthan Gum, is produced by *Xanthomonas compestris bacteria* through the fermentation of glucose. It is an effective food additive used to thicken, emulsify and stabilize water-based foods. It is also used in many different types of food, including salad dressings, sauces, condiments, ice creams and other frozen foods. Recently, Professor Jun-Woo Park and his team of scientists created 'Gingival' gel by using cutting edge Nano Bio-Fusion (NBF) technology, from 'Propolis' which is a natural product collected by honeybees from botanical sources to protect the hive from invasion and infection. Propolis is already known to be one of nature's most powerful natural antibiotics. Thus, NBF Gingival gel is very much beneficial for diabetes, high blood pressure, heart disease,

osteoporosis, compromised immunity and cancer sufferers etc.[10] Some of the naturally available gels are shown in the above **Fig 1.2.**

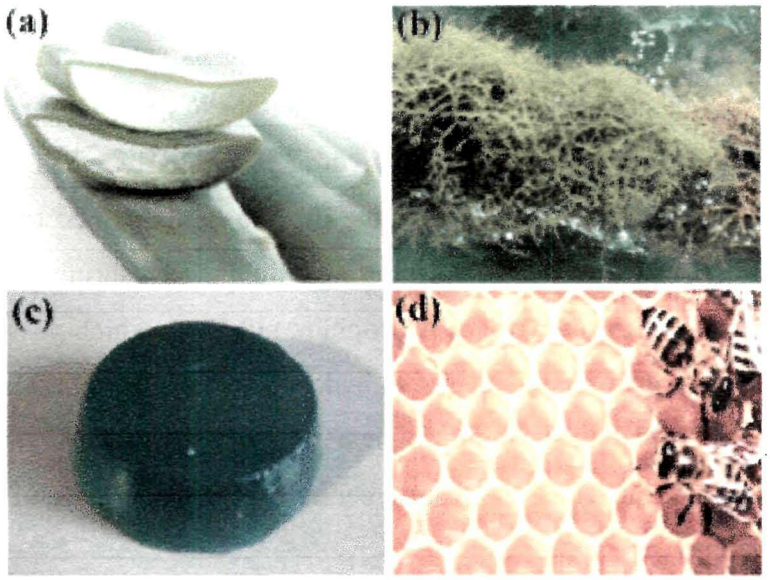

Fig 1.2 Examples of some natural sources of gels: (a) Aloe vera leaves, (b) Carrageenans, (c) Xanthan Gum and (d) Propolis.

Above all, some low molecular weight inorganic molecules also form gels such as, silica gel, alumina gel etc. Silica gel is a granular, vitreous and porous form of silicon dioxide made synthetically from sodium silicate. The utilization of silica gel date back to World War II, where it was used to keep penicillin dry, protect military equipment from moisture damage, as a fluid cracking catalyst for the production of high octane gasoline, as a catalyst support for the manufacture of butadiene from ethanol and also as feedstock for the synthetic rubber program. Alumina gel indicates a varied range of colloidal hydroxides, varied by the media: water, solvent or air. It can act as proficient acid absorber and hence commonly used as gastric antacids.[11] Recently, low molecular-mass organic gelators (LMOGs) have been introduced, which are relatively new and dynamic soft materials capable of numerous possible applications. It is generally accepted that a LMOG is a molecule that in small amounts, (typically <2 wt%), can gel water or organic solvent and combinations thereof, in which the minor solid and major liquid components form a three dimensional continuous phase.[12] Such gels are commonly formed by

dissolving a low percentage (0.1–5.0 wt%) of gelator molecule in an appropriate heated solvent. For example, urea derivatives have been studied for their self-assembling properties and proved to form stable gels in organic solvents: Feringa's group reported geminal bisureas and tripodal tris-urea derivatives capable of gelling in most non-polar solvents.[13,14] More recently, thiourea- based compounds functionalised with n-alkyl chains and N-benzoyl-N′-aryl groups demonstrated their ability to gel in a variety of organic solvents.[15] Some urea-based gelators are shown in **Fig 1.3**.

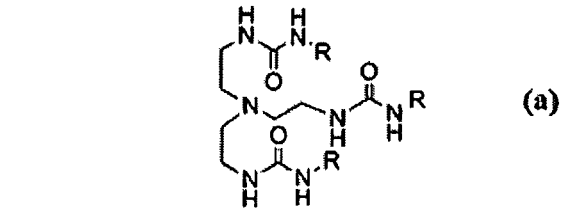

(a)

R= Ph, p-PhNO$_2$, CH$_2$Ph, (CH$_2$)nCH$_3$, CH(C$_2$H$_5$)(CH$_2$)$_3$CH$_3$

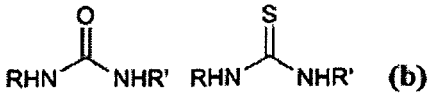

(b)

R=R'= CH$_3$, C$_2$H$_5$
n-C$_3$H$_7$, *n*-C$_4$H$_9$
n-C$_{10}$H$_{21}$, *n*-C$_{18}$H$_{37}$

Fig 1.3 Urea-based gelators of organic solvents.[16]

1.3 Hydrogels

Hydrogels are three-dimensional (3D) macromolecular networks composed of crosslinked hydrophilic polymer chains which can absorb upto thousands of times their dry weight of water or biological fluids.[17] The term hydrogel is composed of 'hydro' (water) and 'gel' and refers to aqueous (water-containing) gels or more precisely, the polymer networks that are insoluble in water. The water holding capacity of the hydrogels arise mainly due to the presence of hydrophilic groups, such as amino, carboxyl and hydroxyl groups in the polymer chains. They uniquely offer moderate-to-high physical, chemical, and mechanical stability in their swollen state. Their high water content renders them

compatible with living tissues and proteins and their rubbery nature minimizes damage to the surrounding tissues when implanted in the host.[18,19] Hydrogels were found to be the first novel bioactive materials rationally designed for human use due to relatively high biocompatibility and have received considerable attention in the past 50 years, due to their exceptional promise in a wide range of applications. Owing to the advantages of hydrogel as a soft material over other polymeric materials, they are currently being considered for various applications such as hygienic products,[20] agriculture,[21,22] waste water treatment,[23-26] carrier of catalyst,[27,28] controlled drug-delivery systems[29,30] and bioengineering material and regenerative medicines [31] etc.

Recently, a new study suggests that, clay hydrogel may be the birth place of life on the Earth. Prof. Dan Luo in his study stated that over billions of years, chemicals confined in those spaces could have carried out the complex reactions that formed proteins, DNA and eventually all the machinery that makes a living cell work. Clay hydrogels could have confined and protected those chemical processes until the membrane that surrounds living cells developed.[32] Although natural hydrogels have been utilized over the past few years, history of modern hydrogels began after the pioneering work of Wichterle and Lim (1955-1960). They developed a synthetic poly-2-hydroxyethyl methacrylate hydrogel, which was extensively used as a revolutionary biomaterial in contact lens production.[33] The main features of their design were: (a) shape stability and softness similar to that of the soft surrounding tissue; (b) chemical and biochemical stability; (c) absence of extractable and (d) high permeability for water-soluble nutrients and metabolites. Since then the research on hydrogel has been steadily increased to a greater extent and with the involvement of a large number of scientists resulted in more understanding on the physicochemical properties of hydrogels and development of new types of hydrogels as, they form a class of soft materials with remote controllable properties that have attracted great attention due to their potential use in diverse applications.[34,35]

Generally, preparation of hydrogel is based on hydrophilic monomers. Sometimes hydrophobic monomers are also used in order to regulate the properties for specific applications. Synthetic hydrogels are mostly produced via bulk, solution and inverse

dispersion techniques.[36] The properties of hydrogels such as crosslinking density, biodegradation, mechanical strength and chemical and biological response to stimuli can be effectively modulated by varying the synthetic factors such as, monomer type, type of crosslinker, crosslinker-to-monomer ratio, monomer concentration etc.

1.4 Water in Hydrogel

Water is the main constituent of a hydrogel. Generally, water inside hydrogel matrices can be categorized into three different types. [37] The experimentally determined separate states of water can be defined as: (a) free water: water that is not intimately bound to the polymer chain and behaves like bulk water, i.e. undergoes thermal transition at temperature analogous to bulk water (at 0°C); (b) semi-bound water: water that is weakly bound to the polymer chain or interacts weakly with nonfreezing water and undergoes a thermal phase transition at a temperature lower than 0°C and (c) bound water (non-freezing water): water tightly bound to the polymer, which does not exhibit a first order transition over the temperature range from -70° to 0°C.[38] Different states of water in hydrogel are shown in **Fig 1.4**.

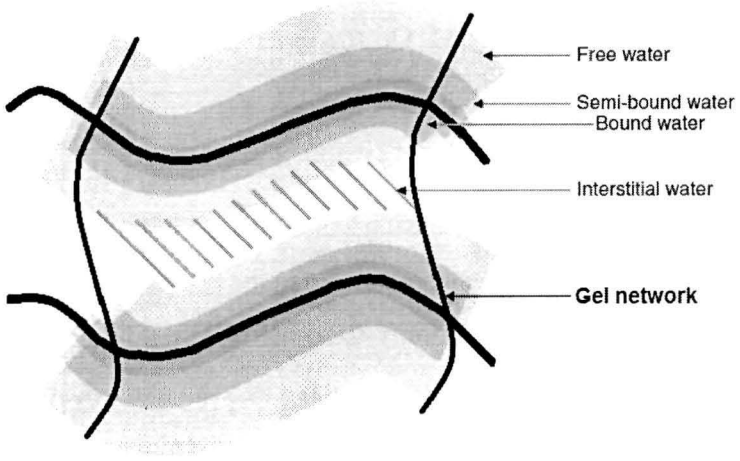

Fig 1.4 Different types of water in hydrogel.[39]

When a dry hydrogel begins to absorb water, the first water molecules entering the matrix will hydrate the most polar, hydrophilic groups, resulting in 'primary bound water'. As the polar groups are hydrated, the network tends to swell and exposes hydrophobic

groups, which also interact with water molecules, resulting in 'secondary bound water'. Primary and secondary bound water are often combined and simply called the 'total bound water'. After the polar and hydrophobic sites have interacted with bound water molecules, the network will imbibe additional water, due to the osmotic driving force of the network chains towards infinite dilution. This additional swelling is opposed by the covalent or physical crosslinks, leading to an elastic network retraction force. In this way, the hydrogel will reach an equilibrium swelling level. The additional swelling water that is imbibed after the ionic, polar and hydrophobic groups become saturated with bound water is called 'free water' or 'bulk water' and is assumed to fill the space between the network chains and/ or the center of larger pores, macropores or voids.[40] All water types in a hydrogels can be identified and characterized in a simple differential scanning calorimeter thermogram.

1.5 Characterization of hydrogels

A hydrogels comprises of chemical and physical structures. Therefore, when two or more monomers are used in the reaction or when a monomer is grafted onto a polymer backbone, analytical techniques, such as FTIR and NMR, are used to monitor the degree of copolymerization or grafting processes. On the other hand, the physical structure of a hydrogels is related to its composite nature. Their physical properties can be characterized by determining the unique swelling and elastic behavior.[41]

Since the weight, volume and dimension values of a hydrogels change during the swelling process **(Fig 1.5)**, any of these factors can be used to characterize swelling behavior of a hydrogels. The most commonly used method is the weight-swelling ratio, which can be expressed in weight unit or in percentage as shown in equation 1.1:

$$Q_t = W_{st} - W_d/W_d \text{ as } g/g \text{ or } Q_t = [W_{st} - W_d/W_d \times 100] \text{ (as \%)} \qquad \textbf{(Eqn. 1.1)}$$

when $W_{st} >> W_d$, the weight-swelling ratio can simply be expressed as in equation 1.2:

$$Q_t = W_{st}/W_d \qquad \textbf{(Eqn. 1.2)}$$

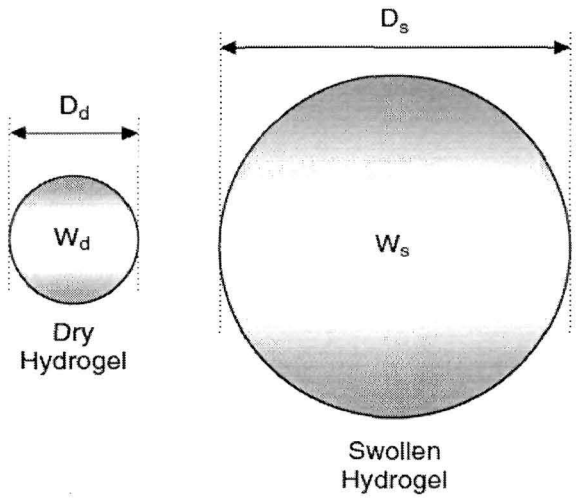

Fig 1.5 Swelling measurement of a hydrogel.[42]

For superabsorbent hydrogels with very high swelling capacities, the above equation is acceptable. When $t \rightarrow \infty$, the Q_t becomes Q_∞, which is the equilibrium swelling capacity or swelling at equilibrium. The Q_∞, is also called a 'power factor' in hydrogels, which can be used to compare the swelling capacity of a hydrogel. The higher the power factor is, the greater the swelling capacity becomes.[42] Swelling in hydrogels can also be expressed as volume-swelling ratio when the ultimate volume of the swollen gels is the goal for a given application. Moreover, since the swelling in hydrogels is driven by swelling pressure, the pressure sensors can be utilized to characterize swelling in hydrogels. It is well known that the initial water uptake process of hydrogels corresponds to the diffusion of water molecules into the gel network. A simple and useful empirical equation, so-called power law equation, is commonly used to determine the mechanism of diffusion,[43] i.e. swelling kinetics in polymeric networks as shown in the equation 1.3:

$$M_t/M_\alpha = kt^n \qquad \textbf{(Eqn. 1.3)}$$

where, M_t and M_α are the weight of the swollen sample at time t and at infinitely equilibrium swollen state, respectively, k is a characteristic constant and n is a characteristic exponent of the mode transport of the water. According to the classification

of the diffusion mechanism, $n = ½$ *and* $½ < n < 1$ indicates a Fickian and anomalous diffusion model respectively.[44]

The properties of a specific hydrogel are extremely important in selecting which materials are suitable for a given application. The mechanical behaviour of hydrogels is best understood using the theories of rubber elasticity and viscoelasticity. These theories are based on time-independent and time-dependent recovery of the chain orientation and structure, respectively. By using theories to describe the mechanical behaviour, it is also possible to analyze the polymer structure and determine the effective molecular weight between the crosslinks as well as to elucidate information about the number of elastically active chains. In their swollen state, most of the hydrogels satisfy the criteria for a rubber. When a hydrogel is in the region of rubberlike behaviour, the mechanical behaviour of the gel is dependent mainly on the architecture of the polymer network. However, at low enough temperatures, these gels can lose their rubber elastic properties and exhibit viscoelastic behaviour.[45] The viscoelasticity theory considers the relationships between elasticity, flow and molecular motion in polymeric materials. In general, hydrogels are not simply elastic materials, but they behave viscoelastically. Thus, the time dependence of the applied stress or strain is as much important as the magnitude in predicting the material's mechanical response.[46]

There are various experimental procedures for testing the mechanical properties of hydrogels. But, the common methods for measuring mechanical properties of hydrogels include tensile (rubber elastic behaviour) or dynamic mechanical analysis (viscoelastic behaviour). Dynamic mechanical analysis provides quantitative information on the viscoelastic and rheological properties of a material by measuring the mechanical response of a sample as it is deformed under periodic stress (or strain). The dynamic modulus, G^*, is defined as:

$$G^* = G' + iG'' \qquad \textbf{(Eqn. 1.4)}$$

here, G' is the real (also elastic or storage) modulus and G'' is the imaginary (also viscous or loss) modulus.

A crosslinked hydrogel with a greater storage modulus and lower loss modulus is considered to have good mechanical property. Once the mechanical characteristics of a hydrogel have been determined, it is often necessary to improve them in some way to make the material suitable for the desired application. Mechanical properties of a hydrogel can be manipulated by altering the co-monomer composition, increasing or decreasing the crosslinking density and the reaction conditions. The mechanical strength of a hydrogel is often derived almost entirely from the crosslinks in the system. Particularly in the swollen state, where physical entanglements are nearly nonexistent, the strength of the material increases dramatically with increasing crosslinking density.[47]

Hydrogels are extensively reported to be used in biomedical applications such as drug delivery, tissue engineering, biosensors and artificial muscles etc.[48] Since these applications involve use of humans or other animals, it is important to study their biocompatibility. Generally, the biocompatibility of a hydrogel can be determined by testing their hemocompatibility and cytocompatibility. Hemocompatibility can be evaluated by examining the hemolysis percentage of blood in presence of the prepared hydrogels. Hemolysis below 5% is reported to be the acceptable limit and the hydrogel is considered to be hemocompatible. Cytocompatibility of a hydrogel is usually determined by MTT assay test. The MTT assay helps in the determination of the viability of the cells when incubated in the presence of hydrogel samples.[49]

1.6 Classification of hydrogels

Hydrogels are classified into several distinct categories depending on their origin, method of preparation, ionic charge and physical structural feature such as nature of crosslinking.

1.6.1 Based on origin

They can be separated into two groups based on their natural or synthetic origins.[50] Hydrogel-forming natural polymers include proteins such as collagen, chitosan and gelatin, and polysaccharides such as alginate, cellulose, starch and agarose etc. All these natural polymers are obtained from various natural origins. Depending on their origin and

composition, various natural polymers have specific utilities and properties. Many natural polymers, such as collagen, hyaluronic acid and fibrin, are derived from various components of the mammalian extracellular matrix. Collagen is the main protein of the mammalian extracellular matrix, while hyaluronic acid is a polysaccharide that is found in nearly all animal tissues. Alternatively, alginate and agarose are polysaccharides that are derived from marine algae sources. The advantages of natural polymers include low toxicity and biocompatibility.[51] Chitosan is another naturally occurring linear polysaccharide derived from chitin. Dissolved chitosan can be crosslinked by increasing pH, by dissolving in a non-solvent or by photo-crosslinking. It can be degraded by the lysosome and is therefore degraded in humans. Chitosan gels can be used for many applications including drug delivery.[52,53] To synthesize gels with enhanced mechanical properties, natural-based hydrogels are usually prepared through addition of some synthetic parts onto the natural substrates, e.g., graft copolymerization of vinyl monomers on polysaccharides. Gelatin is a heterogeneous mixture of water-soluble proteins of high average molecular weights, present in collagen. The proteins are extracted by boiling skin, tendons, ligaments, bones, etc. in water.

On the other hand, most of the synthetic hydrogels are synthesized by traditional polymerization of vinyl or vinyl-activated monomers. The equilibrium swelling of these synthetic hydrogels varies extensively according to the hydrophilicity of the monomers and the crosslinking density. Generally, a bi-functional monomer is added to carry out an in situ crosslinking reaction. Neutral synthetic hydrogels can be generated from derivatives of poly(hydroxyethyl methacrylate) (PHEMA), poly(ethylene glycol) (PEG) and poly(vinyl alcohol) (PVA) etc. PEG hydrogels are one of the most widely studied and used materials for biomedical applications.[54]

1.6.2 Based on preparation method

Based on the method of preparation, hydrogels are classified into (i) homopolymer hydrogels, (ii) copolymer hydrogels, (iii) multipolymer hydrogels and (iv) interpenetrating polymeric hydrogels. Homopolymer hydrogels are crosslinked networks of one type of hydrophilic monomer unit, whereas copolymer hydrogels are produced by crosslinking of

two comonomer units, at least one of which must be hydrophilic to make them swellable. Multipolymer hydrogels are produced from three or more co-monomers reacting together.[55] Interpenetrating polymer networks (IPNs) are defined as a combination of two network polymers, at least one of which is prepared or crosslinked in the immediate presence of the other. Recently, they have gained great attention because their feasibility in biomedical applications. The swelling behaviour and mechanical properties of hydrogels can be greatly improved by this method of preparation.

1.6.3 Based on ionic charges

Based on the ionic charges, hydrogels can be classified into neutral, anionic, cationic and ampholytic hydrogels.[56] Neutral hydrogels, such as poly(N-vinyl pyrrolidone) and poly(ethylene oxide), swell in aqueous medium solely due to water–polymer interactions. Cationic hydrogels display superior swelling at acidic media since their chain dissociation is favored at low pH value. Similarly, anionic hydrogels dissociate more in higher pH media and hence, display superior swelling in neutral to basic solutions. Ampholytic hydrogels possess both positive and negative charges that are balanced at a certain pH (iso-electric point). A change in pH can change the overall ionic (cationic or anionic) properties.

1.6.4 Based on the nature of the crosslinked junctions

Now-a-days, many crosslinking methods have been developed and are presently available for the preparation of hydrogels. Based on the crosslinking method, hydrogels can be divided into two categories: chemically crosslinked networks or permanent gel and physically crosslinked networks or reversible gel.[57] Chemical crosslinking is a versatile method to create hydrogels with good mechanical stability.

Generally, crosslinking by radical polymerization can be obtained by introducing acrylate-based crosslinkers to the polymerization system.[58] Ethylene glycol dimethylacrylate (EGDMA), is one of the most extensively used crosslinker in free radical copolymer crosslinking reactions. Other acrylate-based crosslinkers are (a) trimethylol propane trimethacrylate, (b) 2-hydroxy trimethylene dimethacrylate, (c) 2,3-dihydroxy

tetramethylene dimethacrylate and (d) hexamethylene bis (methacryloyloxy-ethylene carbamate) etc. Structures of these crosslinkers are shown in **Fig 1.6.**

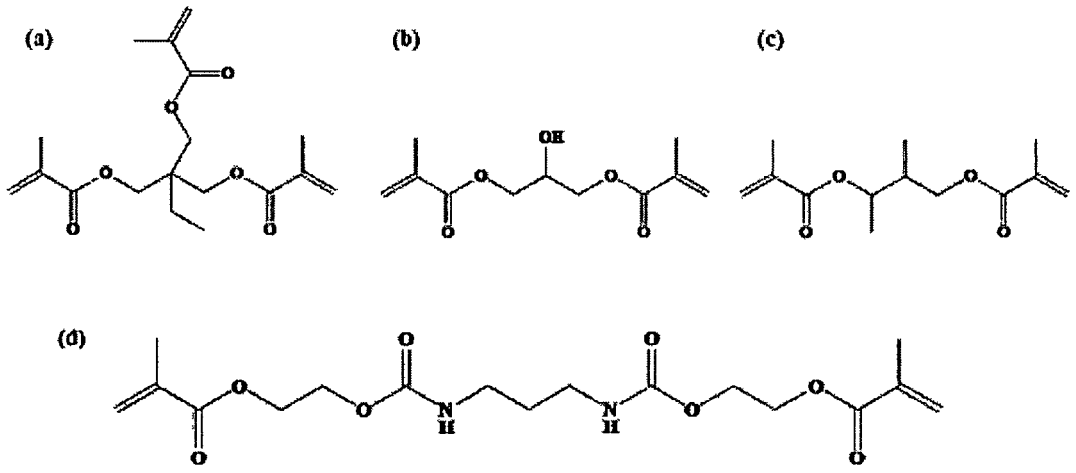

Fig 1.6 (a) Trimethylol propane trimethacrylate, (b) 2-hydroxy trimethylene dimethacrylate, (c) 2,3-dihydroxy tetramethylene dimethacrylate and (d) hexamethylene bis-(methacryloyloxy-ethylene carbamate).

Covalent linkages between polymer chains can also be established by the reaction of functional groups with complementary reactivity, such as an amine-carboxylic acid or an isocyanate OH/NH_2 reaction etc.[59] For example, the reaction of α,ω-hydroxyl poly(ethylene glycol) with a diisocyanate in the presence of a triol as crosslinker as shown in the **Fig 1.7.**

Water-soluble polymers with hydroxyl groups (e.g., poly vinyl alcohol)) can be crosslinked using glutaraldehyde. However, due to the toxicity of glutaraldehyde, alternatives have been developed as shown in **Fig 1.8**. Crosslinking of gelatin using polyaldehydes obtained by partial oxidation of dextran has been reported.[61] High energy irradiation, particularly gamma and electron beam is able to crosslink water-soluble polymers without additional vinyl groups. During irradiation (gamma or electron beam) of aqueous solutions of polymers, radicals can be formed on the polymer chain by e.g., the homolytic scission of C-H bonds.

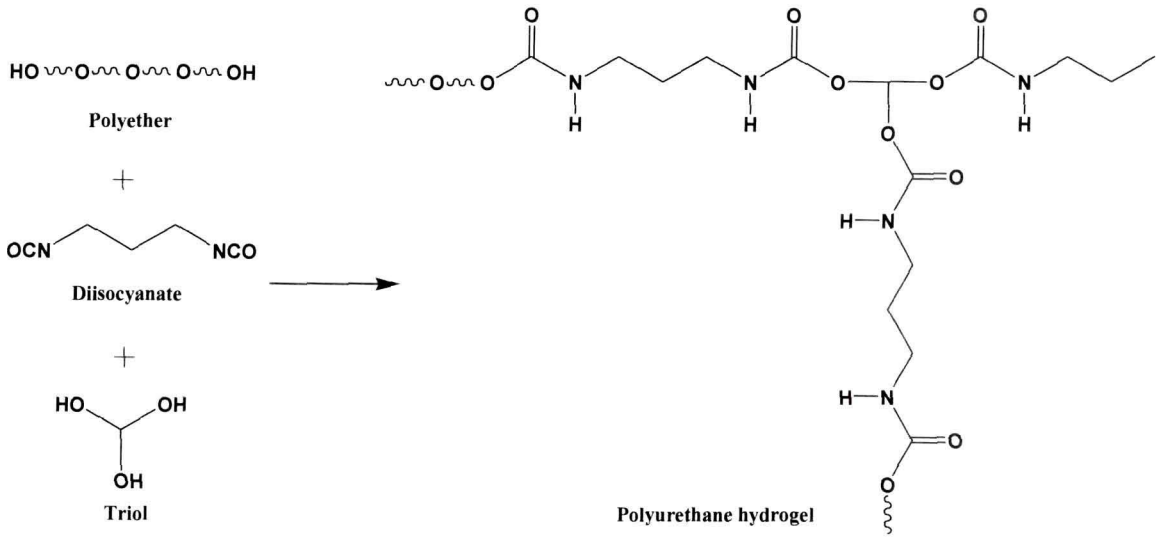

Fig 1.7 The reaction of α,ω-hydroxyl poly(ethylene glycol) with a diisocyanate in the presence of a triol as crosslinker.[61]

Moreover, radiolysis of water molecules generates the formation of hydroxyl radicals which can attack polymer chains also resulting in the formation of macroradicals. Recombination of the macroradicals on different chains results in the formation of covalent bonds and finally in a crosslinked structure.[62]

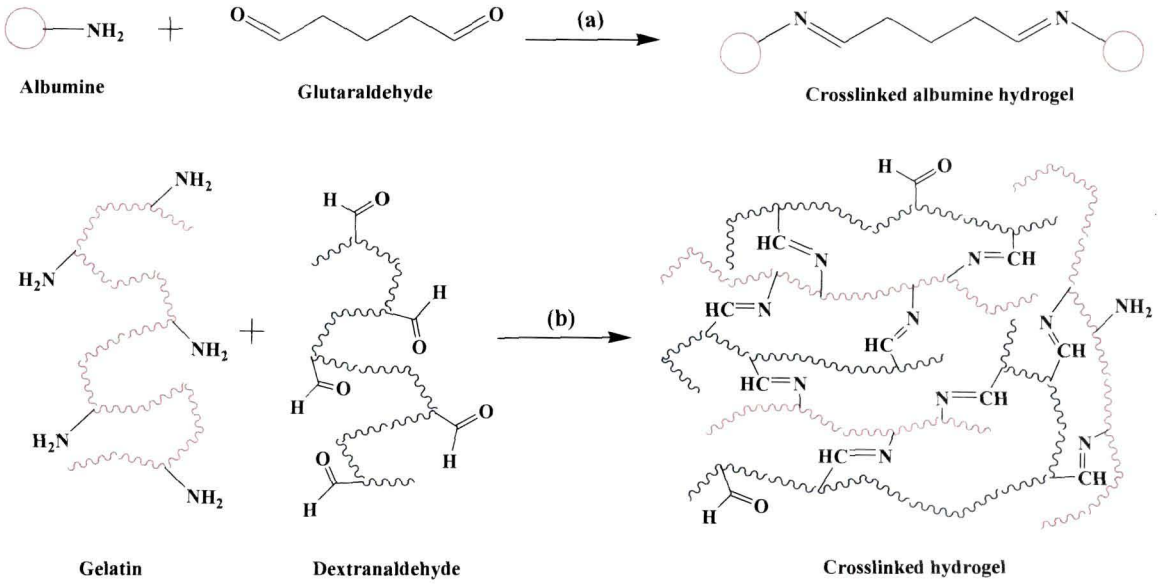

Fig 1.8 Crosslinking by (a) Glutaraldehyde and (b) Dextranaldehyde.

Physical hydrogels are formed due to the physical interactions, such as molecular entanglement, ionic interaction and hydrogen bonding and hydrophobic interactions among the polymeric chains etc.[63] All of these interactions are reversible and can be disrupted by changes in physical conditions or application of stress. In recent years, there has been increasing interest in physically crosslinked gels because the use of crosslinking agents to prepare such hydrogels is avoided. This type of crosslink could be used to reverse the gelling properties of the hydrophilic polymers under the desired conditions. Physically crosslinked hydrogels can be obtained by ionic interactions, by crystallization, stereocomplex formation, hydrogen bonding etc. Ionic bonds exist in polyelectrolyte complexes between the pairs of charge sites on anionic and cationic polyelectrolyte chains. For example, ionically crosslinked chitosan and sodium alginate hydrogel as shown in **Fig 1.9.**

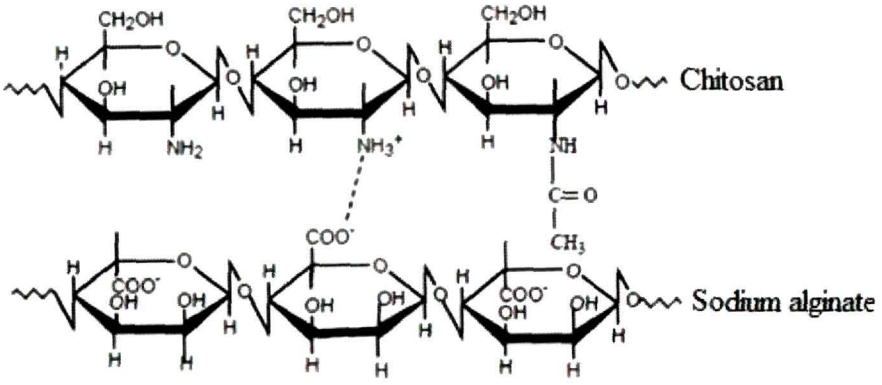

Fig 1.9 Representation of ionically crosslinked chitosan and sodium alginate hydrogel.[64]

1.6.5 Based on crystallinity

On the basis of physical structure and chemical composition can be classified as amorphous hydrogels (non-crystalline), semi-crystalline hydrogels and hydrogen-bonded or complexation structures.[65] In amorphous hydrogels, the macromolecular chains are arranged randomly. On the other hand, semi-crystalline hydrogels are characterized by dense regions of ordered macromolecular chains (crystallites). Finally, hydrogen bonds and complexation structures may be responsible for the three-dimensional structure formed.

1.6.6 Based on environmental response

Hydrogels can also be classified as conventional and stimuli-responsive ones according to their response to different environmental factors.[66] Conventional hydrogels are the crosslinked polymer chains which absorb water when put in an aqueous media and there is no change in the equilibrium swelling with the change in the pH, temperature or electric field of the surrounding environment while the stimuli-responsive (smart or intelligent) hydrogels are the polymeric networks which change their equilibrium swelling with the change of the surrounding environment. Many physical and chemical stimuli can be applied to induce different responses of smart hydrogel systems. Physical stimuli includes temperature, pressure, light, electric, magnetic, sound etc. Chemical or biochemical stimuli comprise pH, ionic strength, ions or specific molecular recognition events.[67,68] The swelling behavior of a stimuli-responsive hydrogel after the response to a specific stimulus can be shown in the **Fig 1.10.**

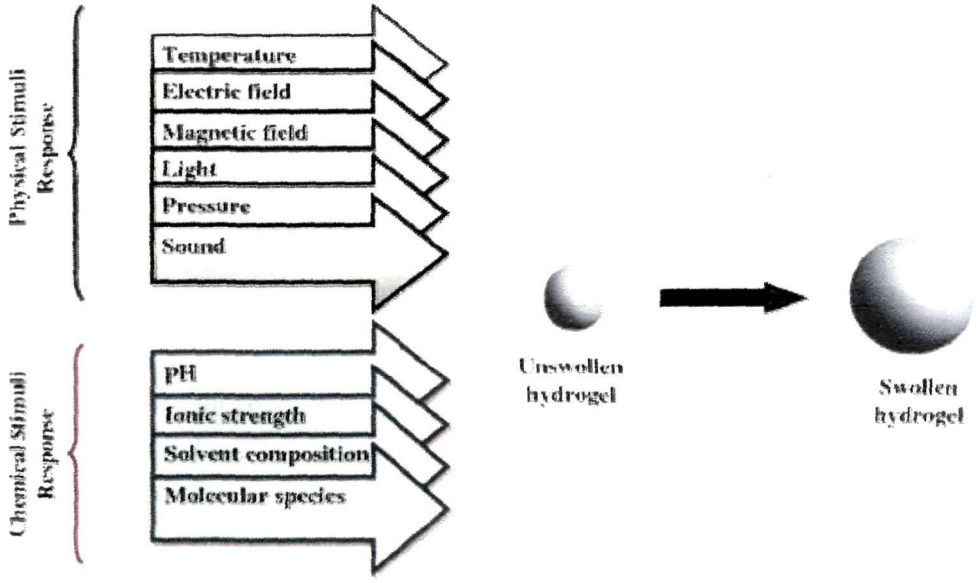

Fig 1.10 Stimuli-responsive swelling of hydrogel.[25]

Stimuli-responsive materials are very much essential for designing of a sustainable future which requires dynamic materials that can respond and adapt with the constantly changing environment. This extraordinary phenomenon of some hydrogels was

discovered by Professor T. Tanaka in 1978 which is called the 'volume phase transition' phenomena.[69,70] Classification of stimuli-responsive hydrogels is based on the external stimuli type. According to their nature, smart hydrogels can be classified as thermo-responsive, pH responsive, electro-responsive, magnetic field responsive,[71] as well as responsive to light, pressure, ionic strength and different molecules such as enzymes, etc. An interesting characteristic of numerous responsive gels is that the mechanism causing the network structural changes can be entirely reversible in nature. Some important classes of stimuli-responsive hydrogels are briefly described below:

pH-responsive hydrogels

The pH-responsive hydrogels are one of the most widely studied stimuli-responsive polymeric hydrogels. They exhibit swelling/deswelling behavior which is related to the environmental pH changes. The pH-responsive polymers consist of ionizable pendant group that can accept and donate protons in response to the environmental change in pH.[72] In aqueous media of appropriate pH and ionic strength, the pendant groups can ionize developing fixed charges on the gel. This, in turn cause differences of internal and external ionic strength and breakage of hydrogen bonds between the molecular segments. As a result, crosslinking density will be decrease and the increase in electrostatic repulsions lead to swelling of the hydrogel. pH-responsive hydrogels may be grouped into three main classes: (a) anionic hydrogels; (b) cationic hydrogels and (c) neutral hydrogels depending on the nature of pendant group present in the network.[73] Anionic hydrogels contain negatively charged fragments of polymer network; cationic ones have positively charged fragments, while neutral hydrogels contain both positively and negatively charged polymer chain fragments.

Anionic hydrogels often contain carboxylic or sulfonic acid groups on their backbone and the most commonly used monomers are acrylic acid (AAc) and its derivatives.[74] The more important parameter in anionic hydrogels is the relation between pKa of the polymer and pH of surrounding medium. In anionic hydrogels having pendent groups such as carboxylic[75] or sulfonic acid,[76] deprotonation occurs when the environmental pH is above the pKa leading to the ionization of the pendent groups.

Therefore, they dissociate more in higher pH media and hence, display superior swelling in neutral to basic solutions.

Cationic pH-responsive hydrogels generally have basic pendants such as primary amine, secondary amine and tertiary amine.[77] They swell at pH lower than pKa of cationic groups. This is due to the fact that amino group is protonated at pH lower than pKa and the amine group will change from NH_2 to NH_3^+, which subsequently increase the hydrophilicity, electrostatic repulsion and swelling rate.[78] On the other hand, driving force for swelling of neutral hydrogels arises from thermodynamic mixing of water and polymer and elastic behaviour of the network. Neutral hydrogels such as poly(*N*-vinyl pyrrolidone) and poly(ethylene oxide) swell in aqueous medium solely due to water-polymer interactions. pH-responsive hydrogels were most frequently used to develop controlled release systems for oral administration. **Fig 1.11** illustrates the structures of anionic and cationic polyelectrolytes and their pH-dependent ionization. Poly(acrylic acid) (PAAc) becomes ionized at high pH, while poly(N,N'-diethylaminoethyl methacrylate) (PDEAEM) becomes ionized at low pH.

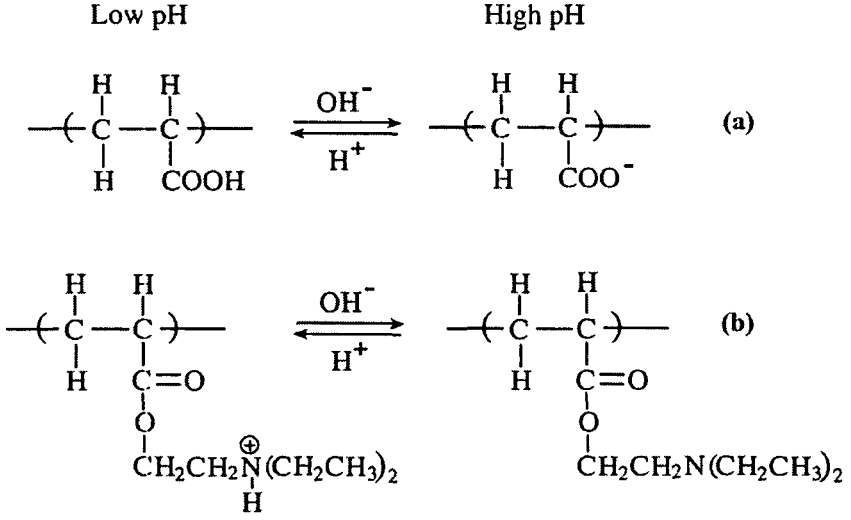

Fig 1.11 pH-dependent ionization of polyelectrolytes: (a) poly(acrylic acid) and (b) poly(N,N'-diethylaminoethyl methacrylate).[74]

Thermo-responsive hydrogels

This is another important class of environmentally sensitive gels which has the ability to swell and shrink when the temperature changes in the surrounding fluid. A unique property of temperature-responsive polymers is the presence of a critical solution temperature, which is the temperature at which the phase of polymer and solution is discontinuously changed according to their composition.[79] They are characterized by the presence of hydrophobic groups, such as methyl, ethyl and propyl groups. One of the most familiar polymers of this type is poly(N-isopropylacrylamide).[80] Thermo-responsive hydrogels can be classified into three categories: negative thermosensitive (negative temperature dependent); positive thermosensitive (positive temperature dependent) and thermally reversible hydrogel. Structures of some thermo-responsive hydrogels are shown in **Fig 1.12**.

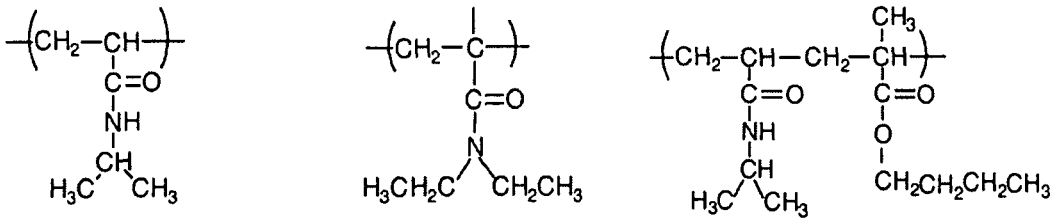

Poly(N-isopropylacrylamide) (PNIAAm) | Poly(N,N-diethylacrylamide) (PDEAAm) | P(NIAAm-co-BMA)

Fig 1.12 Structures of some thermo-responsive polymeric hydrogels.[74]

Negative temperature-sensitive hydrogels have a lower critical solution temperature (LCST), which may be defined as the critical temperature below which the polymer swells in the solution while above it the polymer contracts. Below the LCST, the enthalpy term, related to the hydrogen bonding between the polymer and the water molecules, is responsible for the polymer swelling. But, when the temperature is raised above the LCST, the entropy term (hydrophobic interactions) dominates, leading to polymer contraction. In general, the LCST of polymer with more hydrophobic constituent shift to lower temperature and LCST can be changed by adjusting the percentage ratio of hydrophobic to hydrophilic contents of the structure of the hydrogel.[81] An extensively

studied polymer with LCST at 32°C is poly(N-isopropylacrylamide) which has been widely employed as a negative thermosensitive hydrogel. The main reason for its frequent use is because its phase transition occurs at approximately body temperature.

A positive temperature-sensitive hydrogel bears an upper critical solution temperature (UCST). In this case, at temperatures higher than UCST swelling takes place and the hydrogel starts to contract upon cooling below the UCST. Positive temperature PHGs are shrinking at low temperature because of formation of complex structure by hydrogen bonds. The structure dissociates at high temperature due to breaking of hydrogen bonds and the gel will swell to the maximum possible extent rapidly above the UCST. Examples of positive thermo-responsive hydrogels are, the interpenetrating polymer network (IPNs) based on poly(acrylic acid) and polyacrylamide or poly(AAm-*co*-BMA).[82]

Electro-responsive hydrogels

Electro-responsive hydrogels are a kind of stimuli-responsive hydrogels which undergo swelling, shrinking and bending behavior in response to an external electric field. They are generally prepared from polyelectrolytes and are thus pH-responsive as well. Electro-responsive hydrogels generally deswell or bend, depending on the shape and orientation of the gel under the influence of an electric field. The gel bends when it is parallel to the electrodes, whereas deswelling occurs when the hydrogel lies perpendicular to the electrodes.[83,84] When an electric field is applied, the migration of free ions occurs within hydrogel, which in turn causes inhomogeneity inside and outside the hydrogel. This leads to the variation of osmotic pressure and deformation of hydrogel. Therefore, these hydrogels with ability to transform electric energy to mechanical energy have been investigated extensively as energy converter applied in fields such as robots, sensors, controlled drug release and artificial muscles.[85,86]

Electrically induced anisotropic gel deswelling was first explained by Tanaka et al.[69] The electric field produces a force on both the mobile counter ions and the immobile charged groups of the gel's polymeric network. For example, partially hydrolyzed

polyacrylamide hydrogels which are in contact with both the anode and cathode electrodes undergo volume collapse by an infinitesimal change in electric potential across the gel. When the potential is applied, hydrated H^+ ions migrate to the region of the cathode, which results in a loss of water at the anode side. Simultaneously, the electrostatic attraction that exists between the anode surface and the negatively charged acrylic acid groups creates a uniaxial stress along the gel axis. These two events lead to shrinking of the hydrogel on the anode side.[87,88]

Photo-responsive hydrogels

Another type of stimuli-responsive hydrogel is the photo-responsive hydrogel, which have potential application in developing of optical switches, display units, photo-responsive artificial muscles, memory devices and ophthalmic drug delivery devices etc. Since the light stimulus can be imposed instantly and delivered in specific amounts with high accuracy, light-sensitive hydrogels may possess special advantages over others.[89] Moreover, the capacity for instantaneous delivery of the sol-gel stimulus makes the development of light-sensitive hydrogels important for various applications in both engineering and biochemical fields. They can be classified into UV-sensitive and visible light-sensitive hydrogels; however, visible light-responsive polymers and the hydrogels prepared from them are more advantageous because of their safety, inexpensiveness, readily availability, clean and easy manipulation.

Magnetic field responsive hydrogels

Magnetic field-sensitive hydrogels are often prepared by incorporating or loading magnetic nanoparticles into the crosslinked polymeric hydrogels, i.e. they consist of a polymer matrix and a magnetic component embedded in the matrix.[90] The presence of magnetic nanoparticles gives the hybrid system the capacity to respond to external magnetic stimulus, such as alternating magnetic fields (AMF) and to localize the hydrogel near the target site through the use of an appropriate magnet.[91] They have numerous technological and biomedical applications, including tissue engineering, controlled drug delivery, magnetic separation, MRI contrast agents, hyperthermia and thermal ablation

etc.[92-94] Various methods have been developed to fabricate magnetic hydrogels which includes a blending method,[95] an in situ precipitation method[96] and the grafting-onto method.[97]

1.7 Biomedical applications of stimuli-responsive polymeric Hydrogels

Due to the fascinating properties of the stimuli-responsive hydrogels, such as reversible swelling/deswelling behaviour, sorption capacity, novel mechanical property, high ionic conductivity, high environmental sensitivity, permeability and surface property, hydrogels provide platform for creating novel smart materials for a wide range of applications especially in the biomedical field. They can be conveniently formulated in a variety of physical forms or shapes including slabs, microparticles, nanoparticles, coatings and films etc. As a result, hydrogels are commonly used in clinical practice and experimental medicine for a wide range of applications, including controlled drug delivery,[98] tissue engineering,[99] wound dressing,[100] actuators,[101] sensors[102] and so on. Moreover, there are some high swelling agricultural hydrogels, which can absorb ion-containing aqueous solutions, while being stable to UV- irradiation, oxygen, ozone, acidic rains, temperature variation, microorganisms and soil composition. There are numerous studies which explain the applications of hydrogels in agricultural field.[103] Some of the major applications of stimuli-responsive hydrogels are elaborated below:

1.7.1 Actuator

There have been numerous attempts to mimic the efficient conversion of chemical energy into mechanical energy in living organisms.[104] All living organisms move by the isothermal conversion of chemical energy into mechanical work such as muscular contraction. Stimuli-responsive hydrogels are capable of performing work by converting an external stimulation into mechanical motion can be an effective framework for soft actuators. Therefore, these systems can serve as actuators or artificial muscles in many applications. Conventional actuators require external power (e.g., electromagnetic, electrostatic or thermopneumatic effects) for operation and are relatively complex systems, which limits their use in practical systems. But, stimuli-responsive hydrogels

have a significant advantage over conventional actuators owing to their ability to undergo abrupt volume changes in response to the surrounding environment without the requirement of an external power source. Moreover, hydrogels have been proven to be the low-voltage actuators which are getting considerable interest in the present time due to their possible applications in biomedical devices,[105] machine components[106,107] and micro-electromechanical systems[108] etc. Among various hydrogel systems, polyelectrolyte hydrogels are getting tremendous importance in such applications. The control over swelling, shrinking and bending behaviour of polyelectrolyte gels in response to environmental stimuli enables direct conversion of electrostatic energy into mechanical energy. Due to this capability, polyelectrolyte gels are designated as actuators for technical applications where large swelling and shrinkage is required, such as for artificial muscles or other chemo-electro-mechanical actuators.[109]

Polyelectrolyte gels are also capable of reversible contraction and expansion under physicochemical stimuli that are essential in the development of advanced robotics with electrically driven muscle-like actuators. Electro-responsive hydrogels are the most extensively studied polyelectrolyte hydrogels for actuator application, as in this case the mechanical energy is triggered by an electric signal. They can reversely bend under the application of an electric field **(Fig 1.13)**. Also, for the realization of a powerful actuator, or a material with properties closely resembling those of skeletal muscles, it is necessary to have a polymer gel with both fast and sensitive electric responses with high mechanical strength.[110,111] Several research groups have focused their studies on the actuation behavior of polyelectrolyte gels under the influence of an applied electric field.

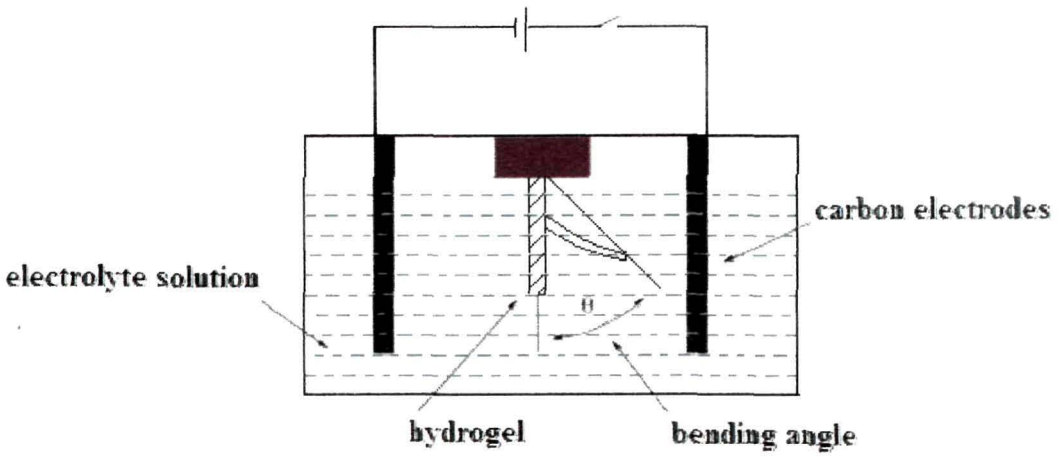

Fig 1.13 Schematic diagram of the apparatus for testing the bending behaviour of hydrogel under an applied electric field.[112]

Osada and his group claimed to be the first to offer an electrically activated artificial muscle system which undergoes contraction under isothermal condition when electric current is passed across water-swollen polyelectrolyte gels. The rate of volume change is proportional to the applied electric current. Hydrogel contraction is believed to be induced from the electrophoretic migration of hydrated ions and concomitant water release.[113] Moschou et al. developed novel artificial muscle material based on acrylic acid, acrylamide and the composite polypyrrole/carbon black. The hydrogel material showed fast and reversible electro-actuation under low applied voltage in near neutral pH environments.[114] Bassil et al. studied the electrochemical properties and actuation mechanisms of polyacrylamide hydrogel for artificial muscle application. They analyzed the volume variation kinetics of the gel responding to various pH stimulations and investigated the electroactivity of PAAm actuators in a fully hydrated gel. They also explained the bending mechanism of the hydrogel actuator based on the phenomenon of diffusion of hydroxide and hydronium ions showing the correlation between the electrical, chemical and mechanical properties of such devices. The bending behaviour was explained by the response of the gel to different pH values. The actuator undergoes a more important contraction (quicker shrink) in an acidic environment than in a basic environment. The gel shrinks and the structure bends toward the anode allowing chemical or electrical energy to be converted into mechanical work.[115]

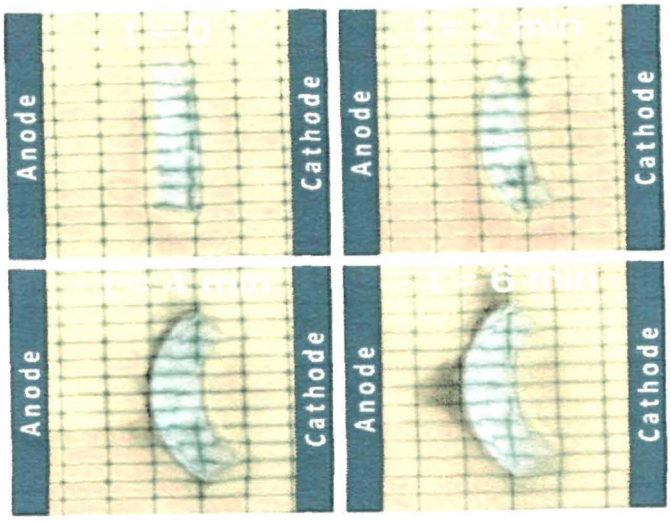

Fig 1.14 Electro-actuation behaviour of polyelectrolyte hydrogel at different time interval.[116]

1.7.2 Controlled drug delivery

Progress in medical science has led to tremendous enhancement of quality of life. Over the past few years, greater attention has been focused on development of controlled and sustained drug delivery systems. The aim in designing these systems is to reduce the frequency of dosing or to increase effectiveness of the drug by localization at the site of the action, decreasing the dose required or providing uniform drug delivery.[117] With the passage of time, newer and more powerful drugs continue to be developed, so increasing attention is being given to the methods by which these active substances are administrated. Conventional delivery systems suffer from the limitations of minimal synchronization between the required time for therapeutically effective drug plasma concentrations and the actual drug release profile exhibited by the dosage form.

Meanwhile, some drugs exert their effects not only at the targeted sites but also at the adjacent sites and cause side effects, which demand to control the drugs distribution after entering humoral system and tissues. To meet the new demands of drug administrations, intelligent drug delivery systems have been developed to release drugs timely, quantitatively and site-specifically in response to the various physiological signals.[118] Moreover, they can also provide pulsatile drug release pattern, where the rapid and transient release of a certain amount of drug molecules within a short time-period

immediately after a predetermined off-release period can be obtained. Schematic representation of the steps involved in preparation of a hydrogel based drug delivery system is shown in the **Fig 1.15.**

In the current niche of drug delivery technologies, hydrogels have made an irreplaceable space because of their unique characteristics. Hydrogel resemble natural living tissue more than any other class of synthetic biomaterials due to their high water content, which also contributes to their biocompatibility. Moreover, stimuli-responsive hydrogels can respond to various environmental stimuli which lead to drastic changes in their volume and shape reversibly and also change in the swelling behavior of these hydrogels. These 'intelligent' or 'smart' polymers play important role in drug delivery since they may determine not only where a drug is delivered, but also when and with which interval it is released.[119] The stimuli that induce various responses of the hydrogel systems include physical (temperature, electric fields, light, pressure, sound and magnetic fields), chemical (pH, ions) or biological (biomolecules) etc. It has been mentioned earlier that stimuli-responsive hydrogels can exhibit dramatic changes in their swelling behaviour, network structure, permeability or mechanical strength in response to different stimuli, both internal and external to the body.[120]

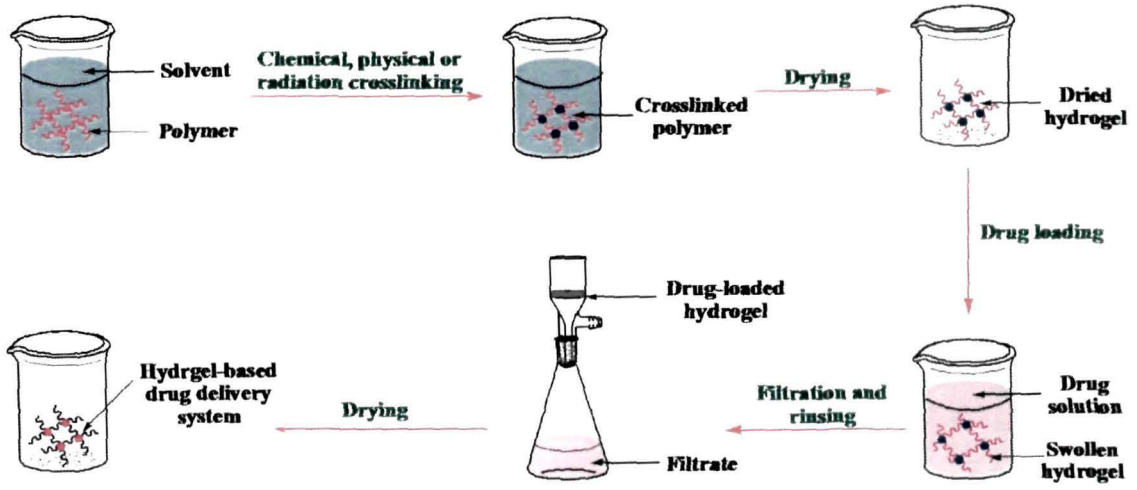

Fig 1.15 Schematic representation of the steps involved in preparation of a hydrogel based drug delivery system.[121]

External stimuli have been produced with the help of different stimuli generating devices, whereas internal stimuli are produced within the body to control the structural changes in the polymer network and to exhibit the desired drug release. Depending on different internal and external stimuli, intelligent drug delivery systems are classified into various categories.

pH-responsive drug delivery systems

The pH range of fluids in various segments of the gastrointestinal tract may provide environmental stimuli for responsive drug release **(Fig 1.16).** For example, oral administration will go through acidic environment in stomach and then neutral or slightly basic intestine, while anti-cancer drugs will come up against lower pH values in tumor and inflammatory tissue (pH ~6.8-7.2) as well as in endosome and lysosome of cells (pH ~5-6) compared with pH ~7.4 in normal tissue and blood.[122] In addition to these, local pH changes in response to specific substrates can be generated and used for modulating drug release. The charge density of the polymers depends on pH and ionic composition of the outer solution (the solution into which the polymer is exposed). Altering the pH of the solution will cause swelling or deswelling of the polymer. Polymers containing acidic groups will be unswollen at low pH, since the acidic groups will be protonated and hence unionized. With increasing pH, they will swell. The opposite holds for polybasic polymers, since the ionization of the basic groups will increase with decreasing pH.

Therefore, the major factors that influence the degree of swelling of ionic polymers are the properties of the polymer (charge, concentration and pKa of the ionizable group, degree of ionization, crosslinking density and hydrophilicity or hydrophobicity) and properties of the swelling medium (pH, ionic strength and the counterion and its valency).[123]

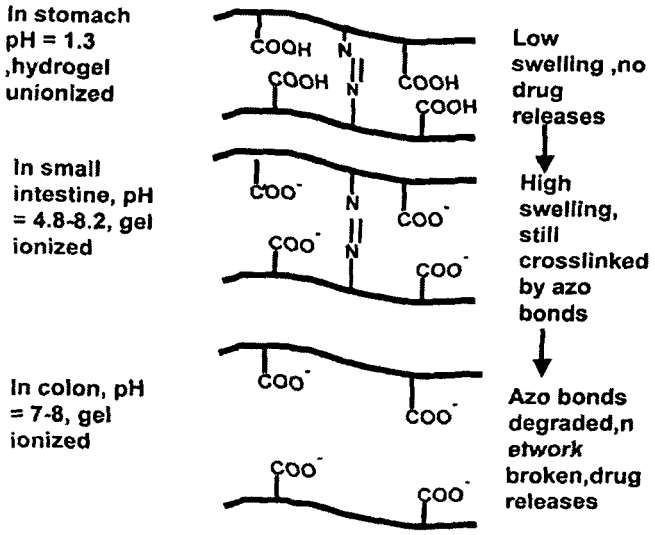

Fig 1.16 Schematic illustration of oral colon-specific drug delivery using pH-sensitive hydrogels.[124]

Most commonly studied ionic polymers for pH-responsive drug delivery include polyacrylamide, poly(acrylic acid), poly(methacrylic acid), poly(diethylaminoethyl methacrylate) and poly(dimethylaminoethyl methacrylate) etc.[125] Various natural polymers such as albumin, chitosan and gelatin have also shown pH-responsive swelling behavior as well as drug release behavior. Thus drug release from matrix devices made from these polymers display release rates that are pH-dependent.[126-129] Numerous attempts have been made by the researchers to develop pH-responsive drug delivery systems. For example, a series of pH-responsive block copolymers were developed by Sant et al. by using PEG as the hydrophilic component and poly(alkyl acrylate-*co*-methacrylic acid) as the pH sensitive core. Depending on the polymer composition, these block copolymers formed micelles with the sizes from 120 nm to 350 nm at pH < 4.5, while releasing drugs as the pH increased up to 7.2.[130]

Also, Park et al. synthesized pH-responsive hydrogels using poly(vinyl alcohol) (PVA) as the networks backbone grafted with poly(acrylic acid) and poly(methacrylic acid). *In vitro* studies on insulin release showed that there was no visible release of insulin in simulated gastric fluid (pH 1.2), but controlled release of insulin was observed in simulated intestinal fluid (pH 6). Further studies on the oral delivery behavior in vivo in

a rat model confirmed that the effectively released insulin could control the level of glucose within 4 hrs.[131] A pulsatile pattern of drug release is required in disease states exhibiting a rhythmic pattern. Pulsatile systems for localized delivery of heparin and streptokinase, based on a poly(N-isopropylacrylamide-*co*-methacrylic acid) hydrogel, were assessed for their swelling behaviour in response to pulses in temperature and pH. The weight: swelling ratio was found to respond quickly for variations in temperature from 33°C to 36°C and in pH from 5.7 to 5.3.[132]

Electro-responsive drug delivery system

The studies on electro-responsive drug delivery are growing day by day due to their advantages over other stimuli. Some advantages of an electric field as an external stimulus are accessibility of equipment, which provides precise control with respect to the magnitude of the current, duration of electric pulses, interval between pulses etc. The mechanical response of polyelectrolyte hydrogels to an applied electric field can be used to control drug release from these gels. Drug may be incorporated into the hydrogels either during gel formation or after the gel has been formed by incubating the gel in a drug solution and allowing drug molecules to diffuse into the network. The effect of electrical stimulation on drug release depends to a large extent on the mechanisms by which the gel responds to the stimulus.[133-135] The principal mechanisms of drug release are forced convection of drug out of the gel along with syneresed water, diffusion and electrophoresis of charged drugs and liberation of drugs upon erosion of electro-erodible gels.

Forced convection of the drug is the most important mechanism of electrically modulated drug release, where the ejection of the drug occurs due to the deswelling of the hydrogel upon electric stimulation. Sawahata et al. showed that drug release only occurred once the applied electrical field was sufficiently high to cause dimensional changes in the gel. They have also shown a lag time of a few minutes between the application of the electric field and drug release from the gel has also been shown, implying that drug release only occurred when the gel deswelled.[136] Yuk et al. demonstrated the higher release rates of hydrocortisone from calcium alginate gels containing increasing amount of

poly(acrylic acid). Increasing PAAc content in the gel leads to increased number of carboxylic acid groups, which can be ionized in response to electrically-induced changes in local pH and which then affect the extent of gel deswelling and drug release. Also, the drug release is stopped when the electric field is switched 'OFF'. Thus, pulsatile drug release pattern can be obtained by switching the electric field 'ON' and 'OFF'.[137]

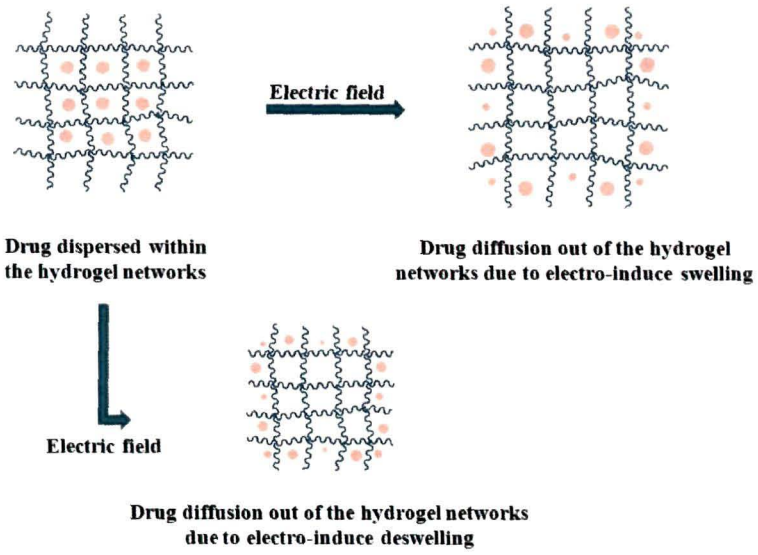

Fig 1.17 Schematic representation of drug release behavior from electro-responsive hydrogels due to electro-induced deswelling-swelling behavior.[138]

Apart from forced convection, drug diffusion out of the gel can also be an important mechanism of release and interesting release profiles have been obtained when diffusion becomes the major mechanism of drug release as shown in **Fig 1.17**. It has been established that electrically-induced drug release from electro-responsive hydrogels is significantly dependent on the experimental set-up. Contacting electrodes induced bulk gel deswelling while non-contacting electrodes only caused deswelling of the gel surface. Consequently, the electrically-induced drug release profiles differed while contacting or non-contacting electrodes were used.[139] As the gel deswelled and the size of the polymer network was reduced, the macromolecule's pathway out of the gel became more difficult and drug diffusion out of the gel was decreased. However, a pulsatile release of the guest molecule was still achieved, except that the drug was released when the electric current

was switched off (when diffusion of macromolecules out of the network could take place unhindered) and release was stopped or reduced when the electric field was switched on.

Therefore, it has been suggested that when electro-responsive release of macromolecules is desired, gels which swell in response to an electric field may be more suitable drug carriers. These type of gels swell in response to an electric field. These carriers allow the diffusion of drug out of the expanded gel network when they were electrically stimulated.[140] For example, Kim et al. developed MWCNT/PVA nanocomposite hydrogels for electro-responsive drug release depending on the electro-induced swelling behavior of the hydrogels. The cumulative amount of released drug and the release rate decreased as the content of MWCNTs increased at 0 V due to the lower swelling of hydrogels. On the other hand, both the cumulative amount of released drug and the release rate increased with the higher content of MWCNTs at 10 V as predicted from the swelling behavior of the nanocomposite hydrogel.[141]

Charged drugs may also be electro-released from hydrogels as the charged entities migrate towards the electrode bearing an opposite charge. Such an additional pathway of drug release has significant effects on the amount of drug that is electro-released. Upon electrical stimulation, the positively charged drugs were displaced from their interactions with the negative charges on the polymer network by H^+ ions generated from water electrolysis at the anode. Kwon et al. studied the release of the positively charged edrophonium ion from the anionic poly(AMPS-*co*-BMA) gel. They suggested that at higher voltages, the H^+ ions produced could migrate faster towards the cathode, resulting in a reduced chance for the H^+ to exchange with the polymer-bound edrophonium ion. Thus, though drug release increases with increasing electric field, it is not linearly proportional.[142] Gel erosion is another mechanism of drug release from gels which erode in response to an electric stimulus.[143] Kwon et al. demonstrated a pulsatile release profile of entrapped insulin from a poly(ethyloxazoline)-poly(methacrylic acid) gel complex which reflected the pulsatile electrical stimulation. Insulin was released in a stepwise manner until 70% of the load had been released. The large deviations in the release rate

were attributed to irregular erosion of the gels which was due to defects in the gel matrix.[140]

In this way, different stimuli-responsive drug delivery systems have undergone a revolutionary advancement in the past few years which further strengthened the link between therapeutic need and drug delivery. With the advent of novel delivery systems, various drug molecules have been revived of their therapeutic and commercial benefits. A lot of research is ongoing in different part of the world to explore stimuli-responsive hydrogels as drug delivery systems for better patient care. The more exploitation of these polymeric networks for improved therapeutic efficacy will open newer arenas in modern drug delivery systems.

1.8 Superabsorbent hydrogel (SAH)

Superabsorbent hydrogels (SAH) are structurally crosslinked hydrophilic polymers, which have the ability to absorb considerable amounts of water or aqueous fluids. These ultrahigh absorbing materials can imbibe deionized water as high as 1,000-100,000% (10-1000 g/g) whereas the absorption capacity of common hydrogels is not more than 100% (1 g/g).[144,145] Commercial production of SAH began in Japan in 1978 for use in feminine napkins. Further developments lead to SAH materials being employing in baby diapers in Germany and France in 1980. In 1983, low-fluff diapers (contained 4-5 g SAH) were marketed in Japan. This was followed shortly by the introduction of thinner superabsorbent diapers in other Asian countries, US and Europe. As a result, superabsorbent hydrogel caused a huge revolution in the personal health care industries in just over ten years.[146] The most commonly used monomers for synthesis of the first generation of SAHs are highly hydrophilic acrylamide, salts of acrylic acid and sulfopropyl acrylate. However, conventional superabsorbent hydrogels are mechanically very weak. Therefore, a composite agent is used in the preparation of superabsorbent hydrogel which serves as the local point of physical crosslinking (or entanglement) of the formed polymer chains during polymerization reaction. The presence of composite agent in SAH composites results in improved mechanical properties over conventional

superabsorbent hydrogels. These types of hydrogels are extensively used in drug delivery applications.

Recently, superabsorbent hydrogel with very high mechanical or elastic properties have been developed by adding a hybrid agent that can be crosslinked after SAH is formed. The hybrid agent is a water-soluble or water-dispersible polymer that can form crosslinked structure (in a manner similar to forming interpenetrating network) through chemical or physical crosslinking. Examples of hybrid agents are polysaccharides including sodium alginate, pectin, chitosan, cellulose, starch and natural gums (such as xanthan, guar and alginates) or synthetic water-soluble hydrophilic polymers such as poly(vinyl alcohol).[147] Superabsorbent hydrogels have tremendous applications in agricultural fields. They help in conservation of water and retain moisture by helping soil increase water holding capacity enabling the survival of plants during drought. They also claim to reduce leaching of fertilizers.

Superabsorbent hydrogels for use in soil to promote plant growth has been reviewed by Kazanskii et al.[103] Crosslinked poly(acrylamide-*co*-sodium acrylate) microgels as well as polyacrylamide, poly(acrylic acid), poly(vinyl alcohol) and potassium polyacrylate have been produced via electron beam irradiation.[148] The average plant height, leaf width, total dry weight and wilting time increased when these hydrogels were added to the soil.[149] The germination of seeds and the growth of young plants were also better with hydrogels based on starch grafted with acrylic acid and acrylamide.[150] In a study, the growth of rice is enhanced in soils containing superabsorbent hydrogels based on crosslinked carboxymethylcellulose and acrylamide.[151] Superabsorbent hydrogels have also been used to reduce the environmental problem of polyphenols and organic contents in olive mill wastewater. They help the wastewater to be immobilized, so that it can be used as plant fertilizer.[152] The superabsorbent hydrogels that have been used in agriculture is coined as 'Jalshakti' which have significant role in seed germination and plant growth in desert.

1.9 Research background and challenges (scope and objectives)

During the past two decades, hydrogels have emerged as a promising biomaterial due to their versatile applications in various fields. The existence of hydrogels dates back to 1960, when Wichterle and Lim first proposed the use of hydrophilic networks of poly(2-hydroxyethyl methacrylate) in contact lenses. Since then, the use of hydrogels has extended to various biomedical and pharmaceutical applications. In comparison to other synthetic biomaterials, hydrogels resemble living tissues closely in their physical properties because of their relatively high water content and soft and rubbery consistency. Hydrogels show minimal tendency to adsorb proteins from body fluids because of their low interfacial tension. The greater part of the work on hydrogels has centered on 'stimuli-responsive' or 'smart hydrogels', due to their ability to respond towards various environmental stimuli such as temperature, pH, ionic strength, magnetic or electric field etc. The stimuli can result in changes in phases, shapes, optics, mechanics, electric fields, surface energies, recognition, reaction rates and permeation rates. Stimuli-responsive hydrogels can perceive the prevailing stimuli and respond by exhibiting changes in their physical or chemical behaviour. Their responses towards different stimuli can be exploited for various applications such as tissue engineering, controlled drug delivery, actuator and sensors etc. Amongst various stimuli, pH and electric field seemed to be promising stimuli.

pH-responsive hydrogels possess a plenty of ionizable groups in the macromolecular networks. As the variation of environmental pH, these ionizable groups are ionized to cause differences of internal and external ionic strength and breakage of hydrogen bonds between the molecular segments. Therefore, pH-sensitive hydrogels have been most frequently used to develop controlled release formulations for oral administration. The pH in the stomach (~ 3) is quite different from the pH in the intestine and such a difference is large enough to elicit pH-dependent behavior of polyelectrolyte hydrogels.

Electro-responsive hydrogels can be synthesized in conjunction with conducting polymers (CP) or by the incorporation of different conducting fillers into the hydrogel

matrix. Conducting polymers such as polyaniline and polypyrrole are the frequently used conducting polymers in this application. Graphite, which is naturally abundant and low cost, has widely been used as electronically conducting filler in preparing conducting polymer composite hydrogels. But, in most of the cases relatively large quantities of graphite are required to reach a critical percolation value. Large amount of graphite concentration always lead to the poor mechanical property of the composite materials. To overcome this problem, the carbon nanotubes have been recently introduced for the preparation of electro-responsive hydrogels. These electric field-sensitive gels can be exploited to construct new types of soft actuators, sensors, micromachines, biomimetic energy-transducing devices and controlled delivery systems.

In the present thesis, efforts have been made to synthesize different types of pH-responsive and electro-responsive hydrogels with plausible applications in actuation and controlled drug delivery systems.

Objectives of the present investigation:

- To develop different stimuli-sensitive polymeric hydrogel, their composites and nanocomposites.
- To study the effect of various parameters such as crosslinking density, pH, electric field etc. on swelling behaviour of the hydrogels.
- To characterize the polymeric hydrogels using FTIR, XRD, SEM, DMA, UV-visible and TGA analysis.
- To evaluate the electrical properties and bending behaviour under the influence of an external electric field.
- Applications of these stimuli-responsive hydrogels for controlled drug delivery and electric-field assisted delivery of drugs.
- Determination of biocompatibility of the prepared hydrogels.

Plan of the work:

To fulfill the above objectives the following plans of work have been adopted:

- Synthesis of hydrogels from acrylic acid/acrylamide/poly(vinyl alcohol)/carboxymethylcellulose/gelatin with a suitable crosslinker.
- Synthesis of conducting hydrogel composites by in situ polymerization of aniline within hydrogel matrix.
- Preparation of composite and nanocomposite hydrogels by the incorporation of graphite, multiwalled carbon nanotubes and OMMT nanoclay into the respective hydrogel matrix.
- Evaluation of pH as well as electro-responsive of the hydrogels and their possible applications in controlled drug delivery and actuation.

References

1. Bunch, B. *The History of Science and Technology*, Houghton Mifflin, New York, 2004.
2. Lapcik, M. & Raab, M. *Materials Science II*, Tomas Bata University, Zlin, Czech Republic, 2004.
3. http://www.nobelprize.org/educational/chemistry/plastics/readmore.htm.(20/11/2014).
4. Maiti, S. *Polymer materials- Science, Technology, Development*, Anusandhan Prakashan, Kolkata, 2009.
5. McCreesh, N.C., et al. *J. Archaeol. Sci.* **38** (12), 3432-3434, 2011.
6. Tager, A. *Physical Chemistry of Polymers*, MIR publishers, Moscow, 1978.
7. Aharoni, S.M., & Edwards, S.F. *Macromolecules* **22** (8), 3356-3361, 1989.
8. Mujawar, N.K., et al. *Int. J. Pharm. Chem. Biol. Sci.* **4** (3), 758-773, 2014.
9. Silberberg, A. Network deformation in flow. in *Molecular Basis of Polymer Networks,* A. Baumgartner et al. eds., Spring-Verlag, 1989, 147-151.
10. Kim, S.M., & Kim, K.W. *J. Oral Maxillofac. Surg. Med. Pathol.* **38** (5), 479-504, 2009.
11. Yoldas, B.E. *J. Mater. Sci.* **10** (11), 1856-1860, 1975.
12. Vintiloiu, A., & Leroux, J.C. *J. Control. Release* **125** (3), 179-192, 2008.
13. de Loos, M., et al. *Eur. J. Org. Chem.* **2000** (22), 3675-3678, 2000.
14. Feringa, B.L., et al. *Chem. Eur. J.* **6** (14), 2633-2643, 2000.
15. Huang, Y.D., et al. *J. Mol. Struct.* **1031**, 43-48, 2013.
16. Skilling, J., et al. *Soft Matter* **10** (2), 237-256, 2014.

17. Peppas, N.A., et al. *Eur. J. Pharm. Biopharm.* **50** (1), 27-46, 2000.

18. Yang, S., et al. *Tissue Eng.* **7**, 679-689, 2001.

19. Drury, J.L., & Mooney, D.J. *Biomaterials* **24** (24), 4337-4351, 2003.

20. Das, A., et al. *J. Appl. Polym. Sci.* **107** (3), 1466-1470, 2008.

21. Teodorescu, M., et al. *Ind. Eng. Chem. Res.* **48** (14), 6527-65234, 2009.

22. Guilherme, M.R., et al. *J. Appl. Polym. Sci.* **117** (6), 3146-3154, 2010.

23. Kaşgöz, H., et al. *Polym. Adv. Technol.* **19** (3), 213-220, 2008.

24. Tang, Q.W., et al. *Sci. Technol. Adv. Mater.* **10**, 015002, 1-7, 2009.

25. Kandile, N.G., & Nasr, A.S. *Carbohyd. Polym.* **78** (4), 753-759, 2009.

26. Li, P., et al. *Compos. B: Eng.* **39** (5), 756-763, 2008.

27. Tang, Q.W., et al. *Eur. Polym. J.* **43** (6), 2214-2220, 2007.

28. Kangwansupamonkon, W., et al. *Polym. Degrad. Stabil.* **95** (9), 1894-902, 2010.

29. Sadeghi, M., et al. *J. Bioact. Compat. Polym.* **23** (4), 381-404, 2008.

30. Pourjavadi, A., et al. *Starch-Stärke* **61** (3-4), 161-72, 2009.

31. Cheung, H.Y., et al. *Compos. B: Eng.* **68** (1), 291-300, 2007.

32. www.sciencedaily.com/releases/2013/11/131105132027.html. (15/11/2014)

33. Wichterle, O., & Lim, D. *Nature* **185** (4706), 117-118, 1960.

34. Aharoni, S.M. *Synthesis, Characterization and Theory of Polymeric Network and Gels*, Plenum Press, New York, NY, 1992.

35. DeRossi, D., et al. *Polymer Gels: Fundamentals and Biomedical Applications*, Plenum Press, New York, NY, 1991.

36. Ottenbrite, R.M., et al. *Biomedical Applications of Hydrogels Handbook*, Springer Science + Business Media, LLC, 2010.

37. Higuchi, A., et al. *Polym. Bull.* **11** (2), 203-208, 1984.

38. Okay, O. General Properties of Hydrogels, in *Hydrogel Sensors and Actuators,* G. Gerlach et al. eds., Springer-Verlag, Berlin Heidelberg, 2009, 1-14.

39. Omidian, H. & Park, K. *Introduction to Hydrogels*, Springer, New York, UK, 2010.

40. Yu, C., et al. *Iran. Polym. J.* **19** (6), 417-425, 2010.

41. Okay, O. *Prog. Polym. Sci.* **25** (6), 711-779, 2000.

42. Adamson, A.W. *Physical chemistry of surfaces.* Wiley-Interscience, New York, 1967.

43. Hickey, A.S. & Peppas, N.A. *Polymer* **38** (24), 5931-5936, 1997.

44. Crank, J. *The Mathematics of Diffusion,* Oxford University Press, Oxford, 1975.

45. Aklonis, J.J. & MacKnight, W.J. *Introduction to Polymer Viscoelasticity.* Wiley-Interscience, New York, 1983.

46. Sperling, L.H. *Introduction to Physical Polymer Science.* Wiley, New York, 1986.

47. Greenberg, A.R., & Kusy, R.P. *J. Appl. Polym. Sci.* **25** (12), 2795-2805, 1980.

48. Lin, C.H., et al. *Colloid Surf. B* **70** (1), 87-95, 2009.

49. Hansen, M.B., et al. *Immunol. Methods* **119** (2), 203-210, 1989.

50. Lee, K.Y., & Mooney, D.J. *Chemical Reviews* **101** (7), 1869-1879, 2001.

51. Lee, C., et al. *Biomaterials* 7 (22), 3145-3154, 2001.

52. Ruel-Gariepy, E., et al. *J. Control. Release* **82** (2-3), 373-383, 2002.

53. Li, J., & Xu, Z. *J. Pharm. Sci.* **91** (7), 1669-1677, 2002.

54. Huh, K., & Bae, Y. *Polymer* **40** (22), 6147-6155, 1999.

55. Lowman, A.M., & Peppas, N.A. *Macromolecules* **30** (17), 4959-4965, 1997.

56. Brannon-Peppas, L. & Harland, R.S. Absorbent polymer technology, in *Studies in polymer science*, Elsevier, Amsterdam, 1990, 147-169.

57. Jen, A.C., et al. *Biotechnol. Bioeng.* **50** (4), 357-364, 1996.

58. Langer, R.S., & Peppas, N.A. *Biomaterials* **2** (4), 201-214, 1981.

59. D.L. Elbert, et al., *Proc. Int. Symp. Controlled Release Bioact. Mater.* **28,** 987-988, 2001.

60. Draye, J.P., et al. *Biomaterials* **19** (1-3), 99-107, 1998.

61. Schacht, E.H., *J. Phys.: Conf. Ser.* **3,** 22-28, 2004.

62. Peppas, N.A. & Mikos, A.G. *Preparation methods and structure of hydrogels*, CRC Press, Boca Raton, FL, 1986.

63. Hoffman, A.S. *Adv. Drug Del. Rev.* **54** (1), 3-12, 2002.

64. Pieróg et al. M., Effect of ionic crosslinking agents on swelling behaviour of chitosan hydrogel membranes, in *Progress on chemistry and application of chitin and its derivatives*, Lodz, Poland, 2009, 25-32.

65. Kishida, A. & Ikada, Y. Hydrogels for biomedical and pharmaceutical applications. in *Polymeric Biomaterials*, S. Dumitriu ed., Marcel Dekker, New York, 2002, 133-145.

66. Kashyap, N., et al. *Crit. Rev. Ther. Drug Carrier Syst.* **22** (2),107-150, 2005.

67. Hoffman, A.S. *Intelligent Polymers. Controlled Drug Delivery: Challenge and Strategies,* American Chemical Society, Washington, DC, 1997.

68. Bae, Y.H. *Stimuli-Sensitive Drug Delivery. Controlled Drug Delivery: Challenge and Strategies,* American Chemical Society, Washington, DC, 1997.

69. Tanaka, T. *Phy. Rev. Lett.* **40** (12), 820-823, 1978.

70. Tanaka, T. *Sci. Am.* **244** (1), 124-138, 1981.

71. Kost, J., & Langer, R. *Adv. Drug Deliv. Rev.* **46** (1-3), 125-148, 2001.

72. Balamuralidhara, V., et al. *Am. J. Drug Dis. Dev.* **1** (1), 24-48, 2011.

73. Prabhakar, S., et al. *Polym. Plast. Technol. Eng.* **51** (4), 1443-1450, 2012.

74. Qiu, Y., & Park, K. *Adv. Drug Deliv. Rev.* **53** (3), 321-339, 2001.

75. Jabbari, E., & Nozari, S. *Iran. Polym. J.* **8** (4), 264-270, 1999.

76. Buchholz, F.L. & Graham, A.T. The structure and properties of superabsorbent. in *Modern superabsorbent polymer technology.* Wiley-VCH, New York, 1998, 251-272.

77. Gil E.S., & Hudson, S.M. *Prog. Polym. Sci.* **29** (12), 1173-1222, 2004.

78. Irie, M. *Adv. Polym. Sci.* **110,** 49-65, 1993.

79. Yoshida, R., et al. *Adv. Drug Deliv. Rev.* **11** (1-2), 85-108, 1993.

80. Bromberg, L.E., & Ron, E.S. *Adv. Drug Deliv. Rev.* **31** (3), 197-221, 1998.

81. Schild, H.G. *Prog. Polym. Sci.* **17** (2), 163-249, 1992.

82. Katono, H., et al. *J. Control. Release* **16** (1-2), 215-227, 1991.

83. Murdan, S. *J. Control. Release* **92** (1-2), 1-17, 2003.

84. Masteikova, R., et al. *Medicina* **39** (2), 19-24, 2003.

85. Ramanathan, S., & Block, L.H. *J. Control. Release* **70** (1-2), 109-123, 2001.

86. Lensen, M., et al. *Eur. J. Pharm. Sci.* **15** (2), 139-148, 2002.

87. Metters, A.T., & Lin C. *Adv. Drug Deliv. Rev.* **58** (12), 1379-1408, 2006.

88. Bawa, P., et al. *Biomed. Mater.* **4** (2), 1-15, 2009.

89. Zhao, Y., & Stoddart, J. F. *Langmuir* **25** (15), 8442-8446, 2009.

90. Schmidt, A.M. *Colloid Polym. Sci.* **285** (9), 953-966, 2007.

91. Hu, S.H., et al. *Macromolecules* **40** (19), 6786-6788, 2007.

92. Reddy, N., et al. *Colloids Surf. A Physicochem. Eng. Asp.* **385** (1), 20-27, 2011.

93. Kim, J., et al. *Biomaterials* **33** (1), 218-222, 2012.

94. Meenach, A., et al. *Acta Biomater.* **6** (3), 1039-1046, 2010.

95. Shin, M.K., et al. *Langmuir* **24** (21), 12107-121011, 2008.

96. Beaune, G., & Menager, C. *J. Colloid Interface Sci.* **343** (1), 396-399, 2010.

97. Liang, Y.Y., et al. *Chem. Phys. Chem.* **8** (16), 2367-2372, 2007.

98. Yang, Z., et al. *J. Biomed. Mater. Res.* **62** (1), 14-21, 2002.

99. Lim, F. Microencapsulation of living cells and tissues-theory and practice. in *Biomedical applications of microencapsulation*, F. Lim, ed., CRC Press, Boca Raton, 1984, 138-153.

100. Kokabi, M., et al. *Eur. Polym. J.* **43** (3), 773-781, 2007.

101. Kim, S.J., et al. *Polym. Int.* **53** (10), 1456-1460, 2004.

102. Buenger, D., et al. *Prog. Polym. Sci.* **37** (12), 1678-1719, 2012.

103. Kazanskii, K.S., & Dubrovskii, S.A. *Adv. Polym. Sci.* **104,** 97-133, 1992.

104. Urry, D.W. *Angew. Chem. Int. Ed. Engl.* **32** (6), 819-841, 1993.

105. Smela, E., et al. *Adv. Mater.* **15** (6), 481-494, 2003.

106. Ding, J., et al. *Synth. Met.* **138** (3), 391–398, 2003.

107. Jager, E.W.H., et al. *Synth. Met.* **102** (1-3), 1309-1310, 1999.

108. Zhou, J.W.L., et al. *IEEE/ASME Trans. Mechatronics* **9** (2), 334-342, 2004.

109. Chiarelli, P., et al. *Biorheology* **29** (4), 383-398, 1992.

110. Shiga, T., et al. *J. Appl. Polym. Sci.* **44** (2), 249-253, 1992.

111. Kishi, R., et al. *Polymer Gels: Fundamentals and Biomedical Applications,* Plenum, New York, 1991.

112. Li, H., et al. *Biosens. Bioelectron.* **19** (9), 1097-1107, 2004.

113. Osada, Y., & Hasebe, M. *Chem. Lett.* **14** (9), 1285-1287, 1985.

114. Moschou, E.A., et al. *Chem. Mater.* **16** (12), 2499-2502, 2004.

115. Bassil, M., et al. *Sensor Actuat. B-Chem.* **134** (2), 496-501, 2008.

116. Glazer, P.J., et al. *RSC Adv.* **4** (4), 1890-1894, 2014.

117. Soppimath, K.S., et al. *Drug Dev. Ind. Pharm.* **28** (8), 957-74, 2002.

118. Ganta, S., et al. *J. Control. Release* **126** (3), 187-204, 2008.

119. Xu, P.S., et al. *Angew Chem. Int. Ed.* **46** (26), 4999-5002, 2007.

120. Lowman, A.M. & Peppas, N.A. Hydrogels. in *Encyclopedia of Controlled Drug Delivery,* E. Mathiowitz ed., John Wiley & Sons, 1999, 397-418.

121. Gehrke, S.H. & Lee, P.I. Hydrogels for drug delivery systems. in *Specialized Drug Delivery Systems*, Marcel Dekker, 1990, 64-67.

122. Patel, V.R., & Amiji, M.M. *Pharm. Res.* **13** (4), 588-593, 1996.

123. Kim, S.W. & Bae, Y.H. Stimuli-modulated delivery systems. in *Transport Processes in Pharmaceutical Systems*, Marcel Dekker, New York, 2000, 547-573.

124. Ghandehari, H., et al. *Biomaterials* **18** (12), 861-872, 1997.

125. Pitt, C.G., et al. *J. Control. Release* **2,** 363-374, 1985.

126. Dong, L.C. & Hoffman, A.S. Drug delivery from environmentally sensitive hydrogels, in *Topical Conference on Emerging Technologies in Materials*, San Francisco, CA, USA, 1989, 192-197,

127. Gliozzi, A., et al. *J. Mem. Biol.* **8** (2), 149-162, 1972.

128. Kopecek, J., et al. *J. Polym. Sci. A* **1** (9), 2801-2815, 1971.

129. Kirstein, D., et al. *Biotech. Bioeng.* **27** (9), 1382-1384, 1985.

130. Sant, V.P., et al. *J. Control. Release* **97** (2), 301-312, 2004.

131. Park, S.E., et al. *J. Appl. Polym. Sci.* **91** (1), 636-643, 2004.

132. Brazel, C.S., & Peppas, N.A. *J. Control. Release* **39** (1), 57-64, 1996.

133. Gehrke, S.H. *Adv. Polym. Sci.* **110,** 81-144, 1993.

134. Jensen, M., et al. *Eur. J. Pharm. Sci.* **15** (2), 139-148, 2002.

135. Yang, Y., & Engberts, J.B.F.N. *Coll. Surf. A: Physicochem. Eng. Aspects* **169** (1), 85-94, 2000.

136. Sawahata, K., et al. *J Control. Release* **14** (3), 253-262, 1990.

137. Yuk, S.H., et al. *Pharm. Res.* **9** (7), 955-957, 1992.

138. Vashist A., & Ahmad, S. *Biomass Bioenerg.* **29** (3), 861-870, 2013.

139. Kim, S.Y., & Lee, Y.M. *J. Appl. Polym. Sci.* **74** (7), 1752-1761, 1999.

140. Kown, L.C., et al. *Nature* **354** (6351), 291-293, 1991.

141. Kim, Y.Y., et al. *Carbon Lett.* **11** (30), 211-215, 2010.

142. Kwon, I.C., et al. *Polym. Sci. Part B: Polym. Phys.* **32** (6), 1085-1092, 1994.

143. Kwon, I.C., et al. *J. Control. Release* **30** (2), 155-159, 1994.

144. Chen, J., et al. *J. Biomed. Mater. Res.* **44** (1), 53- 62, 1999.

145. Askari, F., et al. *J. Appl. Polym. Sci.* **50** (10), 1851-1855, 1993.

146. Brannon-Peppas, L. & Harland, R.S. *Absorbent Polymer Technology,* Elsevier, Amsterdam, 1990.

147. Sannino, A., et al. *J. Biomed. Mater. Res.* **67A** (3), 1016-1024, 2003.

148. Abd El-Rehim, H.A. *Radiat. Phy. Chem.* **74** (2), 111-117, 2005.

149. Abd El-Rehim, H.A., et al. *J. Appl. Polym. Sci.* **93** (3), 1360-1371, 2004.

150. Chen, P., et al. *J. Appl. Polym. Sci.* **93** (4), 1748-1755, 2004.

151. Ibrahim, S.M., et al. *J. Appl. Polym. Sci.* **104** (3), 2003-2008, 2007.

152. Davies, L.C., et al. *Environ. Technol.* **25** (1), 89-100, 2004.

CHAPTER 2

Synthesis of composite hydrogels based on poly(acrylamide-co-acrylic acid)/polyaniline and poly(acrylamide-co-acrylic acid)/graphite and study of their pH, electro-responsive behaviour and biocompatibility.

GRAPHICAL ABSTRACT

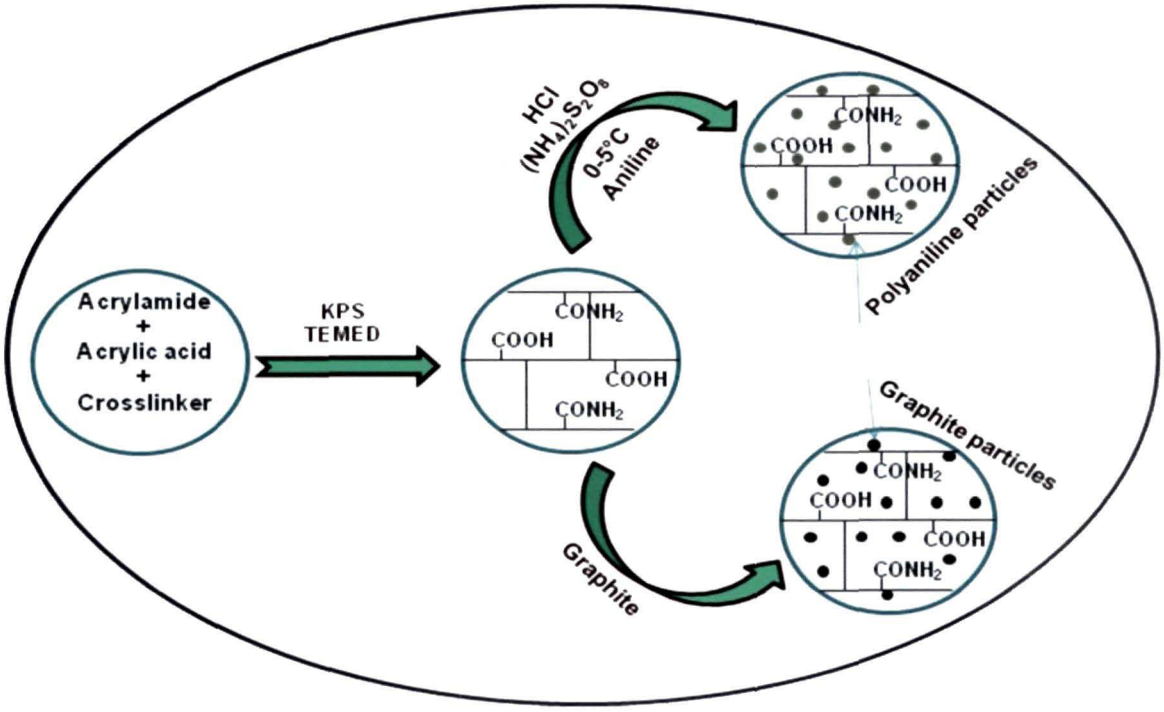

2.1 Introduction

Hydrogels are crosslinked polymer network that can absorb water many times of their original volume. For this excellent water-holding property, hydrogel polymers were introduced into the agriculture, food, cosmetics, diaper and pharmaceutical industries.[1,2] The volume phase transition of certain hydrogels is one of the most fascinating and important phenomena in the polymeric networks. Stimuli-responsive hydrogels, which are also called 'smart polymers' show drastic changes in their volume and shape reversibly due to changes in environmental stimuli such as external pH, temperature, ionic strength, nature and composition of the swelling agent, enzymatic or chemical reaction and electrical or magnetic stimuli[3] etc. The change in the degree of swelling may occur discontinuously at a specific value of stimulus or gradually over a (mostly small) range of stimulus values. An interesting characteristic of responsive gels is their reversible change of network structure.

pH-responsive hydrogels respond to changes in pH of the external environment. They bear readily ionizable side groups attached to impart peculiar characteristics and either accept or release protons in response to changes in environmental pH.[4] Electro-conductive hydrogel describes a polymer that combines the properties of hydrogels as well as that of the conductive system. Under the influence of an electric field, electro-responsive hydrogels generally deswell or bend, depending on the shape of the gel and its position relative to the electrodes.

A part of this chapter is published

M. Boruah, A. Kalita, B. Pokhrel, R. Boruah and S.K. Dolui. *Adv. Polym. Technol.* **32,** E520–E530, 2013

M. Boruah, P. Phukon, B. Saikia and S.K. Dolui. *Polym. Compos.* **35,** 27–36, 2014.

In recent years, intelligent electro-responsive hydrogels are getting special interests because of their exceptional promise in biomedical applications such as sensors, actuators, chemical separation and drug delivery systems[5-9] etc. The ability to directly convert chemical energy into mechanical work makes smart gels suitable for actuator and other devices.[10-15] Electrically-responsive hydrogels are prepared generally from polyelectrolytes which contain relatively high concentrations of ionizable groups along the polymer backbone and are thus pH-responsive, as well as electro-responsive.[16] When the hydrogel is negatively charged, it swells near the anode and contracts near the cathode, the contraction rate being proportional to the external current. So, a gel bar made of polyelectrolyte materials can bend backward and forward by the application of an electric field.[17] The electrical properties of an electro-responsive hydrogel can be significantly improved by the incorporation of different conducting polymers or conducting fillers to the hydrogel matrix. Polyaniline, polypyrrole, thiophene etc. are being used in the preparation of conducting hydrogels.[18-20] Now-a-days, different carbon based conducting fillers like graphite,[21] carbon fibers,[22] carbon black,[23] carbon nanotubes[24] and graphene[25] etc. are also getting considerable importance in the preparation of electro-responsive hydrogels.

Considerable attempts have been made to mimic the efficient conversion of chemical energy into mechanical energy in living organisms. Electro-responsive hydrogels are capable of performing work by converting an external stimulation into mechanical motion can be an effective framework for soft actuators. Therefore, these systems can serve as actuators or artificial muscles in many applications. They are the most extensively studied polyelectrolyte hydrogels for actuator application, as in this case the mechanical energy was triggered by an electric signal. Also, they can reversely bend under the application of an electric field.[26,27]

Several successful attempts have been made by scientists worldwide to prepare electro-responsive hydrogels. Bajpai et al. prepared electrically conducting composite materials consisting of polyaniline (PANI) nanoparticles dispersed in a poly(vinyl alcohol) (PVA)-*g*-poly(acrylic acid) (PAAc) hydrogel medium. They measured the electrical conductivities of the prepared hydrogel and also investigated the electro active

behavior of composite hydrogels swollen in electrolyte solution using effective bending angle (EBA) measurements.[28] Dai et al. made a high quality composite hydrogel of polyacrylamide/polyaniline by interfacial polymerization. They reported that interfacial polymerization is much more economical and effective than conventional methods because the polyaniline (PANI) formed at the water/organic-solvent interface assembles spontaneously and exclusively into the PAAm hydrogel. The resulting composite hydrogels exhibited interesting properties ranging from homogeneous structure, enhanced mechanical strength, high electrical conductivity and reversible interconversion between the doped and undoped states.[20]

Moreover, efforts have also been made for the development of carbon conducting fillers based hydrogels. For example, Fan et al. successfully synthesized the interpenetrating network hydrogel of polyacrylamide/poly(vinyl alcohol)/polyacrylamide/graphite by simple two-step synthesis process and carried out the study of their swelling, conducting and mechanical properties. They found that the conductivity and swelling ratio of the hydrogel depends on the PVA, graphite and crosslinker dosages. Moreover, the prepared hydrogels were found to possess good mechanical strength and thermal stability.[29] Electrically conducting hydrogel based on polyacrylamide and graphite was synthesized by Tang et al. The influence of crosslinker, initiator, monomer, graphite, water absorbency and temperature on the conductivity of the hydrogel was investigated and an adsorbed network structure model for conducting hydrogel was proposed.[30] Lin et al. synthesized conducting composite hydrogels based on polyacrylate and graphite. The influence of crosslinker, initiator, monomer, neutralization degree, graphite, water absorbency and temperature on the electrical conductivity of the hydrogel was investigated. The conducting composite hydrogel was found to possess good electrical conductivity and colloid stability. They concluded that the conductive hydrogel can be potentially used in the field of conductive materials and biomaterials.[31]

In this chapter, we describe the synthesis of two sets of conducting composite hydrogels. In the first set, we performed the synthesis of conducting composite hydrogels of on poly (AAm-*co*-AAc) and polyaniline (PANI) using aqueous polymerization

technique. Impregnation of polyaniline was carried out by interfacial polymerization of aniline at water/organic-solvent interface. The percentage impregnation of PANI into the hydrogel was calculated and effect of crosslinker amount, polyaniline (PANI) content and pH of the media, on swelling behaviour of the composite hydrogels were determined. Variation of conductivity with crosslinker amount and temperature was also studied. In the second set, we carried out the synthesis of composite hydrogel based on poly (AAm-*co*-AAc)/ graphite following the same synthetic route. The influence of crosslinker, graphite content and temperature on the conductivity of the hydrogel was investigated. Also, biocompatibility of the composite hydrogels was determined by hemolytic potentiality test.

2.2 Experimental

2.2.1 Materials

Acrylic acid (AAc) was purchased from Merck Limited (Mumbai, India) and purified by vacuum distillation at 55°C. Acrylamide (AAm), N,N,N′,N′-tetramethylethylenediamine (TEMED), aniline and graphite powder were purchased from Aldrich and were used as received. Potassium persulphate (KPS) and ammonium persulphate (APS), as an initiator, supplied by Merck and was recrystallized before use. Di-sodium phosphate (Na_2HPO_4) and potassium hydrogen phosphate (K_2HPO_4) were purchased from Merck. Other chemicals such as hydrochloric acid, ethylene glycol dimethylacrylate (EGDMA) were also of analytical grade and used without any further purification.

2.3 Synthesis of poly(AAm-*co*-AAc)/PANI composite hydrogel

2.3.1 Fabrication of poly(AAm-*co*-AAc) hydrogel

The composite hydrogel was fabricated by following a two-step procedure. The polymer matrix composed of poly(AAm-*co*-AAc) was prepared by using ethylene glycol dimethacrylate (EGDMA) as crosslinker and KPS/TEMED as a free radical-generating system. In a typical experiment, a mixed solution of acrylamide (AAm, 7 mol%) and

acrylic acid (AAc, 5 mol%) monomer and crosslinker ethylene glycol dimethacrylate (0.03 mol%-0.15 mol%) was mixed well with 15 ml of double distilled water with vigorous stirring. Subsequently, redox initiator potassium persulfate (KPS, 0.18 mol%) and tetramethylethylenediamine (TEMED, 0.05 mol%) were added to the mixture and mixed well. The homogenized mixture was kept in a petridish for 24 hrs. On completion of the reaction, the entire mass got converted into a semi-transparent film which was then purified by equilibrating the film in double distilled water for a week. The swollen gel was dried at room temperature, cut into rectangular pieces and stored in airtight plastic bags. Recipe for the preparation of poly(AAm-*co*-AAc) copolymer hydrogel are shown in **Table 2.1**.

Table 2.1 Recipe for the preparation of poly(AAm-*co*-AAc) copolymer hydrogel with variation of crosslinker (EGDMA) content:

Sample	S(1)	S(2)	S(3)	S(4)	S(5)
Acrylamide (mol%)	7	7	7	7	7
Acrylic acid (mol%)	5	5	5	5	5
Ethylene glycol dimethacrylate	0.03	0.05	0.07	0.10	0.15

Potassium persulfate = 0.18 mol% and tetraethylmethylendiammine = 0.05 mol%.

2.3.2 Impregnation of polyaniline (PANI) into the hydrogel matrix

The impregnation of polyaniline (PANI) into the hydrogel matrix was carried out through interfacial polymerization technique. The prepared hydrogel was dipped into an aqueous solution of 0.25 M ammonium peroxysulfate (APS) and 1 M HCl for 24 hrs. After that the aqueous solution was removed from the solution and the hydrogel was again immersed in a hexane solution containing 0.2 M aniline for 2 hrs. The temperature was maintained at 0-50°C.[32] Aniline was absorbed into the hydrogel matrix leading to contact with oxidative medium resulting into polyaniline after polymerization. Samples of the conducting composite hydrogel of poly(AAm-*co*-AAc)/PANI were dipped in a large amount of 1 M HCl aqueous solution for 1 week to wash out low molecular weight

components of the system as well as the remaining APS and PANI oligomers. Preparation of poly(AAm-*co*-AAc)/PANI composite hydrogel is schematically shown in **Fig 2.1.**

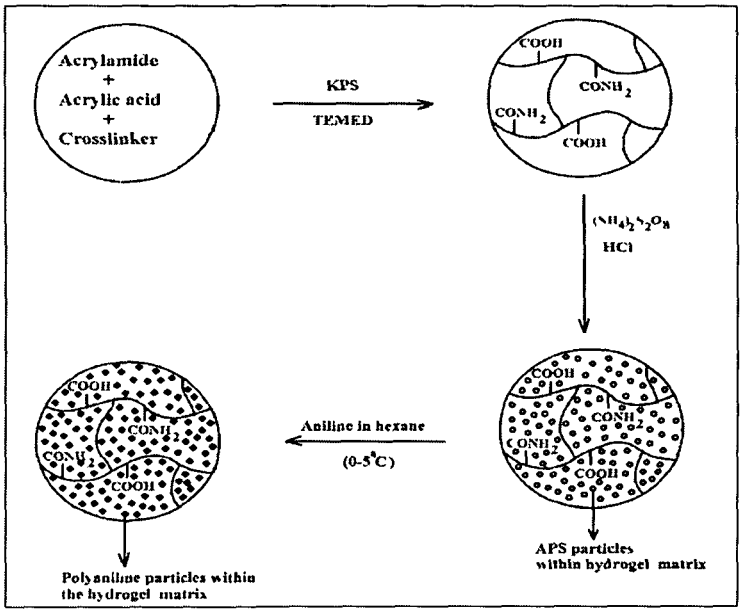

Fig 2.1 Schematic representation of preparation of poly(AAm-co-AAc)/PANI composite hydrogel.

The percentage impregnation of PANI into the gel was calculated by the following equation:

$$\% \, PANI \, impregnation = W_{PANI} - W_{DRY} / W_{DRY} \times 100 \qquad \textbf{(Eqn. 2.1)}$$

where, 'W_{PANI}' is weight of the dry PANI impregnated gel and 'W_{dry}' is the initial weight of polymer gel.

2.4 Fabrication of poly(AAm-*co*-AAc)/graphite composite hydrogel

A polymer matrix composed of poly(acrylamide-*co*-acrylic acid)/graphite was prepared by dissolving a predetermined amounts of acrylamide (AAm) , acrylic acid (AAc) monomer in distilled water. Subsequently, graphite micropowder was dispersed in the above solution thoroughly to form a mixed solution. A given amount of crosslinker ethylene glycol dimethacrylate (EGDMA) was dissolved in the monomer/graphite mixed solution and the whole mixture was ultrasonicated for 30 min. The redox initiator system

potassium persulfate (KPS) and N, N, N′, N′-tetraethylmethylendiammine (TEMED) were added to the mixture under stirring condition. The homogenized mixture was kept in a petridish for 24 hrs. On completion of the reaction, the entire mass got converted into a dark black film which was then purified by equilibrating the film in double distilled water for a week. The swollen gel was dried at room temperature, cut into rectangular pieces and stored in airtight plastic bags.

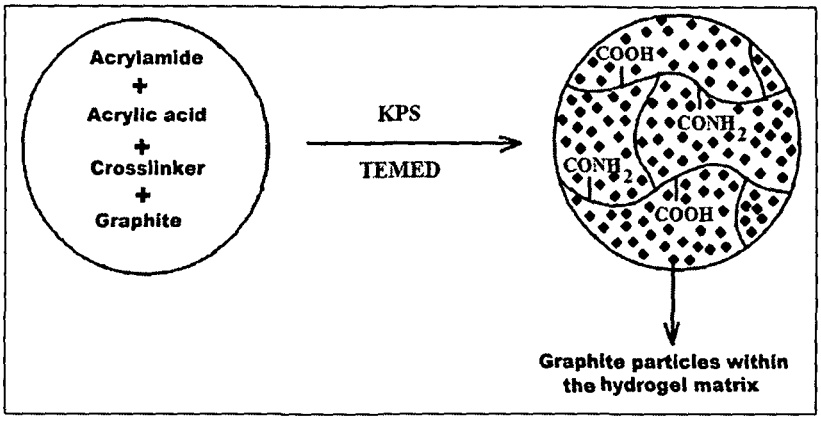

Fig 2.2 Schematic representation for the preparation of poly(AAm-*co*-AAc)/graphite composite hydrogel.

Table 2.2 Recipe for the preparation of poly(AAm-*co*-AAc)/graphite composite hydrogels with variation of graphite content:

Sample	G(1)	G(2)	G(3)	G(4)	G(5)	G(6)
Acrylamide (mol%)	7	7	7	7	7	7
Acrylic acid (mol%)	5	5	5	5	5	5
Graphite (wt %)	3	5	7	9	11	13

Potassium persulfate = 0.18 mol%, ethylene glycol dimethacrylate = 0.07 mol% and tetraethylmethylendiammine = 0.05 mol%.

Preparation of poly(AAm-*co*-AAc)/graphite composite hydrogel is schematically shown in **Fig 2.2** and the compositions of the prepared composite hydrogels are shown in **Table 2.2.**

2.5 Characterization

2.5.1 Fourier transform infrared spectrometer (FTIR)

FTIR is a useful method for the characterization of monomer and polymers. It is primarily used for the detection of functional groups, but analysis of spectra in the lower frequency finger print region can give evidence of degree of polymerization and the effect of substituents on the electronic properties of the polymer backbone.

Spectra were recorded from pressed KBr pellets using a Nicolet, Impact 410 FT-IR spectrometer in the range of 4000-400 cm^{-1} at room temperature.

2.5.2 Powder X-ray diffractometer (XRD)

Powder X-Ray diffraction (XRD) data were collected on a Rigaku Miniflex X-ray diffractometer (Tokyo, Japan) with Cu Kα radiation (λ=0.15418 Å) at 30 kV and 15 mA with a scanning rate of $0.05^{\circ}s^{-1}$ in a 2θ ranges from 20° to 80°.
From the 2θ value for the reflections, d values were calculated using Bragg's equation.

$$n\lambda = 2d\sin\theta \qquad \textbf{(Eqn. 2.2)}$$

where, 'n' is an integer, 'λ' is the X-ray wavelength, 'd' is the distance between crystal lattice planes and 'θ' is the diffraction angle.

2.5.3 Scanning Electron Microscope (SEM)

The scanning electron microscope (SEM) is a type of electron microscope that images the sample surface by scanning it with a high energy beam of electrons in a raster scan pattern. The electrons interact with the atoms that make up the sample producing signals that contain information about the sample's surface topography, composition and other properties such as electrical conductivity.

SEM studies were performed to investigate the surface morphology or microstructure of the samples. JSM-6390LV, JEOL, Japan was used for analysis. The surface of the sample was coated with platinum before SEM analysis.

2.5.4 Tensile strength

A universal testing machine (Zwick 10KN) was used to measure the tensile strength of poly(AAm-*co*-AAc)/PANI and poly(AAm-*co*-AAc)/graphite composite hydrogels, with an extension rate of 10 mm/min at room temperature in wet condition. For measurement, the samples were immersed in water until equilibrium was established.

2.5.5 Evaluation of optical and electrical properties

2.5.5.1 UV-visible spectroscopy

The UV-visible absorption spectra of polyaniline (PANI) powder and poly(AAm-*co*-AAc)/PANI composite hydrogel, in 1-methyl-2-pyrrolidone solvent were recorded in the range 300-800 nm with a UV-visible spectrophotometer (Shimadzu UV-2550).

2.5.5.2 DC electrical conductivity

The electrical conductivities of both sets of composite hydrogels were measured using four probe technique in the temperature range $300K \leq T \leq 413K$. The electrical conductivity of the prepared hydrogels were calculated using the following relation-

$$\rho = (V/I)\, 2\pi S \qquad \textbf{(Eqn. 2.3)}$$

where, 'ρ' is the resistivity of the sample, 'V' is the applied voltage, 'I' is the measured current through the sample and 'S' is the distance between probes. Current-voltage (I-V) characteristics of prepared samples were recorded with a Keithley 2400 source meter at room temperature within the frequency range 102–106 Hz.

2.5.6 Swelling behaviour

To measure the degree of swelling the hydrogels, dried samples were placed in buffer media of different pH values at room temperature until the hydrated gels reached a stable weight. The water absorbed on the surface of the hydrogels was removed using filter paper and the weight noted. The swelling percentages of the composite hydrogels were calculated by using following equation:

$$Swelling\ \% = W_s - W_{dry}/W_{dry} \times 100 \qquad \textbf{(Eqn. 2.4)}$$

where, 'W_s' is the weight of the hydrogels in swollen state and 'W_{dry}' is that of the hydrogels in dry state.

2.5.7 Bending-Angle Measurement

The composite hydrogels were swollen in different concentrations of aqueous NaCl solution at room temperature and cut into rectangular pieces. Then the bending angle of the gels under applied electric fields was measured using a self developed device as shown in **Fig 2.3.** To demonstrate the bending behaviour of the hydrogels, the two carbon electrodes were placed in parallel 30 mm apart. One end of the sample column was fixed and placed vertically between two carbon electrodes in aqueous NaCl solution and the bending behavior was investigated under an applied electric field.

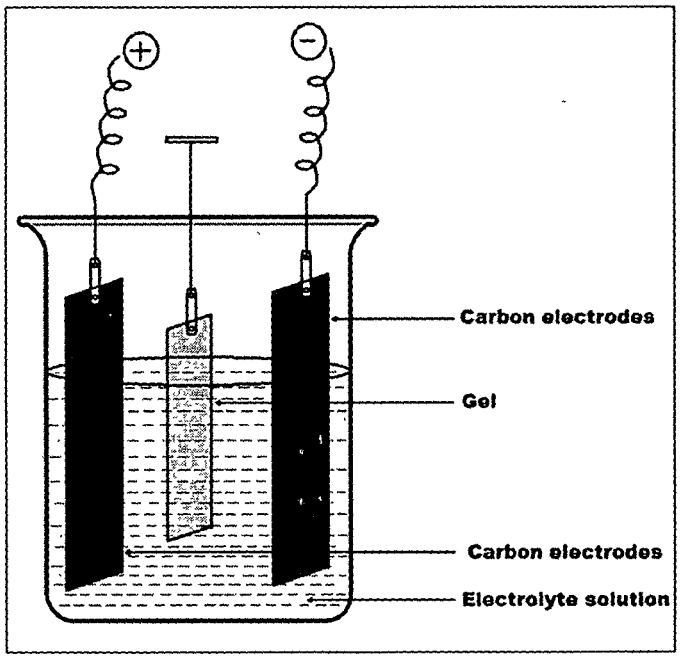

Fig 2.3 Apparatus for measuring bending angle.

2.5.8 Biocompatibility by Hemolytic Potentiality Test

The biocompatibility of the hydrogel is very important for their tissue engineering as well as other biomedical applications. The hemolysis activity tests were performed against some hydrogel samples by following the procedure of Miki et al. with slight

modifications.[33] Blood was collected from a goat intestine using $1/10^{th}$ volume of 3.8% sodium citrate out of the total blood volume. Blood was then centrifuged in a 50 ml centrifuge tube at 3000 rpm for 5 min. The supernatant containing platelet-poor plasma was discarded and the pellet containing RBC was re-suspended in 10 volumes of phosphate buffer saline (PBS) of pH 7.4. The process was repeated two to three times to completely remove the buffy coat of RBC. Finally the cells were suspended in PBS to get a uniform suspension of cells.

Testing samples having uniform thickness (10 mm) were placed in polypropylene test tubes. Prior to this, the surfaces of all the films were sterilized under UV light for 20 min under a sterile laminar air flow hood. After that 2 ml of erythrocyte suspension was added to 10 mg of each type of treated film samples. Each tube was gently inverted and gentle shaking was done to maintain contact of the blood with the material and incubated at 37°C for 90 min. Positive and negative controls were prepared by adding the same amount of erythrocyte suspension to Triton X-100 (Sigma-Aldrich, USA) and PBS (pH 7.4) respectively. After incubation, the samples were centrifuged at 3000 rpm for 5 min to pellet out RBC cells. The supernatants were carefully separated out and used for absorption studies at 540 nm using a UV– visible spectrophotometer against a PBS blank solution. The percentage of hemolytic index (%) was calculated using the following formula:

$$Hemolysis\ (\%) = (A_s - A_c^-) / (A_c^+ - A_c^-) \times 100 \qquad \textbf{(Eqn. 2.5)}$$

where, 'A_s' is the absorbance of the test sample. The absorbance of positive (A_c^+) and negative controls (A_c^-) were found to be 1.30 and 0.007, respectively.

2.6 Results and discussion

2.6.1 poly(acrylamide-*co*-acrylic acid)/PANI composite hydrogel

2.6.1.1 FTIR analysis

Fig 2.4 shows the FTIR spectra of polyaniline (PANI) and poly(AAm-*co*-AAc)/PANI composite hydrogel. The FTIR spectra of PANI exhibited absorption peaks at

3429, 2924, 1630, 1437 and 812 cm^{-1}, due to N-H stretching of secondary amine, stretching of the C-H bonds in phenyl rings, aromatic C=C stretching and N-H bending vibrations respectively **(Fig 2.4a)**.

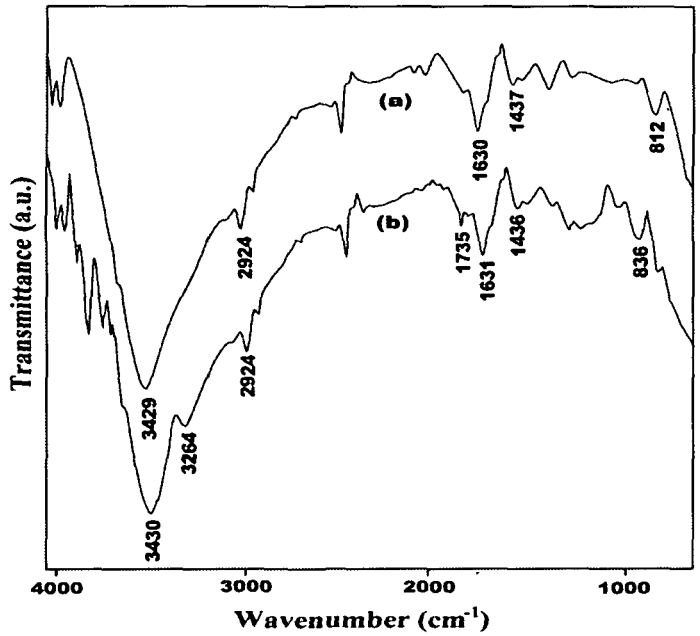

Fig 2.4 FTIR spectra of (a) polyaniline (PANI) and (b) poly(AAm-co-AAc)/PANI composite hydrogel.

The characteristic peaks in the composite hydrogel are shown in the **Fig 2.4b**. Here peak at 3430 cm^{-1} is due to N-H stretching of secondary amine, the one at 3264 cm^{-1} is due to N-H stretching of primary amide group, the one at 2924 cm^{-1} indicates stretching of the C-H bonds in phenyl rings, the one at 1735 cm^{-1} is due to C=O stretching of carboxylic acid group of PAAc and 1631 cm^{-1} is for stretching of C=O of PAAm. Peak at 1436 cm^{-1} is due to aromatic C=C stretching and the peak at 836 cm^{-1} is due to N-H bending vibrations. From the characteristic peaks, the impregnation of polyaniline into the polymer matrix can be confirmed.

2.6.1.2 UV-visible spectral analysis

The UV-visible analysis was carried out in the range 300 to 800 nm **(Fig 2.5)**. The spectra showed two distinct absorption bands at 356 and 630 nm for pure polyaniline

(PANI) powder. In case of PANI impregnated hydrogel, two characteristic peaks were observed at 345 and at 636 nm which indicates the impregnation of polyaniline (PANI) into the gel. This confirms the impregnation of PANI into the gel because the emeraldine form of PANI has two characteristic peaks at 334 and 632 nm originating from π–π^* transition of benzenoid rings and the exciton absorption of the quinoid rings, respectively.

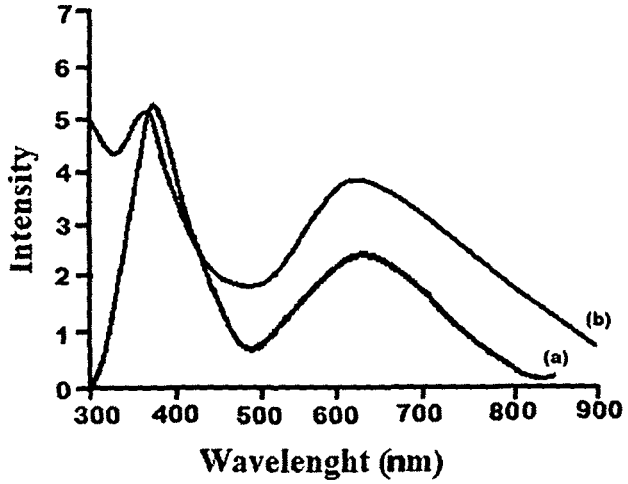

Fig 2.5 UV-visible spectra of (a) polyaniline (PANI) and (b) poly(AAm-co-AAc)/PANI composite hydrogel.

2.6.1.3 XRD analysis

The XRD patterns of the prepared copolymer hydrogel, poly(AAm-*co*-AAc)/PANI composite hydrogel and polyaniline (PANI) powders are shown in **Fig 2.6**. XRD pattern of pure polyaniline (PANI) shows a broad peak at about 25.8°, which is a characteristic peak of amorphous polyaniline **(Fig 2.6c)**. The prominent peak at 25° is present in case of PANI impregnated hydrogel **(Fig 2.6b)**, which is not present in the native gel **(Fig 2.6a)**. Thus, the XRD-patterns of poly(AAm-*co*-AAc)/PANI composite hydrogel confirms the impregnation of polyaniline (PANI) within the polymer matrix.

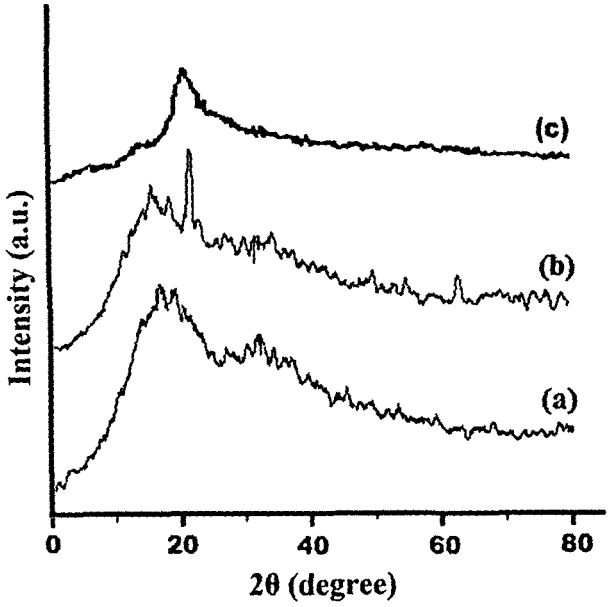

Fig 2.6 XRD spectra of (a) poly(AAm-*co*-AAc) copolymer hydrogel, (b) poly(AAm-*co*-AAc)/PANI composite hydrogel and (c) polyaniline (PANI).

2.6.1.4 Scanning Electron Microscopy (SEM)

From the SEM images of poly(AAm-*co*-AAc) copolymer hydrogel and poly(AAm-*co*-AAc)/PANI composite hydrogel it has been found that the copolymer hydrogel possesses comparatively a smooth surface (**Fig 2.7a**), but heterogeneity develops in the matrix on impregnation of polyaniline (PANI) into the polymer matrix. From **Fig 2.7b,** it is confirmed that polyaniline (PANI) molecules form clusters within the matrix. The polyaniline (PANI) molecules are hydrophobic in nature whereas the polymer matrix is hydrophilic. The formation of polyaniline (PANI) clusters is probably due to their hydrophobic dispersion forces.

The SEM micrograph of the cross-section of the composite hydrogel is shown in **Fig 2.7c**. It also shows the same heterogeneity as that of the surface of poly(AAm-*co*-AAc)/PANI composite hydrogel, which confirms the presence of PANI molecules within the whole matrix. Although, aniline molecules are hydrophobic in nature, they form aniline hydrochloride salt as they come contact with hydrochloric acid. This salt has good solubility in water and absorbed into the hydrogel matrix during swelling of the gel in

water. There, it gets polymerized when comes in contact with ammonium persulphate initiator. So, the polyaniline (PANI) molecules are dispersed within the whole matrix.

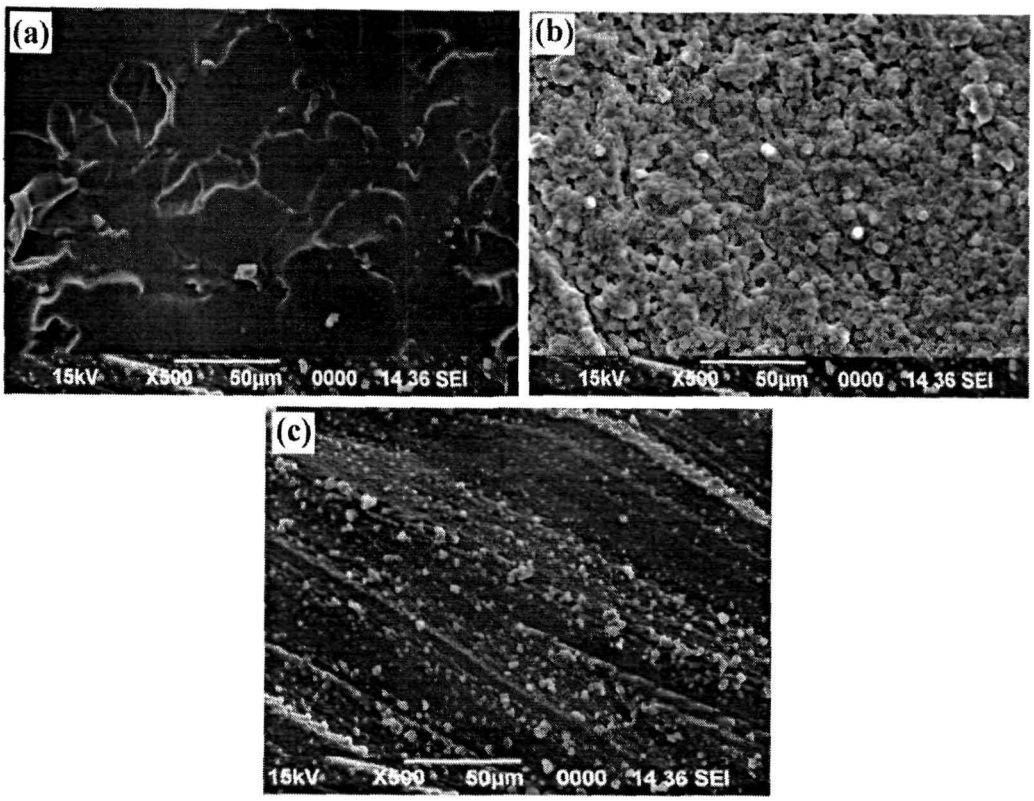

Fig 2.7 SEM micrographs of (a) poly(AAm-*co*-AAc) copolymer hydrogel, (b) poly(AAm-*co*-AAc)/PANI composite hydrogel and (c) cross-section of poly(AAm-*co*-AAc)/PANI composite hydrogel.

2.6.1.5 Tensile strength

Fig 2.8 is a representative tensile strength plot of the conductive composite hydrogels. It has been found that the mechanical strength gradually increases from 0.125 to 0.212 MPa with increase in the crosslinker (EGDMA) amount from 0.03 mol% to 0.15 mol% respectively. This may be due to the perfection affected in the 3D network structure with introduction of increasing amounts of crosslinker. Thus, it is reasonable to suggest that amount of permanent crosslinking between the polymer chains plays a significant role in enhancing the tensile strengths of the composite hydrogel.

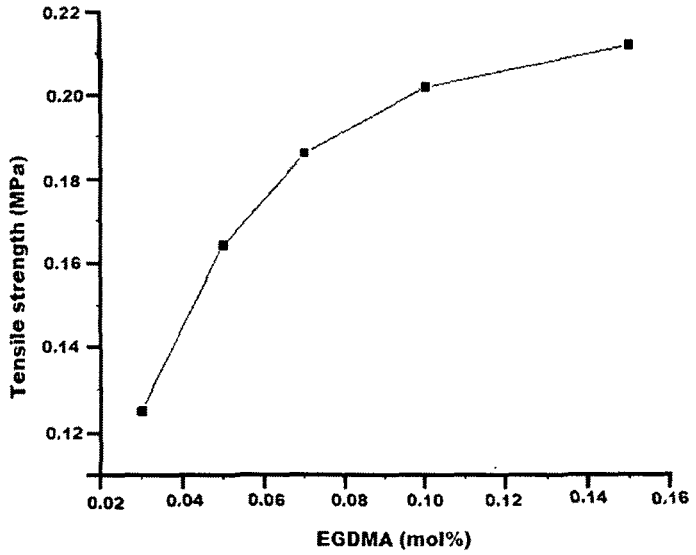

Fig 2.8 Tensile strengths of the hydrogels with the variation of crosslinker content.

The open spaces between polymer networks decreased with high crosslinking density thereby improving the strength. The composite hydrogels possess good tensile strengths as shown in the **Table 2.4.**

2.6.1.6 DC electrical conductivity

2.6.1.6.1 Effect of crosslinker amount on conductivity

The conductivity tends to increase initially from 4.2×10^{-3} Scm^{-1} to 5.6×10^{-3} Scm^{-1} with increase in crosslinker (EGDMA) amount and again decreases to 4.8×10^{-3} Scm^{-1} when amount of crosslinker is highest. Our interpretation of the results is as follows: initial increase in amount of crosslinker facilitates the formation of a proper network structure which in turn enhances the hydrophilicity of the matrix and attracts a large number of aniline hydrochloride molecules to diffuse into the gel which upon subsequent polymerization leads to greater amount of polyaniline (PANI) within the polymer matrix. So the conductivity increases with increasing amount of crosslinking agent. The observation that the conductivity decreases beyond an optimum level of crosslinker amount shows that beyond the optimal level of crosslinker, the network becomes compact

restraining the mobility of both incoming aniline molecules as well as the relaxation of polymer matrix chain. Conductivity values are reported in the **Table 2.3**.

Table 2.3 Variation of % PANI impregnation, conductivity and tensile strengths of the prepared composite hydrogels with different crosslinker (EGDMA) content:

Sample	EGDMA (mol%)	%PANI impregnation	Conductivity (x 10^{-3}Scm^{-1})	Tensile strength (MPa)
S(1)	0.03	12.33	4.23	0.125
S(2)	0.05	18.71	4.75	0.164
S(3)	0.07	26.28	5.12	0.186
S(4)	0.10	42.50	5.63	0.202
S(5)	0.15	31.83	4.81	0.212

2.6.1.6.2 Effect of temperature on conductivity

The dependence of temperature on the conductivity of hydrogel shows that the conductivity of hydrogel rises with the increase of temperature. But conductivity value was found to be low. So, the observed conductivity may be due to the ionic movement. The conductivity increases with the increase in temperature due to the increasing ionic movement of the ions. The conductivity-temperature behavior of the conductive hydrogel can be described by Arrhenius equation:

$$\sigma(T) = A \exp [-E_a / RT] \qquad \textbf{(Eqn. 2.6)}$$

where, 'E_a' is the activation energy, 'R' is the molar gas constant, 'A' is a constant, and 'T' is absolute temperature. According to the experimental data, the E_a is calculated as 6.01 kJ.mol^{-1} and the value of A is 29.22. The Arrhenius behavior of conductivity for the hydrogels suggested that the conduction was due to charge carriers (protons) hopping along the polyaniline chain. The conductivity data are shown in **Table 2.4**.

Table 2.4 Conductivity of poly(AAm-*co*-AAc)/PANI composite hydrogel at various temperatures.

Temperature	Conductivity (x 10^{-3} Scm^{-1})				
(°C)	S (1)	S (2)	S (3)	S (4)	S (5)
27	4.37	4.85	5.18	5.78	4.92
40	4.43	4.93	5.24	5.80	5.03
50	4.56	5.17	5.39	5.87	5.17
60	4.91	5.22	5.42	5.91	5.26
70	5.19	5.28	5.48	6.02	5.33

2.6.1.7 Swelling behavior

Fig 2.9 and Fig 2.10 represent the swelling behavior of the poly(AAm-*co*-AAc) copolymer hydrogels and poly(AAm-*co*-AAc)/PANI composite hydrogels respectively. In both the cases, swelling behaviour was found to be same, but the values tend to decrease slightly with incorporation of PANI into the hydrogel matrix. It may be due to the hydrophobic nature of the PANI molecules present within the hydrogel matrix.

The hydrogels were allowed to swell in different pH media and variation of swelling behavior with respect to the crosslinker amount and pH were studied. With diminishing acidity of the media (larger pH), ionization of the carboxylic acid groups occurs, resulting in both electrostatic repulsion between the carboxylate ($-COO^-$) groups as well as expansion of the space network.[34] Therefore, the swelling percentage is found be highest in basic medium (higher pH).

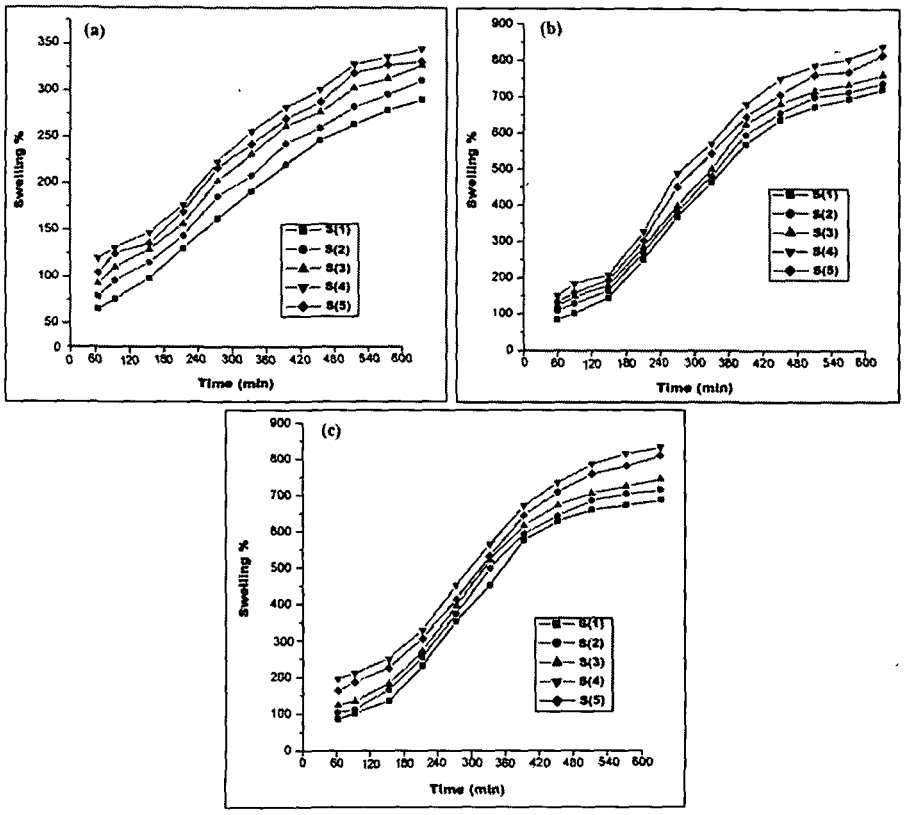

Fig 2.9 Swelling % of poly(AAm-*co*-AAc) copolymer hydrogels in different pH medium: (a) pH 4, (b) distilled water and (c) pH 7.4

Furthermore, presence of crosslinker is an important pre-requisite for formation of ideal three-dimensional networks of hydrogels. Under lower crosslinker concentrations, the polymerization reaction does not occur adequately and the 3D network of the polymer does not form effectively; water molecules cannot be held in the 3D network, which leads to the decrease of swelling percentage. So, as the amount of crosslinker increases, the 3D network of the polymer forms effectively and after an optimum level of crosslinker amount, the network density increases which results in a compact network. It is clearly seen from the **Fig 2.10** that percentage swelling increases with increase in crosslinker amount in samples S(1) to S(4) but is found to decrease in case of sample S(5). It can be explained that the amount of crosslinker may be higher than the optimum level in case of sample S(5), thereby decreasing the percentage swelling.

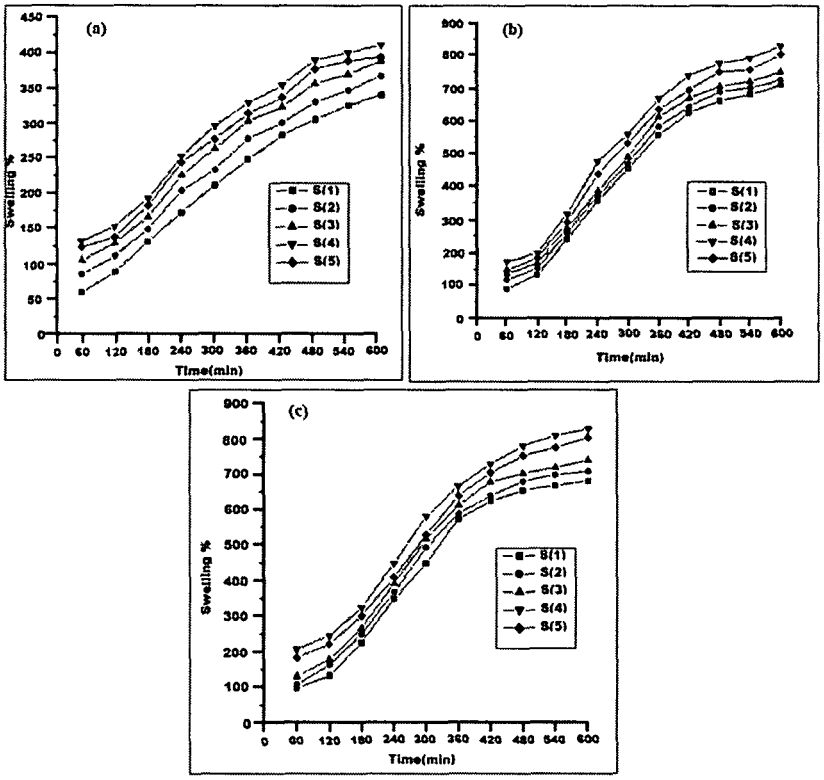

Fig 2.10 Swelling % of poly(AAm-*co*-AAc)/PANI composite hydrogels in different pH medium: (a) pH 4, (b) distilled water and (c) pH 7.4.

2.6.1.8 Bending angle measurements

The bending behavior of poly(AAm-*co*-AAc)/PANI composite hydrogels under varying concentrations of the electrolyte solution and applied voltages are shown in **Fig 2.11**. It is clear that the bending behavior is low when applied voltage is low and tends to increase with increase in applied voltage. The increase in effective bending angle may be attributed to the fact that with increase in voltage, the charged matrix is attracted more and more towards the electrodes leading to the said observation. It also indicates that bending is induced by an electric current.[35]

The bending behaviour of the gel was studied in NaCl solutions of concentrations 0.1 and 0.2 N separately. It was found that bending angle tends to decrease at higher concentrations of the electrolyte **(Fig 2.11b)**. It may be due to the fact that beyond a critical electrolyte concentration, the ions present in the polymer chain are shielded by the

other ions in the electrolytic solute leading to electrostatic repulsion of the polyions and a decrease in the degree of bending.[36] Also, according to Flory's theory, an increasing amount of ions could reduce the electrostatic repulsion of the polyions by the screening of fixed charges and bring about a decrease in the degree of bending. So, bending angles are found to decrease with increase in electrolyte concentration.[37]

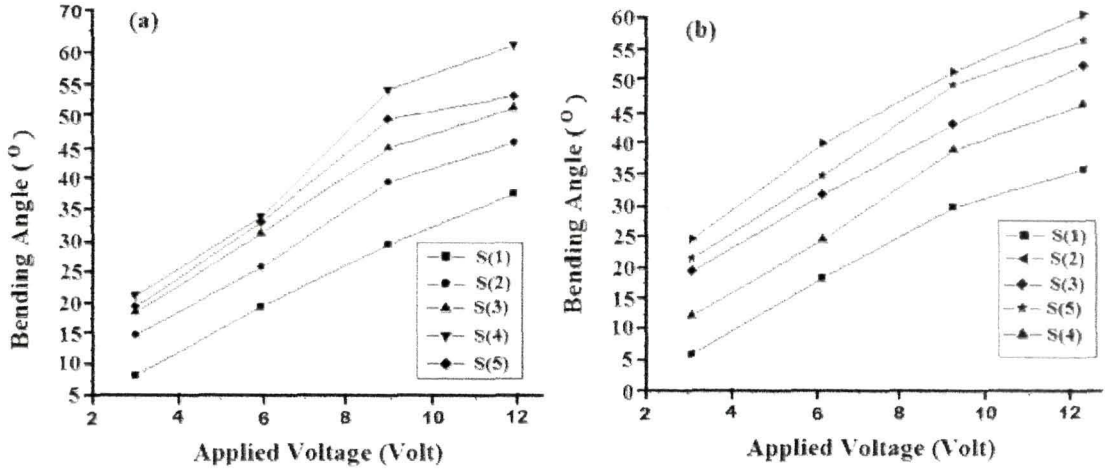

Fig 2.11 Effective bending angles of poly(AAm-*co*-AAc)/PANI composite hydrogel in: (a) 0.1 N NaCl solution and (b) 0.2 N NaCl solution.

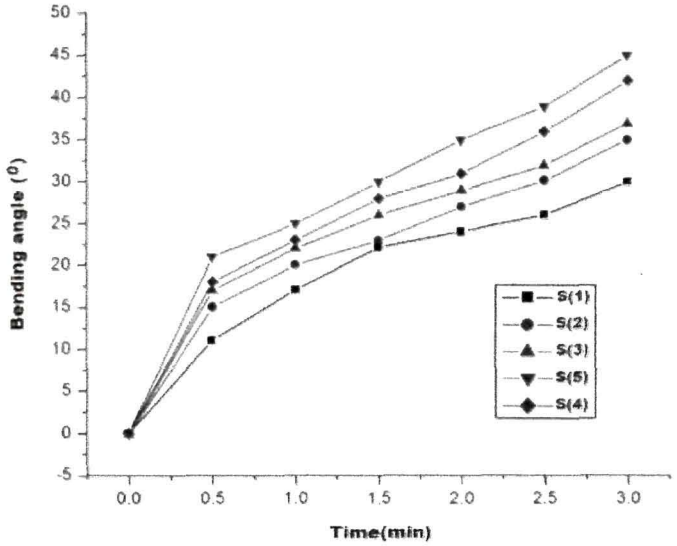

Fig 2.12 Effective bending angles of poly(AAm-*co*-AAc)/PANI composite hydrogels with respect to time.

Also, the bending behavior of the hydrogels with time is studied. All conducting hydrogels show good response in a short time. But, sample S(4) (containing highest % of PANI) is found to show highest bending within the given time interval. Bending angles with respect to time are shown in **Fig 2.12.**

2.6.1.9 Hemolytic potentiality test

The biomedical application of any material involves the use of humans or other animals, it is important to study their biocompatibility with blood. The prepared composites hydrogels were subjected to hemolytic potentiality test to evaluate their *in vitro* blood compatibility.

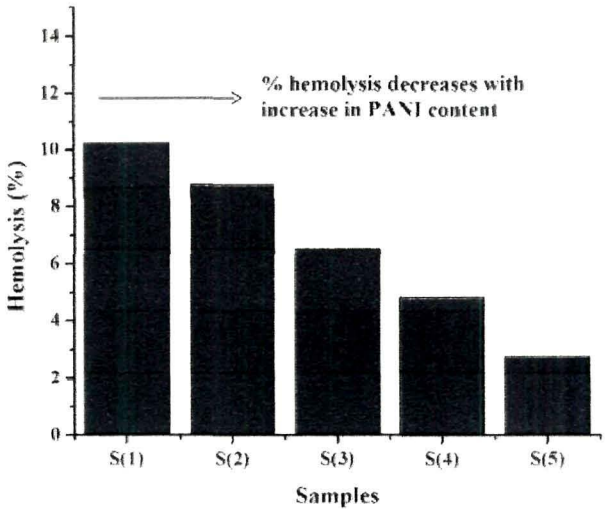

Fig 2.13 The percentage of hemolytic activity of poly(AAm-*co*-AAc)/PANI composite hydrogel at concentration (5 mg/2ml) at 540 nm.

The test showed overall less hemolysis activity by all the tested samples and the data obtained are at the permissible limit for their biomedical applications. Also, hemolysis percentage was decreased with increase in polyaniline impregnation into the hydrogel matrix. **Fig 2.13** represents the hemolysis percentage of the composite hydrogels.

2.6.2 poly(acrylamide-*co*-acrylic acid)/graphite composite hydrogel

2.6.2.1 FTIR analysis

FT-IR analysis was carried out to elucidate the composition of the hydrogel and is shown in the **Fig 2.14**. FT-IR spectrum of the composite hydrogel shows peaks at 3468, 3410, 3185, 2925, 1726, 1630, 1437, 1266 and 442 cm^{-1}. The characteristic peak at 3468 cm^{-1} is assigned to the O-H stretching from carboxylic group. Peak at 3410 cm^{-1} is due to N-H stretching vibration, at 3185 cm^{-1} is due to N-H bending vibration from $-CONH_2$ group of PAAm.

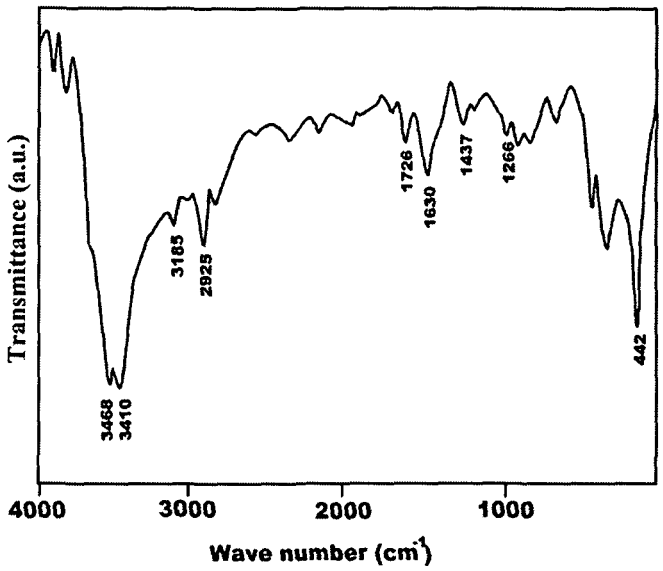

Fig 2.14 FTIR spectrum of poly(AAm-*co*-AAc)/graphite composite hydrogel.

Also, the characteristic peaks at 1726 cm^{-1} is due to C=O stretching of carboxylic acid group of PAAc and at 1630 cm^{-1} is for C=O stretching of PAAm. Peak at 1437 cm^{-1} is due to the aromatic C=C stretching vibration, 1266 cm^{-1} is due to the C-N stretching vibration and at 442 cm^{-1} is due to the $-NH_2$ out of plan rocking. The results indicate the formation of poly(AAm-*co*-AAc)/graphite composite hydrogel.

2.6.2.2 XRD analysis

The XRD patterns of poly(AAm-*co*-AAc) copolymer hydrogel and poly(AAm-*co*-AAc)/ graphite composite hydrogels are shown in **Fig 2.15**. The different peaks were

observed at 2θ, 26.6, 44.6 and 54° respectively and are matched with (002), (101) and (004) planes of the hexagonal system with primitive structure of graphite.[38] These peaks were absent in the native gel. Thus, the XRD-patterns provide an evidence of impregnation of graphite within the polymer matrix (**Fig 2.15b**).

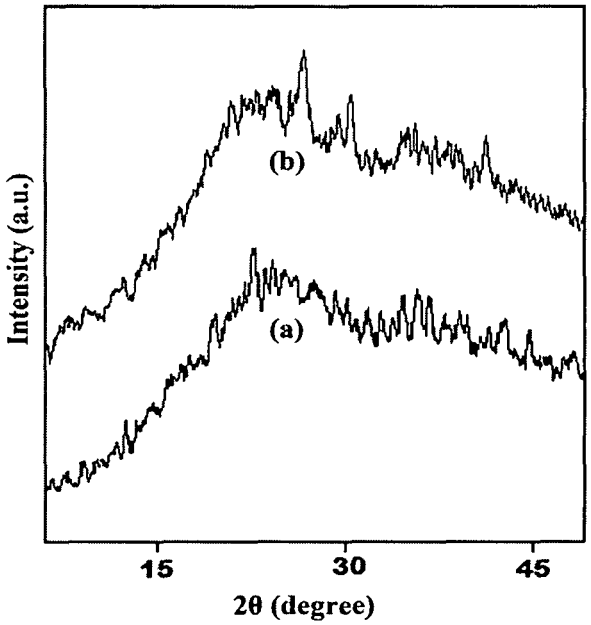

Fig 2.15 XRD spectra of (a) poly(AAm-*co*-AAc) copolymer hydrogel and (b) poly(AAm-*co*-AAc)/graphite composite hydrogel.

2.6.2.3 SEM morphological observation

Fig 2.16 illustrates the scanning electron micrographs of poly(AAm-*co*-AAc) copolymer hydrogel with and without graphite. The surface morphology of the hydrogel without graphite appears to be rough while with graphite it is found to be smooth. Here, the graphite particles may act as nucleating centre over which polymer grows with uniform rate (**Fig 2.16b**).

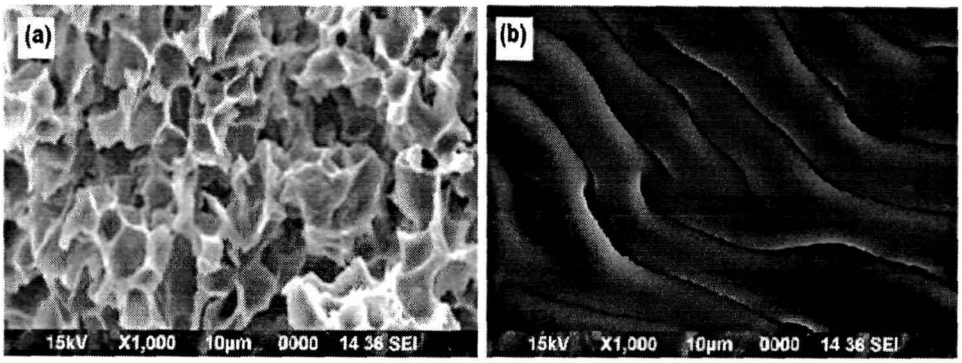

Fig 2.16 SEM images of (a) poly(AAm-*co*-AAc) copolymer hydrogel and (b) poly(AAm-*co*-AAc)/graphite composite hydrogel.

2.6.2.4 Tensile strength

It has been found that the mechanical strength gradually increases from 0.112 to 0.282 MPa with increase in the crosslinker (EGDMA) amount from 0.03-0.15 mol% (**Fig 2.17**). This may be due to the formation of the 3D network structure with introduction of increasing amounts of crosslinker. Thus, amount of crosslinker plays a significant role in enhancing the tensile strengths of the composite hydrogel. The open spaces between polymer networks decreased with high crosslinking density thereby improving the mechanical strength. The composite hydrogels possess good tensile strengths for which they may find applications in flexible electronics and soft machines.

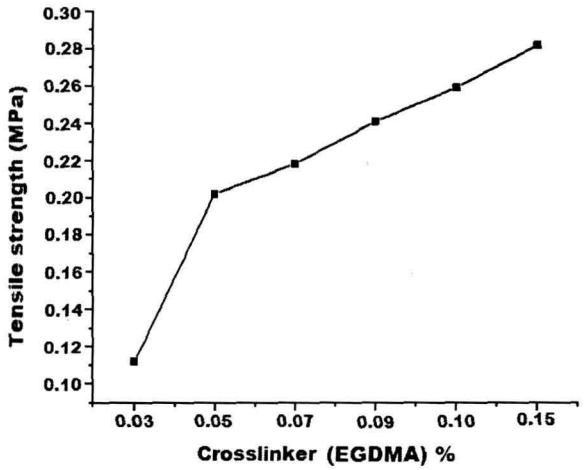

Fig 2.17 Tensile strength of the poly(AAm-*co*-AAc)/graphite composite hydrogels (with different amount of crosslinker).

2.6.2.5 DC electrical conductivity

2.6.2.5.1 Influence of crosslinker concentration on the conductivity of hydrogel

The structure of the polymeric network plays a significant role in the electrical conductivity of hydrogel. The conductivity tends to increase initially with increase of crosslinker (EGDMA) amount from 0.03-0.09 mol% and again decreases beyond a crosslinker amount of 0.10 mol% as shown in **Fig 2.18.**

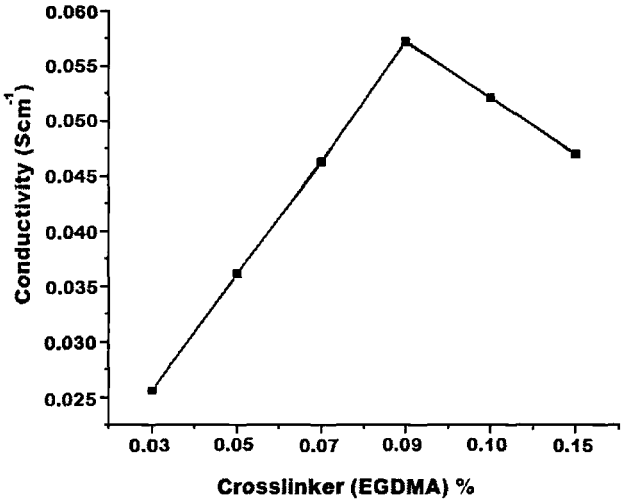

Fig 2.18 Conductivity of the poly(AAm-*co*-AAc)/graphite composite hydrogels with the variation of crosslinker amount.

Initial increase in amount of crosslinker facilitates the formation of a proper network structure which in turn enhances the uniformity in distribution of graphite into the hydrogel matrix. So the conductivity increases with increasing amount of crosslinking agent. Again, beyond an optimum level of crosslinker amount, the network becomes compact restraining the mobility of the charge carriers. So, at higher crosslinking density, the connection between graphite particles decreases thereby decreasing the electrical conductivity of the hydrogel.

2.6.2.5.2 Influence of graphite amount on the conductivity of hydrogel

Fig 2.19 represents the conductivities of the prepared hydrogels with the variation of graphite amount. The electrical conductivity of the prepared hydrogels is mainly

accounted for the presence of graphite micropowder component. It was observed that the conductivity values increases with the increase in graphite content from 3 to 9 w%.

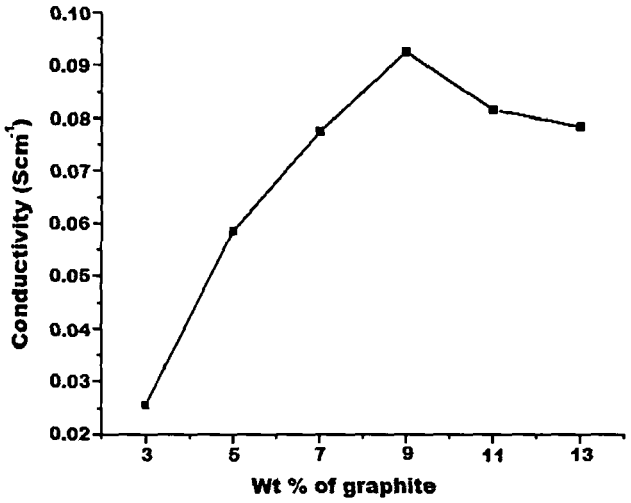

Fig 2.19 Conductivity of the poly(AAm-*co*-AAc)/graphite composite hydrogels with the variation of graphite amount.

With the increase of graphite amount, the contact between the graphite particles increase which leads to the enhancement of conductivity. On the other hand, conductivity tends to decrease when amount of graphite exceeds 9 w%. It may be due to the fact that, with increase in amount, graphite particles tend to form agglomerates thereby restricting the uniform distribution of graphite within the hydrogel matrix. So, a little decrease in the conductivity value was observed.

2.6.2.5.3 Influence of temperature on the conductivity of hydrogel

The conductivity of hydrogel also depends on temperature. The conductivity of hydrogel rises with the increase of temperature as shown in **Fig 2.20**. It may be due to the fact that, as temperature increases, the mobility of liquid within the polymeric network increases which again enhances the connectivity between the graphite particles. This leads to the increase in conductivity. The conductivity-temperature behavior of the conductive hydrogel can be described by Arrhenius equation.

$$\sigma(T) = A \exp [-E_a / RT] \qquad \textbf{Eqn. 2.7}$$

where, 'E_a' is the activation energy, 'R' is the molar gas constant, 'A' is a constant, and 'T' is absolute temperature. According to the experimental data, the E_a is calculated as 6.01 kJ mol^{-1} and the A is 29.22.

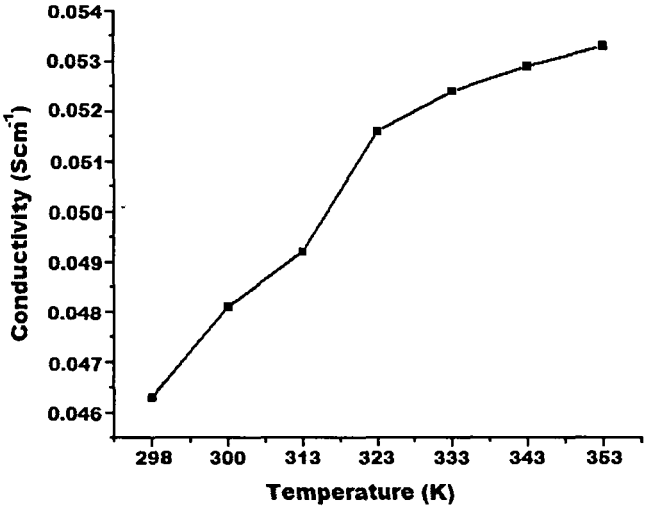

Fig 2.20 Conductivity of the poly(AAm-*co*-AAc)/graphite composite hydrogels with the variation of temperature.

2.6.2.6 Swelling behaviour

The swelling behavior of hydrogels is a measure of their utility as biomaterials in various fields. So, the swelling behaviors of the composite hydrogels without graphite and with graphite are investigated and shown in **Fig 2.21** and **Fig 2.22**. In both the cases, swelling behaviours are found to be same, but the values tend to decrease slightly with incorporation of graphite into the hydrogel matrix due to the hydrophobic nature of the graphite molecules.

The hydrogels were allowed to swell in different pH media. The swelling percentage is found be highest in basic medium (higher pH). With diminishing acidity of the media (higher pH), ionization of the carboxylic acid groups occurs, resulting in both electrostatic repulsion between the carboxylate ($-COO^-$) groups as well as expansion of the space network.[28] Also, there is development of a large osmotic swelling force caused by the presence of the ions.

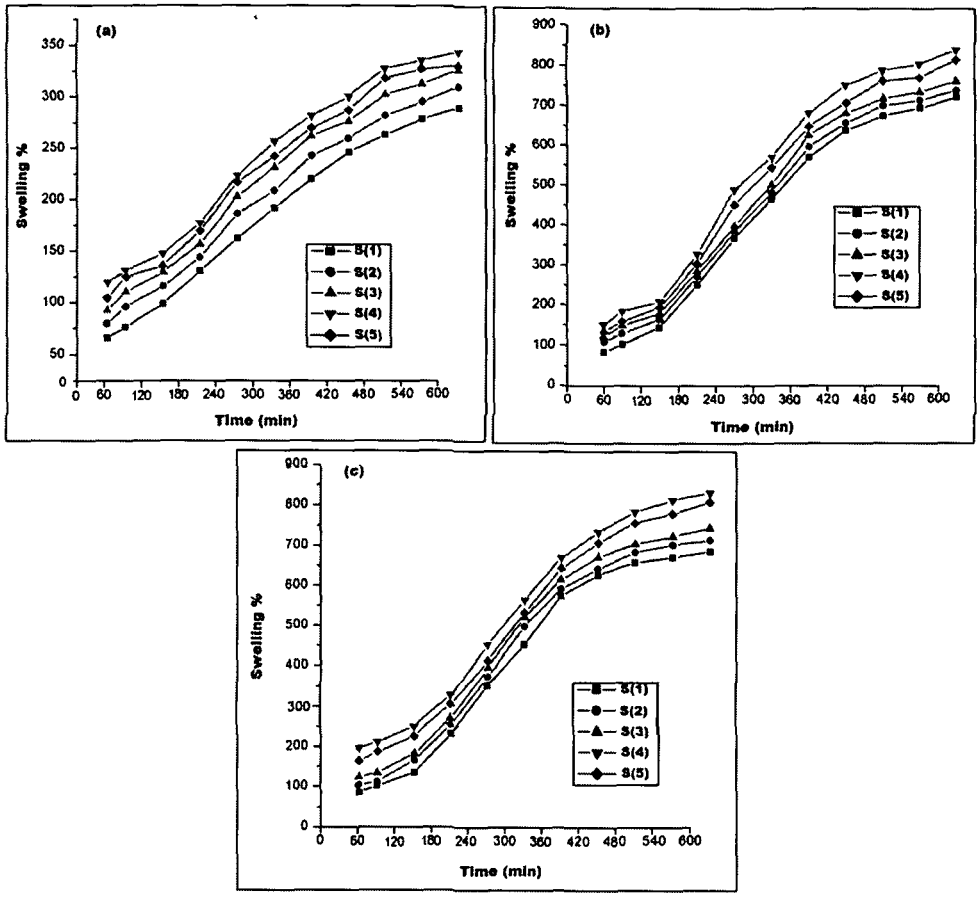

Fig 2.21 Swelling % of poly(AAm-*co*-AAc) copolymer hydrogel in different pH medium: (a) pH 4, (b) Distilled water and (c) pH 7.4.

Furthermore, presence of crosslinker is an important pre-requisite for formation of ideal three-dimensional networks of hydrogels. Under lower crosslinker concentrations, the 3D network of the polymer does not form effectively in the gel. Thereby 3D network of gel cannot hold sufficient water which leads to decrease in swelling percentage. So, as the amount of crosslinker increases, the 3D network of the polymer forms effectively. After an optimum level of crosslinker amount, the network density increases which results in a compact network causing decrease in swelling.

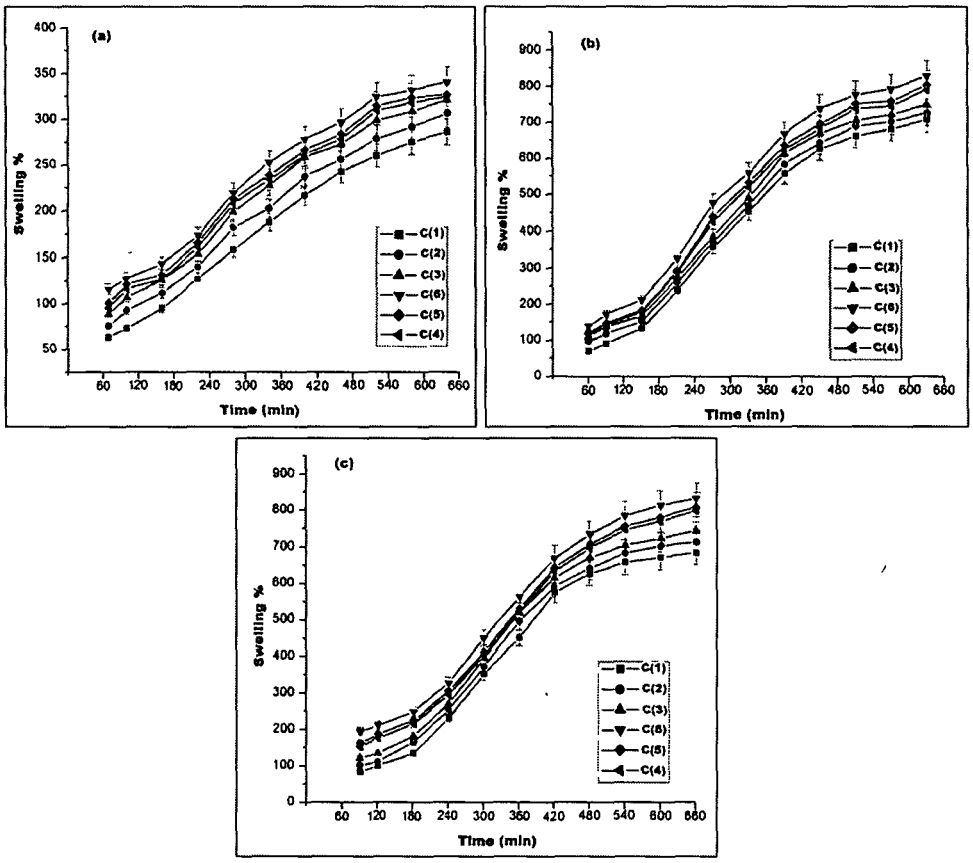

Fig 2.22 Swelling % of poly(AAm-*co*-AAc)/graphite composite hydrogels in different pH medium: (a) pH 4, (b) distilled water and (c) pH 7.4.

2.6.2.7 Bending angle measurements

When an electric field was applied to a strip of the hydrogel in an aqueous NaCl solution, the hydrogel showed significant and quick bending towards the cathode. When the electric stimulus was removed, it returned to its original position. The bending behavior of the hydrogels under varying concentrations of the electrolyte solution and applied voltages are shown in **Fig 2.23**. It is clear that the bending angle is low when applied voltage is low and tends to increase with increase in applied voltage. The increase in effective bending angle may be attributed to the fact that with increase in voltage, the charged matrix is attracted more and more towards the electrodes leading to the said observation. However, bending was not found in pure water and this indicates that bending was induced by the electric current.[36] The effect of voltage on bending

phenomenon has been investigated in the range 3 0 to 12 0 V. No bending was observed below 3.0 V, so, lower critical voltage (LCV) found in this case is 3.0 V

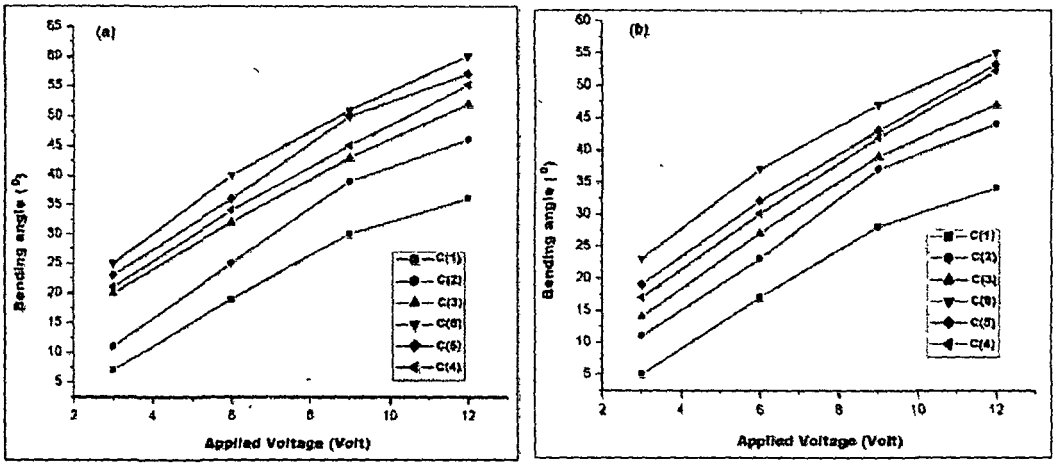

Fig 2.23 Effective bending angles of poly(AAm-*co*-AAc)/graphite composite hydrogel in: (a) 0.1 N NaCl solution and (b) 0.2 N NaCl solution.

The influence of the medium ionic concentration on the bending behavior of the hydrogel in response to an electric stimulation was determined by varying the concentrations of aqueous NaCl from 0.1 N and 0 2 N separately It was found that bending angle tends to decrease at higher concentrations of the electrolyte. This may be due to the fact that beyond a critical electrolyte concentration, the ions present in the polymer chain are shielded by the other ions in the electrolytic solute which leads to the electrostatic repulsion of the polyions and a decrease in the degree of bending.[35] Also, according to Flory's theory, an increasing amount of ions could reduce the electrostatic repulsion of the polyions by the screening of fixed charges and bring about a decrease in the degree of bending So, bending angles are found to decrease with increase in electrolyte concentration.[37] A similar result was reported by Sun and Mak in their study of the mechano-electrochemical behavior of a hydrogel fiber based on chitosan/poly(ethylene glycol).

Moreover, the bending behavior of the hydrogels with time is studied. All conducting hydrogels show good response in a short time. But, sample containing highest weight % of graphite is found to show highest bending within the given time interval. Bending angles with respect to time are shown in **Fig 2.24**.

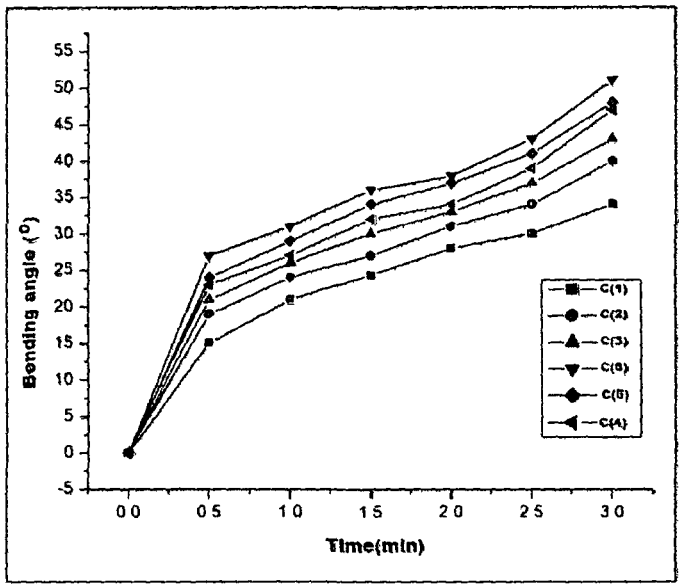

Fig 2.24 Effective bending angles of poly(AAm-co-AAc)/graphite composite hydrogel with respect to time

2.6.2.8 Hemolytic potentiality test

The hydrogel samples were tested for hemolytic activity and the results obtained are shown in **Fig 2.25** The test showed overall less hemolysis activity by all the tested samples and the data obtained are at the permissible limit [39] These results reveal that the hydrogel samples are hemocompatible and may be potentially used for biomedical applications

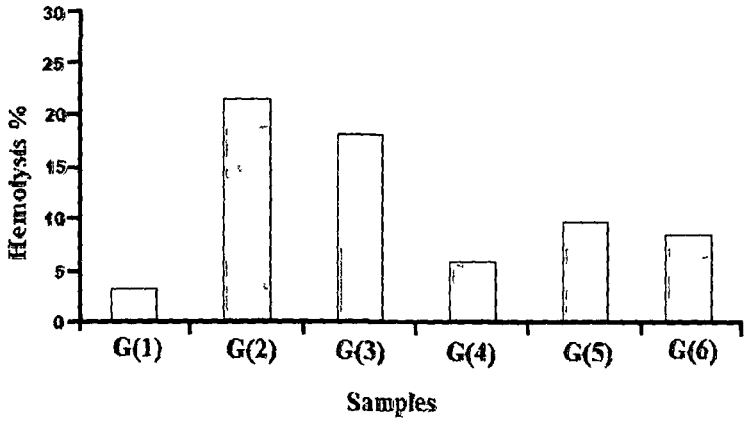

Fig 2.25 Bar diagram showing the percentage of hemolytic activity by different samples at concentration (10 mg/2ml) at 540 nm

2.7 Conclusion

- Two sets of composite hydrogels with poly(AAm-*co*-AAc)/PANI and poly(AAm-*co*-AAc)/graphite were prepared by solution polymerization process in presence of redox initiator potassium persulfate (KPS)/TEMED and crosslinker (EGDMA).
- The FTIR spectrum shows the characteristic peaks of the functional groups of constituent polymers. The presence of polyaniline and graphite in the hydrogel matrix was confirmed by XRD and SEM analysis.
- The swelling behaviour of both the composite hydrogels were found to be pH-responsive upon study across varying pH media. Also, the swelling is found to be the highest in basic medium (pH 7.4).
- The mechanical properties of the composite hydrogels were improved with an increase in crosslinker (EGDMA) content due to the formation of a compact network structure.
- The prepared conducting composite hydrogels were found to possess gratifying conductivity which was significantly dependent on crosslinker (EGDMA) content, temperature and amount of the conducting filler.
- The hemolytic potentiality test reveals that, all the composite hydrogels are biocompatible in nature.
- Both the composite hydrogels show significant bending behaviour when exposed to an external electric field.
- The properties of composite hydrogels confirmed in this chapter indicate that the hydrogels can find possible application in artificial organ components, especially as actuator.

References

1. Buchholz, F. & Graham, A. *Modern superabsorbent polymer technology*, New York, Wiley-VCH, 1997.
2. Weaver, M.O., Bagley, E.B., Fanta, G.F. & Doane, W.M. *Highly absorbent starch-containing polymeric compositions,* **U. S. Patent No. 3, 997, 1484,** December 14, 1976.
3. Bajpai, A.K., et al. *Prog. Polym. Sci.* **33** (11), 1088-1118, 2008.
4. Gunasekaran, S., et al. *J. Appl. Polym. Sci.* **102** (5), 4665-4671, 2006.
5. Tanaka, T. *Phy. Rev. Lett.* **40** (12), 820-823, 1978.
6. Suzuki, A., & Tanaka, T. *Nature* **346** (6282), 345-347, 1990.
7. Kiler, J., et al. *Macromolecules* **23** (23), 4944-4949, 1990.
8. Kown, L.C., et al. *Nature* **354** (6351), 291-293, 1991.
9. Yoshida, R., et al. *Nature* **374** (6519), 240-242, 1995.
10. Angeles, G.H., et al. *Eur. Polym. J.* **59,** 341-352, 2014
11. Hoffman, A.S. *Adv. Drug. Deliv. Rev.* **54** (1), 3-12, 2002.
12. Novikov, G.F., et al. *Russ. J. Phys. Chem. A* **88** (10), 1790-1794, 2014.
13. Sun, X., et al. *Solid State Ionics* **175** (1-4), 713-716, 2004.
14. Shinji, N., et al. *Electrochem. Acta.* **48** (6), 749-753, 2003.
15. Lewandowski, A., et al. *Electrochem. Acta.* **46** (18), 2777-2780, 2001.
16. Wu, J.H., et al. *Photochem. Photobiol. A* **181** (1), 227-333, 2006.
17. Scranton, A.B., et al. Biomedical applications of polyelectrolytes, in *Biopolymers II.* N.A. Peppas et al. eds., Springer Berlin Heidelberg, 1995, 1-54.
18. Chen, G., et al. *Carbon* **42** (8-9), 753-759, 2004.
19. Kurkuri, M.D., et al. *Smart Mater. Struct.* **15** (2), 417-423, 2006.
20. Dai, T., et al. *Compos. Sci. Technol.* **70** (3), 498-503, 2010.
21. Xiao, Y., et al. *J. Mater. Chem.* **22** (48), 8076-8082, 2012.
22. Kim, B., & Osada, Y. *Korea Polym. J.* 7 (6), 350-355, 1999.
23. Yang, S., et al. *Carbon* **43** (2), 827-834, 2005.
24. Jia, S., et al. *Radiat. Phys. Chem.* **75** (4), 524-531, 2006.

25. Zhang, X., et al. *Carbon* **43** (10), 2186-2191, 2005.

26. Kuilla, T., et al. *Prog. Polym. Sci.* **35** (11), 1350-1375, 2010.

27. Dispenza, C., et al. *Polymer* **47** (4), 961-971, 2006.

28. Bajpai, A.K., et al. *eXPRESS Polym. Lett.* **2** (1), 26-39, 2008.

29. Fan, S., et al. *J. Mater. Sci.* **43** (17), 5898-5904, 2008.

30. Tang, Q., et al. *J. Appl. Polym. Sci.* **108** (3), 1490-1495, 2008.

31. Lin, J., et al. *React. Funct. Polym.* **67** (4), 275–281. 2007.

32. Stejskal, J. *Pure Appl. Chem.* **74** (5), 857-867, 2002.

33. Miki, M., et al. *Arch. Biochem. Biophys.* **258** (2), 373-380, 1987.

34. Pourjavadi, A., et al. *React. Funct. Polym.* **67** (7), 644-658, 2007.

35. Kim, S.J., et al. *Polym. Int.* **53** (10), 1456-1460, 2004.

36. Sun, S., & Mak, A.F.T. *J. Polym. Sci. Pol. Phys.* **39** (3), 236-239, 2001.

37. Flory, P.J. *Principles of Polymer Chemistry,* Ithaca, Cornell University Press, 1992.

38. Konwer, S., et al. *J. Appl. Polym. Sci.* **116** (2), 1138-1145, 2010.

39. Mishra, A., & Chaudhary, N. *Trends Biomater. Artif. Org.* **23** (3), 122-128, 2010.

CHAPTER 3

Synthesis of electric field responsive poly (vinyl alcohol)-g-poly(acrylic acid)/OMMT nanocomposite hydrogels and their swelling kinetics.

GRAPHICAL ABSTRACT

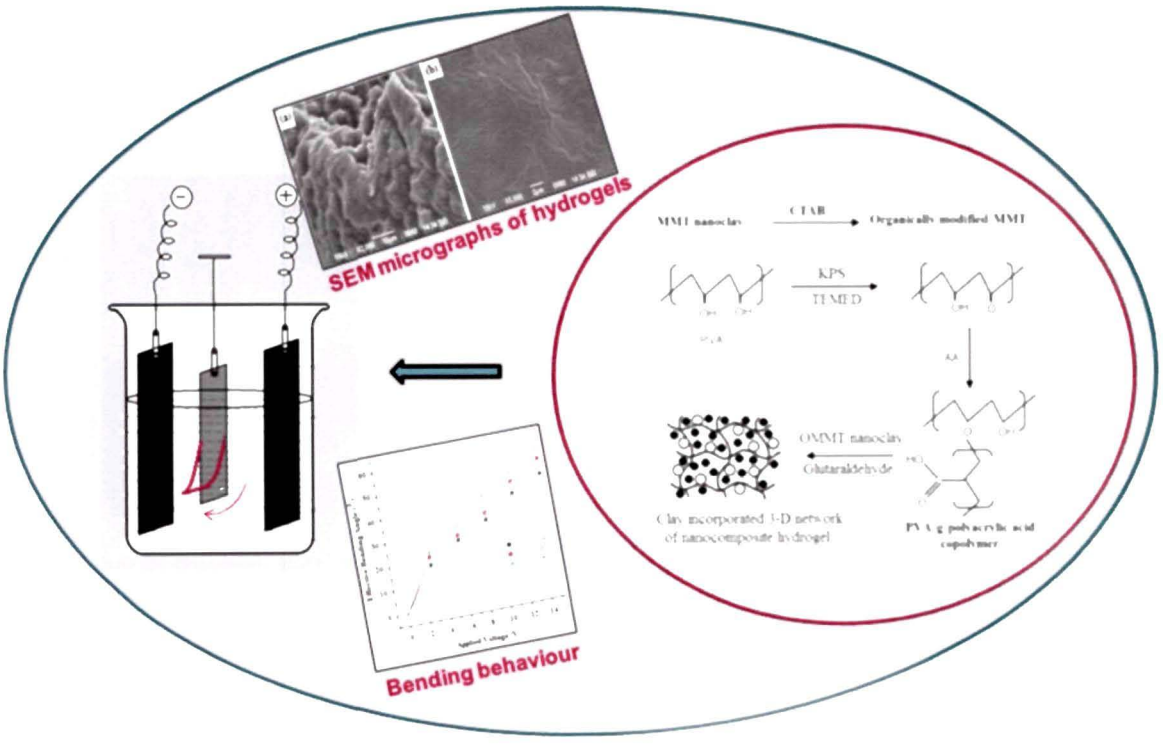

3.1 Introduction

During the past decades, there has been an explosion of advances in the fields of structured and intelligent materials science and nanomaterials properties. Nanocomposite hydrogels have been introduced as suitable novel materials for a variety of applications such as wound dressing,[1,2] drug delivery system[3,4] and agriculture[5] as well as waste-water treatment[6,7] etc. Smart polymeric hydrogels can change their volume and shape reversibly depending on several environmental stimuli such as temperature, pH, ionic strength, pressure, electronic and magnetic field etc. Among these possibilities, electro-responsive polymer hydrogels seem to be particularly interesting because mechanical energy has been triggered by an electric signal.[8]

Nanocomposite refers to a composite material, in which reinforcing agent has at least one dimension in nanometer scale.[9] In recent years, organic-inorganic nanocomposites have attracted great research interests because of their high water absorbency, relatively low production cost and considerable range of applications.[10,11] Also, natural inorganic clays have been widely utilized in this field for improving performance and reducing cost.[12] For a successful nanocomposite to be prepared, the dispersion of inorganic material with the polymeric matrix is necessary. But, the intrinsic incompatibility of hydrophilic clay layers with hydrophobic polymer chains prevents the dispersion of clay nanolayers within polymer matrix. The weak interfacial interactions again hinder the exfoliation of clay. For this reason modification of clay layers with hydrophobic agents is necessary in order to render the clay layers more compatible with polymer chains.[13]

A part of this chapter is published

M. Boruah, M. Mili, S. Sharma, B. Gogoi and S. K. Dolui, *Polym. Compos.* DOI: 10.1002/pc.22909, 2014.

The organophilized filler shows compatibility with the relatively hydrophobic polymer matrix due to the hydrophobic surface. These fillers may help to improve the swelling, the mechanical properties, as well as the thermal stability of the polymers. Layered silicates, e.g., montmorillonite (MMT), have been used in polymer nanocomposites with a significant improvement in the properties.[14,15] Due to unique structure of montmorillonite, the mineral platelet thickness is only one nanometer, although its dimensions in length and width can be measured in hundreds of nanometers, with a majority of platelets in 200-400 nm range after purification. Furthermore, being lamellar clay, MMT has intercalation, swelling and ion exchange properties and it can expand considerably more than other clays due to the water penetrating the interlayer molecular spaces and concomitant adsorption.[16] Moreover, Poly vinyl alcohol (PVA) and polyacrylic acid (PAAc) are hydrophilic polymers used in many biomedical researches, previously. Polyvinyl alcohol (PVA) is a well known biologically friendly, non-toxic, semi-crystalline synthetic polymer with properties such as water solubility, biodegradability and biocompatibility for which it finds use in a broad spectrum of applications.

Currently, several successful methods have been carried out to obtain functional polymer/organo clay nanocomposite hydrogels to improve the properties of hydrogel, such as swelling and deswelling properties, thermal properties etc. For example, Wu et al. reported the preparation of starch-*g*-polyacrylamide/clay and poly(acrylic acid)/mica composites with striking capability of water absorption by grafting the monomers on the inorganic clay/mica.[17] Zheng et al. studied the effect of cation-exchanged montmorillonite on water absorbency of poly(acrylic acid-*co*-acrylamide)/montmorillonite/sodium humate superabsorbent composite. Their results showed that the properties of the composite including water absorbency, swelling behavior and deswelling capability were dependent strongly on the kinds of cation exchanged.[18]

Electro-sensitive hydrogels are generally made of polyelectrolytes which contain relatively high concentrations of ionisable groups along the polymer backbone.[19] The

response of electro-sensitive hydrogels generally exhibits in the form of swelling, shrinking or bending behaviors. Several research groups have extensively studied the mechanism of such behaviors of this kind of hydrogels. Kim et al. reported a poly(vinyl alcohol)/chitosan (PVA/chitosan) IPN hydrogel that exhibited the electro-sensitive behavior in an aqueous NaCl solution.[20] The bending angle and the bending speed of the PVA/chitosan hydrogel increased with an increasing applied voltage and the concentration of the aqueous NaCl solution. Sun and Mak demonstrated that a hydrogel fiber based on chitosan/poly(ethylene glycol) displayed mechano-electro-chemical (MEC) behaviour. They also showed the reversibility of the bending behavior under an applied electric field.[21]

This chapter includes the synthesis of a new type of electro-responsive organic/inorganic nanocomposite hydrogel, by introducing the organically modified MMT nanoclay into the poly(vinyl alcohol)-*g*-poly(acrylic acid) polymer network. Molecular structure and surface morphology of the prepared hydrogels are investigated thoroughly. The influence of clay content and the crosslinker amount on the swelling properties of the nanocomposite hydrogels were determined. In addition, the bending behaviour of the swollen hydrogels under an electric field at various applied voltages was also evaluated.

3.2 Experimental

3.2.1 Materials

Acrylic acid monomer (Aldrich) was distilled under reduced pressure prior to use. Polyvinyl alcohol (MW=1,25,000 g/mol, 98.5-99.5% hydrolyzed), potassium persulfate (initiator), glutaraldehyde as a crosslinking agent, MMT nanoclay, and N, N, N′, N′-tetramethylethylene diamine were supplied by Aldrich (A.R. grade). Cetyl trimethylammonium bromide (CTAB) was supplied by G.S Chemical testing lab and allied industries, New Delhi. Sodium hydroxide and ethanol were purchased from Merck and were of A. R grade.

3.3 Synthesis of poly(vinyl alcohol)-*g*-polyacrylic acid/OMMT nanocomposite hydrogel

3.3.1 Preparation of organo-MMT nanoclay

The organophilic clay was prepared by treating the clay with cetyl trimethylammonium bromide (CTAB) as reported elsewhere.[22] 3 g clay (Na^+-MMT) was dispersed in 250 ml of deionized water under vigorous stirring (700 rpm). A solution of CTAB (1.318g, 3.615x 10^{-3} mol) in 100 ml of deionized water was slowly added to the dispersion, under continuous stirring. The resultant dispersion was stirred for a further 6 hrs. The dispersion was filtered and obtained cake was thoroughly washed with deionized water. Samples of the filtrate were taken in regular intervals and tested with a solution of 0.1 M silver nitrate for the presence of released counterions. Washing was discontinued only when the filtrate did not give a positive test to silver nitrate. The washed cake was dried overnight under reduced pressure (vacuum) at 40°C and ground in a mortar.

3.3.2 Preparation of PVA-*g*-PAAc/OMMT nanocomposite hydrogel

Poly(vinyl alcohol)-*g*-poly(acrylic acid) /OMMT nanocomposite hydrogels were prepared by free radical polymerization in distilled water. Before polymerization, 2 g of PVA was dissolved in 30 ml of hot double distilled water and 1.5 ml of partially neutralized (60%) acrylic acid monomer was added to this solution. Also, a certain amount of OMMT nanoclay was dispersed in the deionized water under the ultrasonic vibration for 30 min. Both the solutions were mixed well and subsequently, glutaraldehyde (0.3-1.5 mol%), potassium persulfate (0.18 mol%) and tetramethylethylene diamine (0.05 mol%) were added to the mixture under continuous stirring. Nitrogen was used to remove dissolved oxygen from the reactive solution. The reactive solution was first prepolymerizd at 70°C for 30 min under stirring, and then poured into a petri dish quickly. The post polymerization was carried out at 65°C for 15 hrs. When the reaction completed, the hydrogel was cut into same size and immersed in repeatedly changed deionized water for 72 hrs to remove the residual monomers.

Table 3.1 Compositions of PVA-*g*-PAAc/OMMT nanocomposite hydrogels with various crosslinker (Glutaraldehyde) content:

Ingredients/Sample	S(1)	S(2)	S(3)	S(4)	S(5)	S(6)	S(7)
PVA(g)	2	2	2	2	2	2	2
Acrylic Acid (ml)	1.5	1.5	1.5	1.5	1.5	1.5	1.5
OMMT (wt%)	5	5	5	5	5	5	5
KPS (mol%)	0.18	0.18	0.18	0.18	0.18	0.18	0.18
Glutaraldehyde (mol%)	0.3	0.5	0.7	0.9	1.2	1.3	1.5
TEMED (mol%)	0.05	0.05	0.05	0.05	0.05	0.05	0.05

Table 3.2 Compositions of PVA-*g*-PAAc/OMMT nanocomposite hydrogels with various OMMT nanoclay content:

Ingredients/Sample	G(1)	G(2)	G(3)	G(4)	G(5)	G(6)
PVA(g)	2	2	2	2	2	2
Acrylic Acid (ml)	1.5	1.5	1.5	1.5	1.5	1.5
OMMT (wt%)	1	3	5	7	9	11
KPS (mol%)	0.18	0.18	0.18	0.18	0.18	0.18
Glutaraldehyde (mol%)	0.9	0.9	0.9	0.9	0.9	0.9
TEMED (mol%)	0.05	0.05	0.05	0.05	0.05	0.05

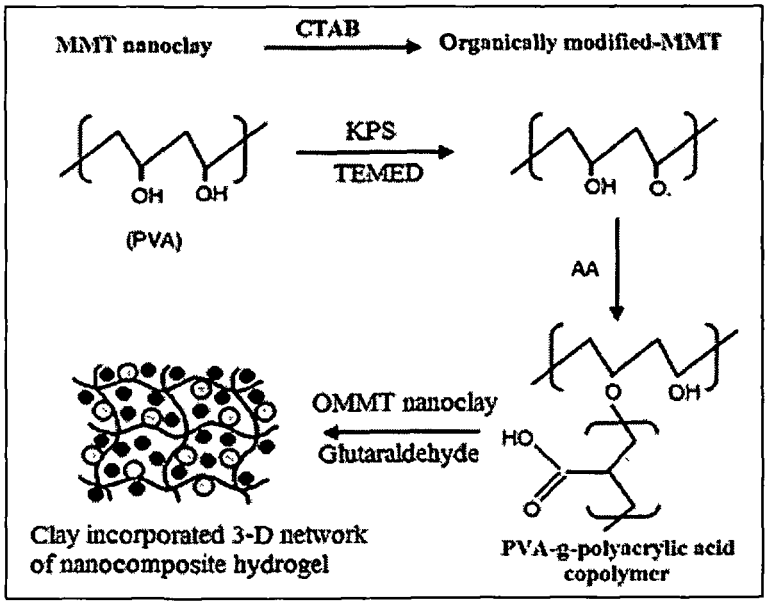

Fig 3.1 Schematic representation for the preparation of PVA-*g*-PAAc/OMMT nanocomposite hydrogel.

3.4 Characterization

3.4.1 Fourier transform infrared spectrometer (FTIR)

To gain insights into the structural information of prepared hydrogels, the IR spectra of the hydrogels were recorded with a Nicolet Impact-410 IR spectrometer (USA) in KBr medium at room temperature in the region 4000-450 cm^{-1}.

3.4.2 Powder X-ray diffraction (XRD)

Powder X-Ray diffraction (XRD) data were collected on a Rigaku Miniflex X-ray diffractometer (Tokyo, Japan) with Cu Kα radiation (λ=0.15418 Å) at 30 kV and 15 mA with a scanning rate of $0.05^{o}s^{-1}$ in a 2θ ranges from 10°-70° for the native gel and 0-45° for OMMT nanoclay and nanocomposite hydrogel.

3.4.3 Scanning Electron Microscope (SEM)

The surface morphology of the composites was observed using a scanning electron microscope (SEM) (Model- JSM-6390LV, JEOL, Japan). The surface of the sample was platinum coated before SEM analysis.

3.3.4 Thermo Gravimetric analysis (TGA)

Thermal analysis was done in a Shimadzu TA-60 thermo gravimetric analyzer. A pre weighted amount of the latex was loaded in a platinum pan and heating was done under nitrogen atmosphere at a heating rate of 10°C/min in the range of 0-600°C.

3.4.5 Swelling behaviour

To measure the degree of swelling the hydrogels, dried samples were placed in buffer media of different pH values at room temperature until the hydrated gels reached a stable weight. The water absorbed on the surface of the hydrogels was removed using filter paper and the weight noted.

The swelling percentages of the composite hydrogels were calculated by using following equation:

$$Swelling\ \% = W_s - W_{dry}/W_{dry} \times 100 \qquad \textbf{(Eqn. 3.1)}$$

where, W_s is the weight of the hydrogels in swollen state and W_{dry} is that of the hydrogels in dry state.

3.4.6 Bending-Angle Measurement

The composite hydrogels were swollen in different concentrations of aqueous NaCl solution at room temperature and cut into rectangular pieces. Then the bending angle of the gels under applied electric field was measured using a self developed device as shown in **Fig 3.2.** To demonstrate the bending behaviour of the hydrogels, the two carbon electrodes were placed in parallel 30 mm apart. One end of the sample column was fixed and placed vertically between two carbon electrodes in aqueous NaCl solution and the bending behavior was investigated under an applied electric field.

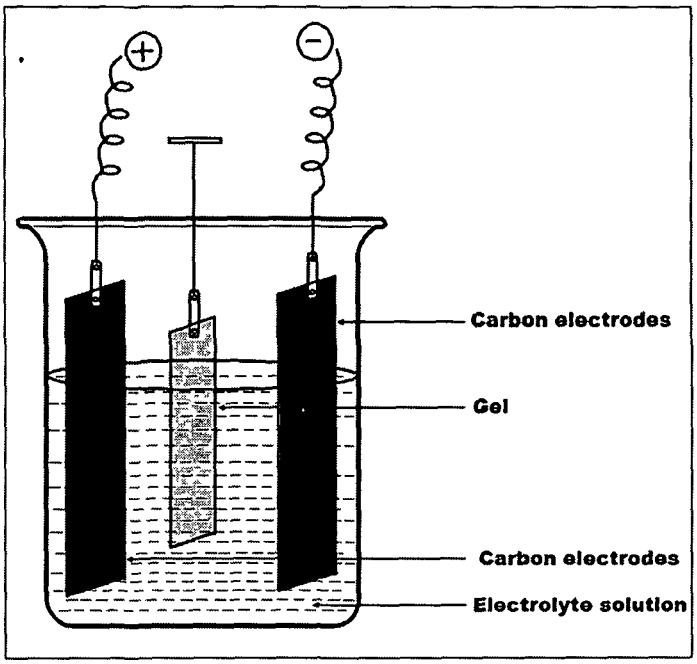

Fig 3.2 Apparatus for measuring bending angle.

3.4.7 Swelling kinetics

The swelling capacity of a hydrogels can be determined by the amount of space inside the hydrogels network available to accommodate water. Three forces; polymer–water interactions, electrostatic and osmosis expand the hydrogels network to accommodate water inside it. The maximum amount of water that can be absorbed by a hydrogel is called its 'equilibrium swelling capacity' which depends on many factors including hydrogel structure, crosslinking density, ionic content and hydrophilic content. The suitability of hydrogels as biomedical materials and their performance in a particular application depend to a large extent on their bulk structure. Three important parameters can define the structure of a hydrogel, the polymer volume fraction in swollen state $v_{2,s}$, the number average molecular weight between the crosslinks ($\overline{M_c}$) and the correlation length (ξ).[23]

In our work, the polymer volume fraction of the hydrogel in swollen state $v_{2,s}$ was estimated using the equation:

$$v_{2,s} = v_d/v_s \qquad \textbf{(Eqn. 3.2)}$$

where, V_d is the polymer volume fraction in dry state and V_s is the polymer volume fraction in swollen state. The value of V_d and V_s are determined by using the buoyancy principle with equation **(3.3)** and **(3.4)** as follows:

$$V_d = m_a - m_h/\rho_h \qquad \textbf{(Eqn. 3.3)}$$

$$V_s = m_{a,s} - m_{h,s}/\rho_h \qquad \textbf{(Eqn. 3.4)}$$

where, m_a is the mass of the initially dry polymer in air, m_h is the mass of the dry polymer in n-heptane, $m_{a,s}$ is the mass of swollen hydrogel in air after reaching equilibrium swelling, $m_{h,s}$ is the mass of swollen hydrogel in n-heptane after reaching equilibrium swelling and ρ_h is the density of n-heptane (0.684 g/cm^3 at 37±0.1°C). Prepared hydrogels were weighed in air and in n-heptane where a brass wire (0.04 mm in diameter) basket was suspended for placing samples.

3.4.8 Effective molecular weight of the polymer chain between two neighbouring crosslinks, $\overline{M_c}$

The molecular weight between two consecutive crosslinks, which can be either chemical or physical in nature, is a measure of the degree of crosslinking of the polymer. But due to the random nature of the polymerization process only average values of $\overline{M_c}$ can be calculated. Based on the equilibrium swelling data, effective molecular weight of the polymer chain between two neighbouring crosslinks, $\overline{M_c}$ was calculated using equation:[24]

$$\frac{1}{\overline{M}_c} = \frac{2}{\overline{M}_n} - \frac{\left(\frac{\bar{v}}{V_1}\right)\left[\ln(1-v_{2,s}) + v_{2,s} + \chi_{12} v_{2,s}^2\right]}{v_{2,s}^{1/3} - \frac{v_{2,s}}{2}} \qquad \textbf{(Eqn. 3.5)}$$

where, $\overline{M_n}$ is the number average molecular weight of PVA before crosslinking and taken as 1,25,000. $\bar{v}$ is the specific volume of PVA before crosslinking and was taken as 0.788 cm^3/g,[25] V_1 is the molar volume of the solvent (water) - 18 cm^3mol^{-1}. $v_{2,s}$ is the polymer volume fraction in swollen state and was calculated using equation **3.2**. The value of Flory Huggins polymer water interaction parameter equal to 0.494.

3.4.9 Mesh size, ξ

An important structural parameter for analyzing hydrogels is the space available between macromolecular chains. This space is often regarded as the molecular mesh or pore which is denoted by ξ. Also, it can be reported only as an average value. Using the calculated values of number average molecular weight between crosslinks, mesh size for the hydrogel was estimated using equation:

$$\xi = v_{2,s}^{-1/3} \left[C_n(2M_o/M_r)\right]^{1/2} .\ell \qquad \textbf{(Eqn. 3.6)}$$

where, C_n is the Flory characteristics ratio for PVA = 8.3, ℓ is the carbon-carbon bond length along the polymer backbone which is equal to 1.54 Å, M_r is the average molecular weight of the repeating units of PVA and acrylic acid in $gmol^{-1}$.

3.5 Results and discussion

3.5.1 FTIR analysis

FTIR spectra of OMMT nanoclay, PVA-*g*-PAAc copolymer and PVA-*g*-PAAc/OMMT nanocomposite hydrogels were recorded to investigate the formation of the nanocomposite as shown in **Fig 3.3**. The FTIR spectrum of OMMT nanoclay shows characteristics peaks at 3631 cm^{-1}, -OH stretching; 1637 cm^{-1}, -OH bending; 1108 cm^{-1}, Si-O stretching (out-of-plane); 1044 cm^{-1}, Si-O stretching (in-plane); 830 cm^{-1}, Al-Mg-OH bending vibrations and at 522 cm^{-1} due to the bending vibrations of Si-O. Also, the characteristics peaks were found for PVA-*g*-PAAc copolymer at 1730–1850 cm^{-1} due to the presence of C=O stretching vibration and the peak observed at 639 cm^{-1} is due to the -OH out of plane vibration of the carboxylic groups of PAAc, which obviously confirms the grafting reaction. The characteristic peaks at 3468 cm^{-1} and 3420 cm^{-1} are due to -OH stretching vibration of PVA and PAAc, respectively, which also confirms the grafting of PAAc into PVA. Other characteristics peaks for PVA are found at 2890 cm^{-1} for $-CH_2$ stretching, 1402 cm^{-1} for –O=C-OR stretching and at 860 cm^{-1} for –CH stretching vibrations respectively.

From the FTIR spectrum of PVA-*g*-PAAc/OMMT nanocomposite hydrogel, it was found that, characteristics peaks occur at 1735-2010 cm^{-1} due to the presence of C=O stretching vibration, 3600-3450 cm^{-1} due to -OH stretching vibrations. Also, the characteristics peaks at 1050-1000 cm^{-1} are found for OMMT nanoclay. When OMMT nanoclay was incorporated into the PVA-*g*-PAAc gel matrix, it was observed that peaks intensity related to PVA-*g*-PAAc gel have increased. So, it can be said that OMMT nanoclay is acting here as active fillers.

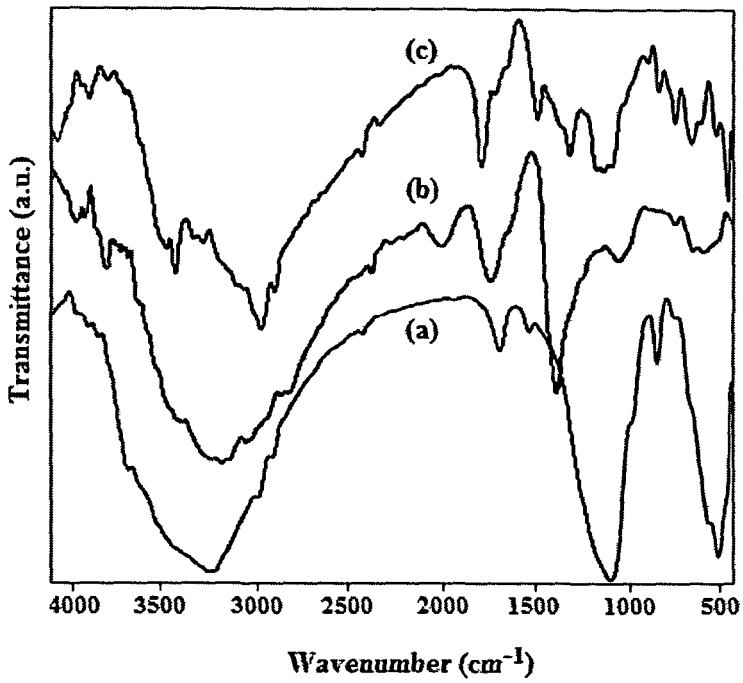

Fig 3.3 Representative FTIR spectra of (a) OMMT nanoclay, (b) PVA-*g*-PAAc copolymer and (c) PVA-*g*-PAAc/OMMT nanocomposite hydrogel.

3.5.2 XRD analysis

XRD experiments were run to gather information on the structure of PVA-*g*-PAAc/OMMT nanocomposite hydrogel. **Fig 3.4** shows the XRD spectrum of the PVA-*g*-PAAc copolymer gel and **Fig 3.5** represents that of the OMMT nanoclay and the nanocomposite hydrogel respectively. A prominent peak is observed near 19.4° (d-spacing of 4.57 Å) in the XRD spectrum of PVA-*g*-PAAc, which corresponds to the (101) plane of the PVA crystal. Other minor peaks around 21 and 22° could be attributed to minor crystallites of grafted polyacrylic acid chains. Pure OMMT displays a diffraction peak at 6.24°, corresponding to a d-spacing of 14.12 Å. But after incorporation of 3.0 wt% of the mineral clay (OMMT) in the polymer matrix, a peak at 4.69° corresponding to a d-spacing of 18.6 Å was found. This increase in d-spacing indicates the increasing of layers spacing due to the intercalation or exfoliation of organophilic clay into the PVA-*g*-PAAc copolymer matrix.

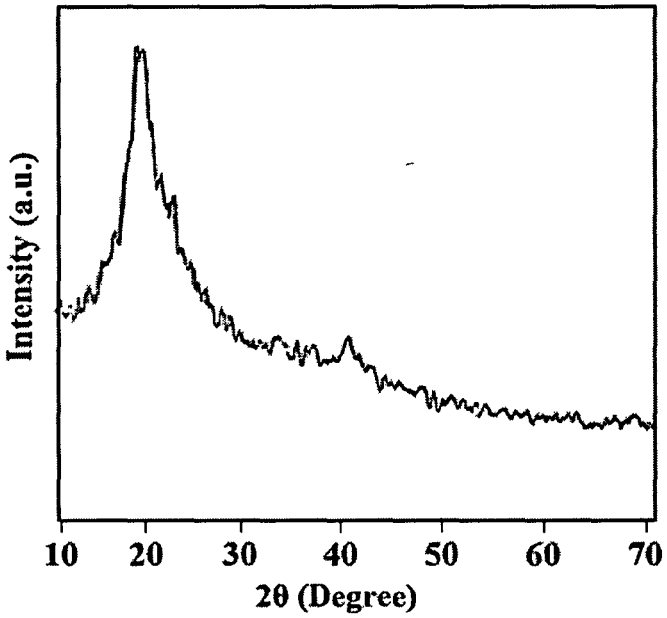

Fig 3.4 XRD pattern of PVA-*g*-PAAc copolymer hydrogel.

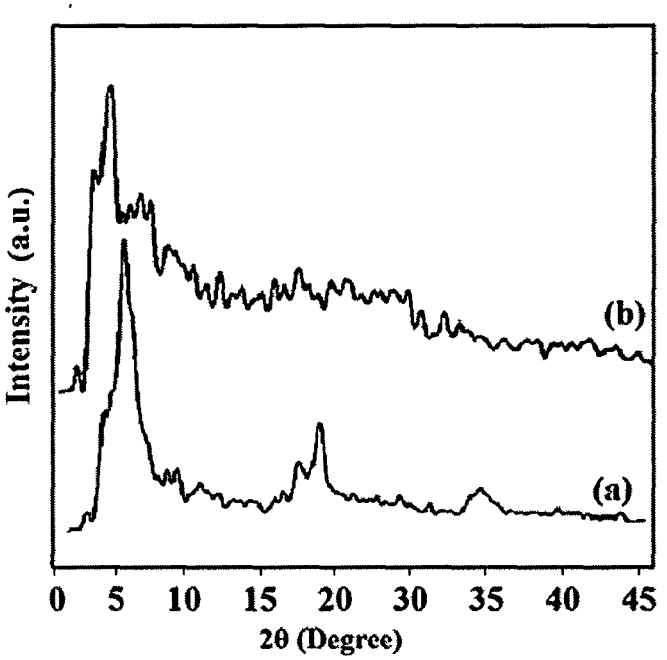

Fig 3.5 XRD patterns of (a) OMMT nanoclay and (b) PVA-*g*-PAAc/OMMT nanocomposite hydrogel.

3.5.3 SEM analysis

One of the most important properties that must be considered is hydrogel composite microstructure morphologies. The morphological image of the nanocomposite hydrogel was studied by SEM. The SEM images in **Fig 3.6** show that the morphology of PVA-*g*-PAAc/OMMT becomes smoother than pure polymer. Also, the clay incorporated hydrogel matrix is found to be filamentous. Since PVA is crystalline in nature. So, this morphological change can be attributed to the re-ordered crystalline phase of the PVA matrix, causing a packed network.

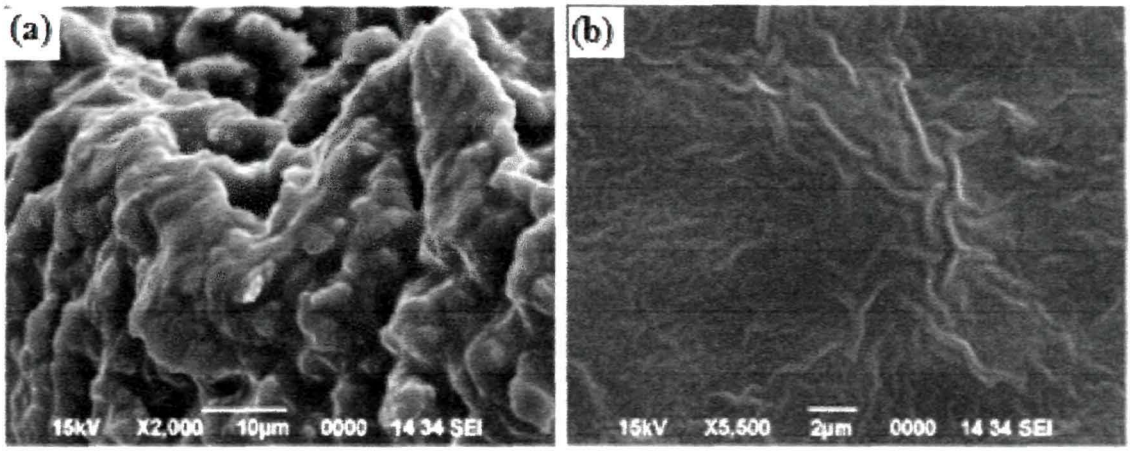

Fig 3.6 SEM micrographs of (a) PVA-*g*-PAAc hydrogel and (b) PVA-*g*-PAAc/OMMT nanocomposite hydrogel.

3.5.4 Thermal behaviour

The thermogravimetic analysis (TGA) of the OMMT nanoclay incorporated nanocomposites and copolymer are shown in **Fig 3.7**. Both TGA curves show a very small weight loss below 100°C, implying a loss of moisture. The initial decomposition for the copolymer starts at 230°C whereas that for clay incorporated polymer was found at 270°C.The major weight loss of the copolymer is found at 340°C, while for the nanocomposite it was found at 415°C. So, it can be concluded that the nanocomposites are thermally more stable. Thus, the incorporation of clay fillers into the polymer matrices results in the improvement of their thermal stability. The clay layers act as superior insulation and mass transport barrier against the volatile compounds generated during the decomposition of polymer under thermal conditions.

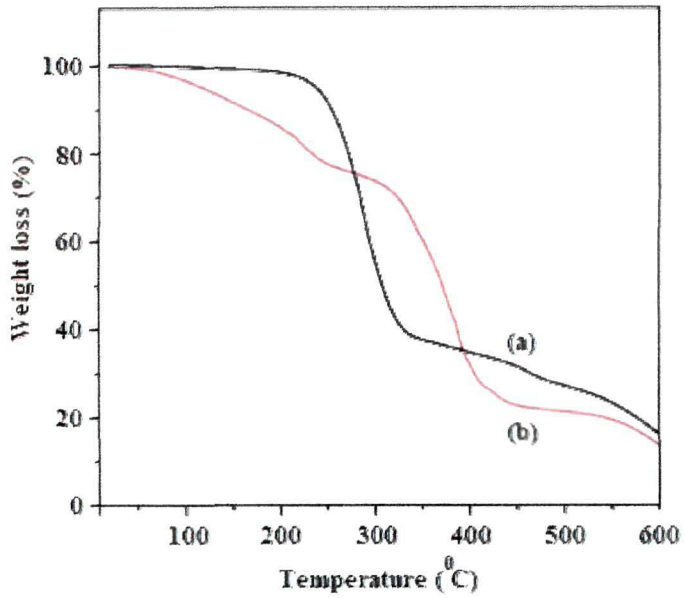

Fig 3.7 TGA curves of (a) PVA-*g*-PAAc/OMMT nanocomposite hydrogel and (b) PVA-*g*-PAAc copolymer hydrogel.

3.5.5 Swelling behaviour

The swelling behavior of hydrogels is a measure of their utility as biomaterials in various fields. **Fig 3.8** represents the swelling behaviour of the composite hydrogels with the variation of crosslinker and with different OMMT content as a function of time, from which some differences can be observed. It was observed that the water absorbency decreased with the increase of clay content. It may be due to the fact that, inorganic clay mineral particle in network acted as an additional network point. The crosslinking density of composite increased with the increase of OMMT content, which resulted in a decrease in water absorbency. **Fig 3.9** represents the influence of clay amount on swelling behaviour of the nanocomposite.

Presence of crosslinker is an important pre-requisite for formation of ideal three-dimensional networks of hydrogels. It was observed that the swelling capacity of the nanocomposite hydrogels decreased with the increase in crosslinker amount. According to Flory's theory, the excessive crosslinking may cause the generation of more crosslinking points during radical polymerization and the increase of crosslinking

density of polymer network.[26] Therefore, the water absorption of the hydrogel was decreased with increasing the concentration of crosslinker.

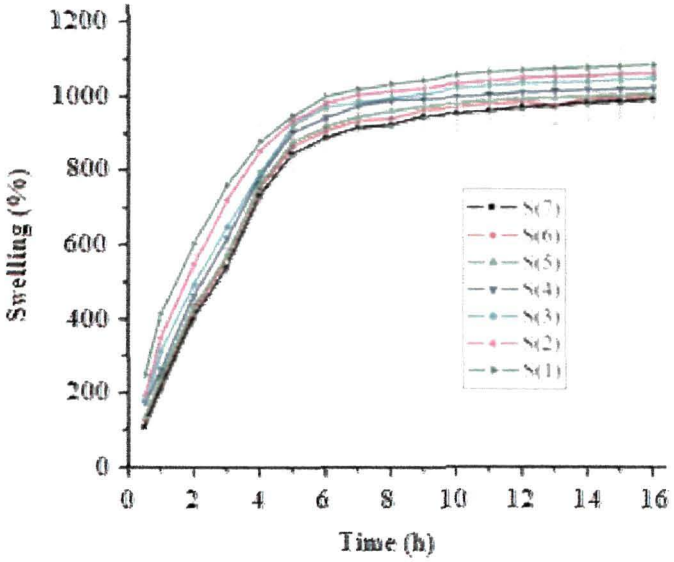

Fig 3.8 Swelling curves of PVA-*g*-PAAc/OMMT nanocomposite hydrogel with various crosslinker amounts.

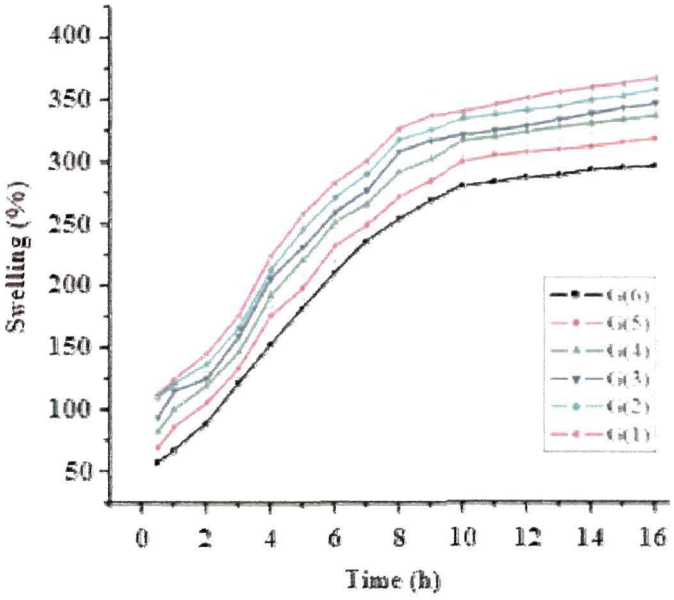

Fig 3.9 Effect of OMMT nanoclay content on the swelling properties of PVA-*g*-PAAc/OMMT nanocomposite hydrogel.

Swelling behaviour is observed to be varied with the network parameters such as the polymer volume fraction in swollen state $v_{2,s}$, molecular weight of the polymer chain between two neighboring crosslinking points ($\overline{M_c}$) and the correlation length or mesh

size (ξ). **Table 3.3** represents the calculated values of these parameters found in case of the prepared nanocomposite hydrogel. It can be seen that mesh size (ξ) decreases with increasing polymer volume fraction and accordingly swelling % decreases. Also, gradual increase of crosslinker leads to a compact network which results low value of ξ and $\overline{M_c}$, indicating that the network meshes were less open with the higher amount of crosslinker. For that, there will be a fall in the swelling percentage of the hydrogels.

Table 3.3 Swelling Kinetics Parameters: polymer volume fraction in swollen state ($v_{2,s}$), number average molecular weight between the crosslinks ($\overline{M_c}$) and the correlation length (ξ) for PVA-*g*-PAAc/OMMT nanocomposite hydrogel:

Sample	GA (mol%)	$v_{2,s}$ (Eqn. 3.2)	ξ, Å (Eqn. 3.6)	$\overline{M_c}$, g/mol (Eqn. 3.5)	'*n*' value
S(1)	0.3	0.256	56.2	1296	0.50
S(2)	0.5	0.288	42.3	1189	0.54
S(3)	0.7	0.317	37.0	1056	0.75
S(4)	0.9	0.330	31.6	994	0.81
S(5)	1.1	0.352	28.8	973	0.87
S(6)	1.3	0.376	22.1	912	0.91

3.5.6 Modelling of the swelling kinetics of the hydrogels

It is well known that the initial water uptake process of hydrogels corresponds to the diffusion of water molecules into the gel network.[24] A simple and useful empirical equation, so-called power law equation, is commonly used to determine the mechanism of diffusion in polymeric networks.

$$M_t/M_\alpha = kt^n \qquad \textbf{Eqn. 3.7}$$

where, M_t and M_α are the weight of the swollen sample at time t and at infinitely equilibrium swollen state, respectively, k is a characteristic constant and n is a characteristic exponent of the mode transport of the water. **Table 3.3** shows the 'n' values obtained for the PVA-*g*-PAAc/OMMT hydrogels. According to the classification of the diffusion mechanism, n - ½ means Fickian and $½ < n < 1$ indicates

an anomalous diffusion model respectively.[27] The '*n*' value was found to be 0.5 in case of the sample with lowest crosslinker amount and it is found to be increased from 0.50-0.94 with increase in crosslinker amount. So, the *n* values found in our work indicate that the transport mechanism for the PVA-*g*-PAAc/OMMT nanocomposite hydrogels changes from Fickian to non-Fickian as the crosslinking density increases.

3.5.7 Bending behaviour under an electric field

The exact mechanism of bending of ionic polymer films has not been fully understood, it is generally thought that the deformation of a hydrogel film under an electric field is due to the voltage-induced motion of ions. When a strip of PVA-*g*-PAAc/OMMT nanocomposite hydrogel, in an aqueous solution of NaCl, was subjected to an electric filed, the hydrogel showed significant and quick bending towards the cathode. Again, if the electric stimulus was removed, it returned to its original position. The same behaviour was not observed in pure water. This implies that the bending of the hydrogels was induced by electro-chemical reactions. The bending behaviors of the hydrogels under different applied voltages are shown in **Fig 3.10**.

It can be seen that both the bending speed and the maximum bending angle of hydrogel increased with the increasing of applied voltage, indicating that bending is induced by an electric current.[28] It is thought that the counterions (cations) of the polyion, which is an ionic group in the polymer network, moves toward the negative electrode. The polyion (anion) remains immobile. The free ions in the surrounding solution move towards their counter electrode and come in contact with the gel. Therefore, the osmotic pressure of the gel polymer network near the positive electrode increases and becomes larger than that of the negative electrode side. Consequently, the osmotic pressure difference occurs within the gel and is the driving force that controls bending toward the negative electrode. The effect of voltage on bending phenomenon has been investigated in the range 3.0 to 12.0 V. No bending was observed below 3.0 V; so, lower critical voltage (LCV) found in this case is 3.0 V.

The influence of the medium ionic concentration on the bending behavior of the nanocomposite hydrogels were determined by varying the concentrations of aqueous NaCl solution from 0.05 N to 0.2 N respectively. It was observed that the bending degree increased when the concentration of aqueous NaCl solution was increased from 0.05 N to 0.1 N, but again decreased when concentration of NaCl exceeds 0.1 N. May be, an increase in the electrolyte concentration in a solution induces an increase of the free ions moving from the surrounding solution toward their counter electrode or into the hydrogel.

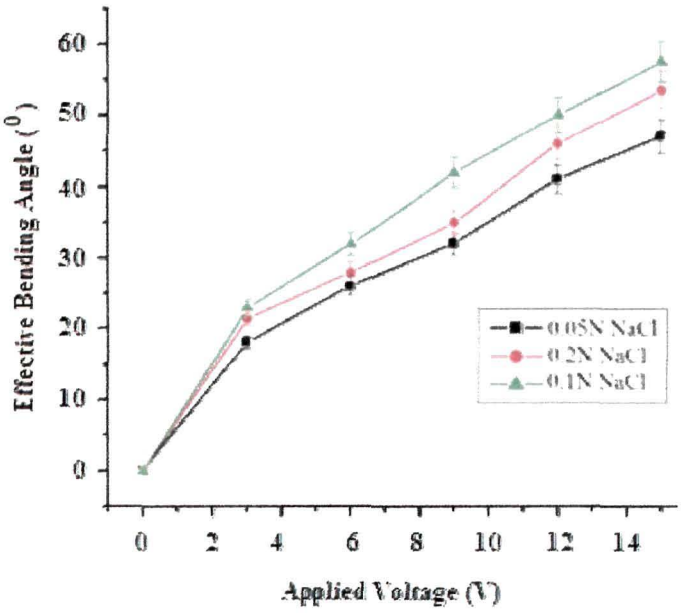

Fig 3.10 Effect of aqueous NaCl solution concentration on the equilibrium bending angle (EBA) at different applied voltages.

So, the bending degree of the hydrogel increased when concentration of NaCl was increased from 0.05 N to 0.1 N. But after an optimum electrolyte concentration, the shielding effect of the polyions by the ions in the electrolytic solute occurs which leads to a reduction in the electrostatic repulsion of the polyions and a decrease in the degree of bending. A similar result was reported in our previous study of bending behaviors of composite hydrogels composed of poly(acrylamide-*co*-acrylic acid) and polyaniline.[29]

3.6 Conclusion

- Nanocomposite hydrogels based on PVA, partially neutralized acrylic acid and organically modified OMMT clay were prepared by free radical graft polymerization reaction and the grafting of acrylic acid on PVA was confirmed by FTIR analysis.
- X-ray diffraction analysis showed that the nanocomposite forms a partially exfoliated or intercalated structure. Also, SEM studies demonstrated a finer dispersion of the *clay particles in nanocomposite.*
- From thermogravimetric analysis, it was observed that introduction of OMMT to the polymer network results in an increase in thermal stability.
- Since, crosslinking density of composite increased with the increase of OMMT content, so there was decrease in water absorbency with an increase in OMMT content.
- Swelling kinetics of the prepared hydrogels shows that transport mode of water in the nanocomposite hydrogels exhibited Fickian diffusion which gradually changes to non-Fickian diffusion with increase in crosslinker amount.
- The nanocomposite hydrogels showed significant and quick bending towards the cathode under an applied electric field.
- The observed behaviour suggest the possible applications of PVA-*g*-PAAc/OMMT nanocomposite hydrogels as artificial muscle, sensors, switches and electric current modulated drug delivery systems etc.

References

1. Kosemund, K., et al. *Regul. Toxicol. Pharm.* **53** (2), 81-89, 2009.
2. Chang, C., et al. *Eur. Polym. J,* **46** (1), 92-100, 2010.
3. Reddy, N.N., et al. *Colloid Surf. A: Physicochem. Eng. Aspects* **385** (1), 20-27, 2011.
4. Liang, R., et al. *Carbohydr. Polym.* 77 (2), 181-187, 2009.
5. Wang, L., et al. *Colloid Surf. A, Physicochem. Eng. Aspects* **322** (1-3), 47-53, 2008.
6. Orozco-Guareno, E., et al. *J. Colloid Interface Sci.* **349** (2), 583-593, 2010.
7. Kuckling, D., et al. *Macromol. Mater. Eng.* **288** (2), 144-151, 2003.
8. Kim, S.Y., et al. *J. Appl. Polym. Sci.* **73** (9), 1675-1683, 1999.
9. Kim, S.J., et al. *J. Appl. Polym. Sci.* **86** (9), 2285-2289, 2002.
10. Li, A., et al. *J. Appl. Polym. Sci.* **92** (3), 1596-1603, 2004.
11. Kawasumi, M., et al. *Macromolecules* **30** (20), 6333-6338, 1997.
12. Pavlidou, S., & Papaspyrides, C.D. *Prog. Polym. Sci.* **33** (12), 1119-1198, 2008.
13. Changa, J.H., et al. *Polymer* **44** (13), 3715-3720, 2003.
14. Chang, J.H., et al. *J. Polym. Sci. B Pol. Phys.* **41** (1), 94-103, 2003.
15. Giannelis, E.P., et al. *Adv. Polym. Sci.* **138,** 107-147, 1999.
16. Ramsay, J.D.F., et al. *J. Chem. Soc. Faraday Trans.* **86,** 3919-3926, 1999.
17. Wu, J.H., et al. *Macromol. Rapid. Commun.* **21** (15), 1032-1034, 2000.
18. Zhang, J.P., et al. *Eur. Polym. J.* **41** (10), 2434-2442, 2005.
19. Kim, S.J., et al. *React. Funct. Polym.* **55** (3), 291-298, 2003.

20. Sun, S., & Mak, A.F.T. *J. Polym. Sci. B Polym. Phy.* **39** (2), 236-246, 2001.

21. Peppas, N.A. & Mikos, A.G. Preparation, methods and structure of hydrogels, in *Hydrogels in medicine and pharmacy,* N.A. Peppas et al. eds., CRC Press, Boca Raton, 1986, 1-27.

22. Samakande, A., et al. *Polymer* **48** (6), 1490-1499, 2007.

23. Zheng, Y., & Wang, A. *Polym. Compos.* **30** (8), 1138-1145, 2009.

24. Hickey, A.S., & Peppas, N.A. *Polymer* **38** (24), 5931-5936, 1997.

25. Jin, X., & Hsieh, L.Y. *Polymer* **46** (14), 5149-5160, 2005.

26. Flory, P.J. *Principles of Polymer Chemistry,* Cornell University Press, Ithaca, 1992.

27. Crank, J. *The Mathematics of Diffusion*, Oxford University Press, Oxford, 1975.

28. Boruah, M., et al. *Polym. Compos.* **35** (1), 27-36, 2014.

29. Boruah, M., et al. *Adv. Polym. Technol.* **32** (S1), E520-E530, 2013.

CHAPTER 4

pH-responsive, biocompatible carboxymethylcellulose-g-poly(acrylic acid)/OMMT nanocomposite hydrogels for in vitro release of vitamin B_{12}.

GRAPHICAL ABSTRACT

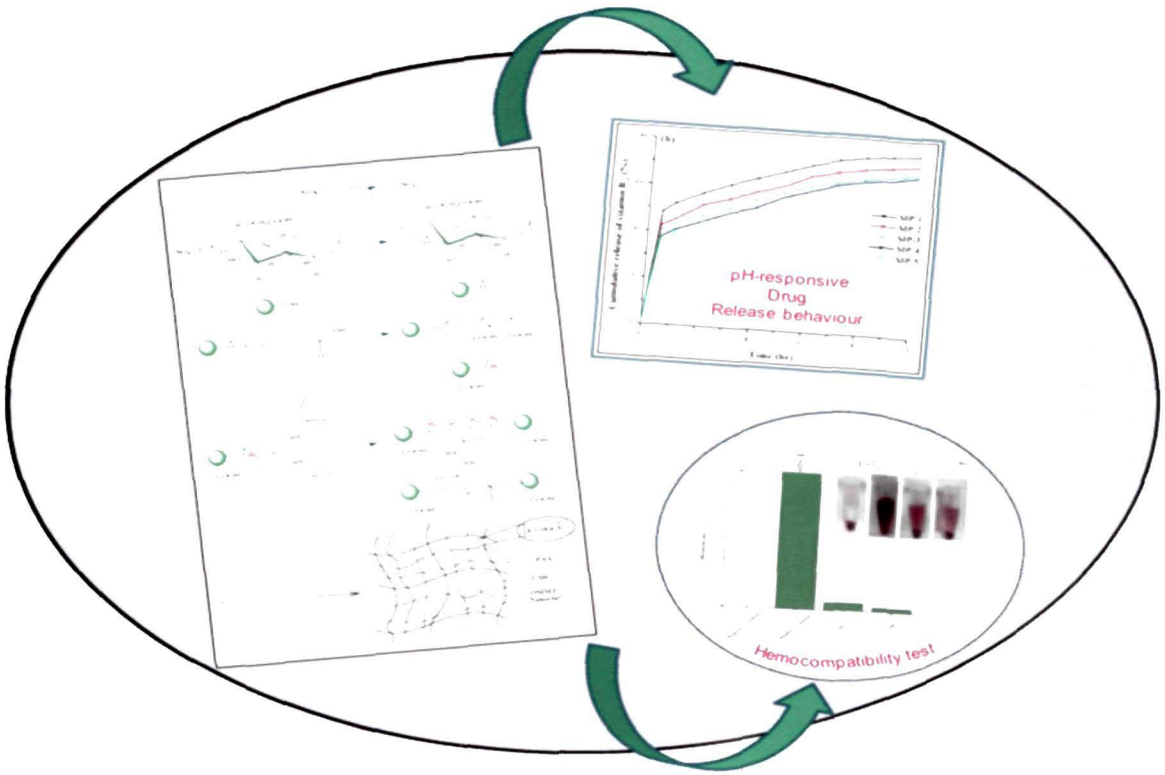

4.1 Introduction

In recent years, stimuli-responsive polymeric hydrogels have attracted attention as 'intelligent materials' because of their ability to mimic natural systems. They can sense a stimulus as a signal and give rise to volume changes in response to small changes in external stimuli, such as solvent composition,[1] temperature,[2] pH,[3] salt concentration,[4] electrical pulses[5] etc. Amongst the stimuli-responsive systems, pH-responsive hydrogel has been extensively studied in the biomedical field because the pH can be easily controlled and is applicable both in vitro and in vivo conditions.[6]

Carboxymethyl cellulose (CMC) is a type of cellulose derivative with carboxymethyl groups (-CH_2-COOR) bound to some of the hydroxyl groups present on the cellulose backbone. It can be easily produced by the alkali-catalyzed reaction of cellulose with chloroacetic acid. The polar carboxyl groups provide solubility, chemical reactivity to cellulose and make it strongly hydrophilic in nature. But, the main disadvantage of natural polymer based hydrogels is their poor mechanical properties due to extensive swelling. To get rid of this problem, attempts have been made to modify their structures by the incorporation of different nanofillers, grafting,[7] developing interpenetrating polymer networks[8] (IPNs) or by physical blending with other polymers.[9] Poly(acrylic acid) is a hydrophilic polymer owing to the existence of hydrophilic -COOH group and it has the capacity to absorb large amounts of water. For this reason, poly(acrylic acid) has been extensively used in controlled drug delivery system.

Nanocomposites exhibit superior properties when compared to micro- and macro-composites. The strong interfacial interactions between the dispersed clay layers and the polymer matrix give rise to improved mechanical and thermal properties than that of the virgin polymer.[10]

A part of this chapter is published

M. Boruah, P. Gogoi, A.K. Manhar, M. Khannam, M. Mandal & S.K. Dolui. *RSC Adv.* **4**, 43865-43873, 2014.

Clays have been widely utilized in this field due to improved performance and low cost.[11] Montmorillonite (MMT) is smective-type clay composed of an expandable 2:1 type of aluminosilicate clay mineral which has a layered structure and also relatively high cation exchange capacity, large specific surface area, good swelling capacity and high platelet aspect ratio.[12] The organic cations can enter into the surface of clay by cation exchange reaction and clay can be modified into organophillic in nature.[13]

Biocompatibility is a prime requirement for the development of functional biomaterials. It is governed mainly by the interface between foreign materials and host living cells/tissues. So, fundamental aspect of any biocompatibility evaluation is to know the effects of the polymers on living cells.[14] Thus, suitability of a hydrogel for biological applications can be confirmed by determining the potential toxicity of all materials which have been used for fabrication of gel.

Now-a-days, researchers are concentrating on developing natural polysaccharide based hydrogels due to their enhanced pH-responsive characteristics.[15] Sadeghi et al. reported the novel CMC-*g*-(PNVP-*co*-PAMPS) based hydrogels for the controlled release of metronidazole. They investigated the release behavior of metronidazole from this kind of responsive hydrogel by control of pH of the surrounding environment.[16] Wang et al. synthesized a series of carboxymethyl cellulose/organic montmorillonite (CMC/OMMT) nanocomposites and studied their adsorption behavior for Congo red dye from wastewater. MMT clay was organically modified by using cetyl trimethylammonium bromide (CTAB). The prepared nanocomposites exhibited improved thermal properties. The effect of various parameters such as CTAB content, weight ratio of CMC to OMMT, reaction time and reaction temperature on adsorption behaviour of congo red dye was thoroughly investigated.[17] Also, Irani et al. synthesized linear low-density polyethylene-*g*-poly(acrylic acid)/organo-montmorillonite superabsorbent hydrogel composites. They determined the optimum reaction conditions and effect of different parameters on the swelling behaviour of the superabsorbent hydrogels along with the equilibrium swelling. The gel strength of the nanocomposite hydrogel was increased with the increase in OMMT content.[18]

To combine the advantages of synthetic and natural polymers and at the same time maintain the beneficial properties of natural polymers, we have prepared pH-sensitive hydrogels based on carboxymethylcellulose, acrylic acid and organically modified MMT nanoclay for the controlled release of vitamin B_{12}. It is a water-soluble vitamin with a key role in the normal functioning of the brain and nervous system and for the formation of blood. Therefore, Vitamin B_{12} was chosen as a model drug. This chapter deals with in vitro release studies on nanocomposite hydrogel formulations loaded with different amounts of vitamin B_{12}. The drug release kinetics was studied and effect of pH and crosslinker content on the release behavior of the prepared hydrogels have been determined.

4.2 Experimental

4.2.1 Materials

Acrylic acid monomer (Aldrich) was distilled under reduced pressure prior to use. Carboxymethylcellulose was supplied by Aldrich (M_w = 2,50000). Potassium persulfate (KPS, analytical grade), methylene bis-acrylamide (MBA, chemically pure) as a crosslinking agent, montmorillonite nanoclay, and N, N, N', N'- tetramethylethylene diamine were supplied by Aldrich (A.R. grade). Cetyltrimethylammonium bromide (CTAB) was supplied by G.S Chemical testing lab & allied industries, New Delhi. Sodium hydroxide and ethanol (A. R grade) were purchased from Merck, Mumbai. Vitamin B_{12} ($C_{63}H_{88}CoN_{14}O_{14}P$) was purchased from Merck, Mumbai (M.W= 1355.4 g/mol).

4.3 Synthesis of carboxymethylcellulose-*g*-poly(acrylic acid)/OMMT nanocomposite hydrogel

4.3.1 Preparation of organo-MMT nanoclay

The organophilic MMT-nanoclay was prepared by treating the pristine clay with cetyltrimethylammonium bromide (CTAB) as reported elsewhere.[19] 3 g of pristine clay was dispersed in 250 ml of deionized water under vigorous stirring. Then, a solution of

CTAB (1.318 g in 100 ml of deionized water) was slowly added to the dispersion, under continuous stirring for 6 hrs. The dispersion was filtered and obtained product was thoroughly washed with deionized water. To determine the presence of released counterions, samples of the filtrate were taken in regular intervals and tested with 0.1 M silver nitrate solution. Washing was stopped only when the filtrate did not give a positive test to silver nitrate. The washed product was dried overnight under reduced pressure (vacuum) at 40°C and finally ground in a mortar.

4.3.2 Preparation of CMC-*g*-PAAc/OMMT nanocomposite hydrogels

Carboxymethylcellulose-*g*-poly(acrylic acid)/OMMT nanocomposite hydrogels were prepared by free radical polymerization in distilled water. 2 g of CMC was dissolved in 30 ml of double distilled water and 1.5 ml of partially neutralized (60%) acrylic acid monomer in 10 ml of double distilled water was added to it. Also, a certain amount of OMMT nanoclay (0-20 wt%) was immersed in 5 ml of deionized water for 2 hrs and dispersed under the ultrasonic vibration for 30 min. Both the solutions were mixed well and subsequently, methylene bis-acrylamide (0.05-0.25 wt%), potassium persulfate (0.1-1.0 wt%) and TEMED (0.05 ml) were added to the mixture under continuous stirring. Nitrogen was used to remove dissolved oxygen from the reactive solution. The reactive solution was first prepolymerizd at 70°C for 30 min under stirring, and then poured into a petri dish quickly. The post polymerization was carried out at 65°C for 15 hrs. When the reaction completed, the nanocomposite hydrogel was cut into the same size (3×4 cm) and immersed in repeatedly changed deionized water for 72 hrs to remove the residual monomers. **Tables 4.1-4.3** outline the feed compositions of subsequently prepared hydrogels. Also, the formation of nanocomposite hydrogel has been presented in **Fig 4.1**.

Table 4.1 Recipe in the preparation of CMC-*g*-PAAc/OMMT nanocomposite hydrogel with the variation of initiator (KPS):

Recipe	CP-1	CP-2	CP-3	CP-4	CP-5
Carboxymethyl cellulose (g)	2	2	2	2	2
Acrylic acid (ml)	1.5	1.5	1.5	1.5	1.5
Methylene bis-acrylamide (wt%)	0.2	0.2	0.2	0.2	0.2
Potassium persulfate (wt%)	0.1	0.3	0.5	0.8	1.0

Tetramethylethylene diamine (ml) = 0.05 ml, OMMT (wt %) = 10.

Table 4.2 Recipe in the preparation of CMC-*g*-PAAc/OMMT nanocomposite hydrogel with the variation of crosslinker (MBA) and '*n*' value:

Recipe	MP-1	MP-2	MP-3	MP-4	MP-5
Carboxymethyl cellulose (g)	2	2	2	2	2
Acrylic acid (ml)	1.5	1.5	1.5	1.5	1.5
Methylene bis-acrylamide (wt%)	0.05	0.1	0.15	0.2	0.25
'n' value determined	0.63	0.71	0.78	0.83	0.87

Potassium persulfate (wt%) = 0.5, tetramethylethylene diamine (ml) = 0.05 ml and OMMT (wt%) = 10.

Table 4.3 Recipe in the preparation of CMC-*g*-PAAc/OMMT nanocomposite hydrogel with the variation of organo-MMT nanoclay content and gel fraction:

Recipe	NP-1	NP-2	NP-3	NP-4	NP-5
Carboxymethyl cellulose (g)	2	2	2	2	2
Acrylic acid (ml)	1.5	1.5	1.5	1.5	1.5
Methylene bis-acrylamide (wt%)	0.2	0.2	0.2	0.2	0.2
Organo-MMT nanoclay (wt%)	0	5	10	15	20
Gel Fraction (%) determined	74	78	84	89	93

Potassium persulfate (wt %) = 0.5 and tetramethylethylene diamine (ml) = 0.05 ml.

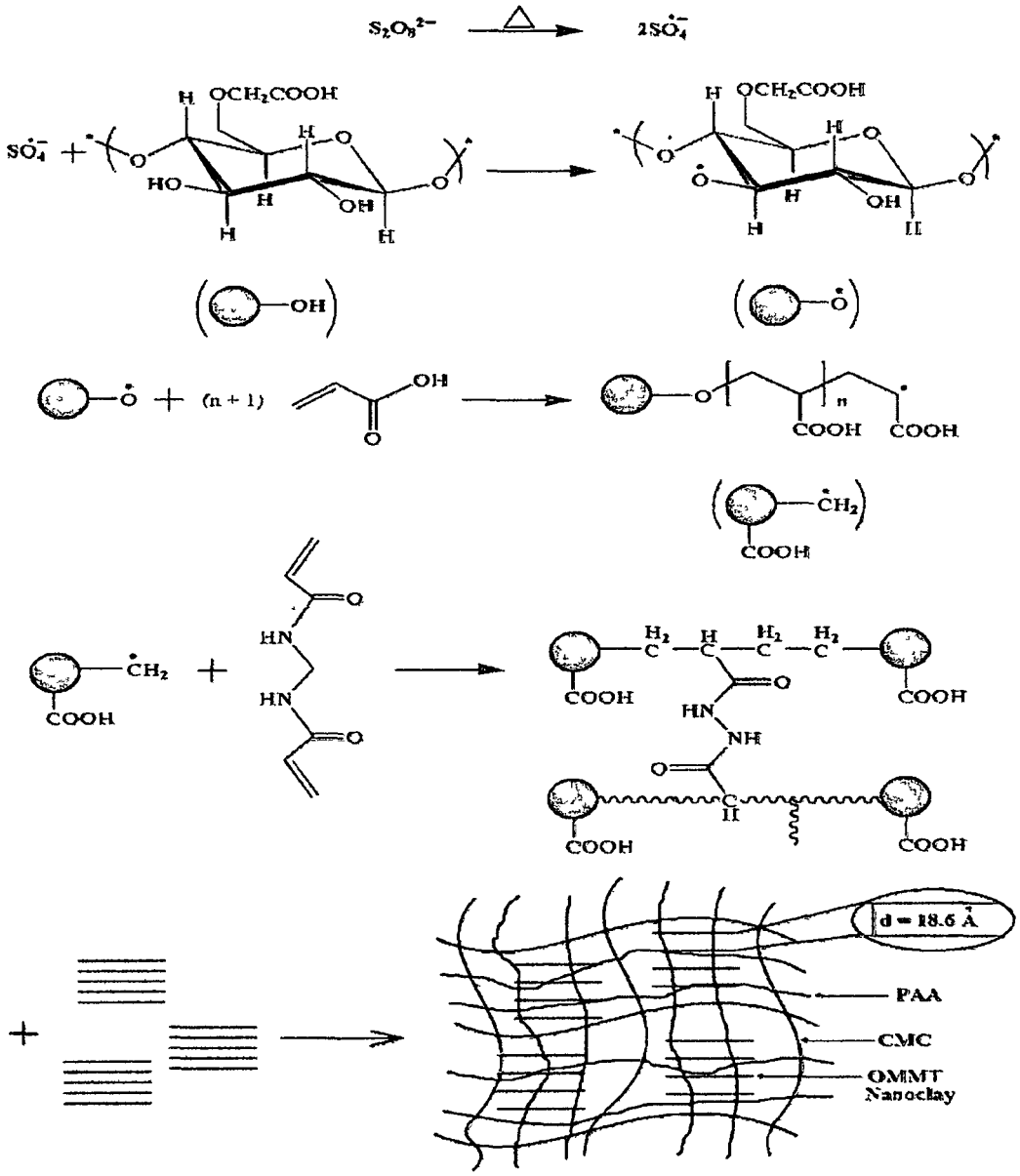

Fig 4.1 Proposed reaction mechanism for the formation of CMC-*g*-PAAc/OMMT nanocomposite hydrogels.

4.4 Characterization

4.4.1 Fourier transform infrared spectrometer (FTIR)

To gain insights into the structural information of prepared hydrogels, the IR spectra of the hydrogels were recorded with a Nicolet Impact-410 IR spectrometer (USA) in KBr medium at room temperature in the region 4000–450 cm^{-1}

4.4.2 Powder X-ray diffractometer (XRD)

Powder X-Ray diffraction (XRD) data were collected on a Rigaku Miniflex X-ray diffractometer (Tokyo, Japan) with Cu Kα radiation (λ=0.15418 Å) at 30 kV and 15 mA with a scanning rate of $0.05^{o}s^{-1}$ in a 2θ ranges from 10°-70° for the native gel and 0-45° for OMMT nanoclay and nanocomposite hydrogel.

4.4.3 Scanning Electron Microscope (SEM)

The surface morphology of the composites was observed using a scanning electron microscope (SEM) (Model- JSM-6390LV, JEOL, Japan). The surface of the sample was platinum coated before SEM analysis.

4.4.4 Dynamic Mechanical Analysis

The mechanical properties of the hydrogels were determined by dynamic mechanical analysis (DMA). The equilibrated swollen hydrogel samples were used for the measurement. The samples were cut in cylindrical shapes with about 6 mm diameter and 4 mm thickness. The samples were then loaded into a DMA (PerkenElmer DMA 8000), which applied a sinusoidally oscillating tensile strain, measured the resulting force waveform, and using the input geometrical parameters determined the resulting stress waveform. The frequency sweeping test experiments were performed under constant strain amplitude (1%) at frequency range 0.1 Hz to 10 Hz and storage moduli G' and loss moduli G'' were monitored as a function of frequency. In DMA, dynamic stress and dynamic strain are obtained describing the viscoelastic behavior of a material. The dynamic modulus, G^*, is defined as:

$$G^* = G' + iG'' \qquad \textbf{(Eqn. 4.1)}$$

where, G' = storage modulus, G'' = loss modulus.

4.4.5 Swelling properties

To measure the degree of swelling the hydrogels, dried samples were placed in buffer media of different pH values at room temperature until the hydrated gels reached a

stable weight. The water absorbed on the surface of the hydrogels was removed using filter paper and the weight noted.

$$Swelling\ \% = W_s - W_{dry}/W_{dry} \times 100 \quad \textbf{(Eqn. 4.2)}$$

where, 'W_s' is the weight of the hydrogels in swollen state and 'W_{dry}' is that of the hydrogels in dry state.

4.4.6 Gel fraction

The weight ratio of the dried hydrogels in rinsed and unrinsed conditions can be assumed as an index of degree of crosslinking or gel fraction. The pieces of hydrogel samples (3×3 cm) were dried for 6 hrs at 50°C under vacuum. Same sample (3×3 cm) was immersed into excess of DDW for 4 days to rinse away unreacted parts. The gels were dried again at 50°C under vacuum. The gel fraction percentage was calculated by the following equation[20]:

$$Gel\ fraction\ \% = W_f / W_i \times 100 \quad \textbf{(Eqn. 4.3)}$$

where, W_i = Initial weight before rinse and W_f = Final weight after rinse.

4.4.7 Blood compatibility by hemolytic activity assay

The hemolytic test was performed following the protocol of Das Purkayastha, M. et al. with slight modification.[21] Briefly, fresh goat blood from a slaughterhouse was collected in a centrifuge tube containing anticoagulant, trisodium citrate (3.2%) and was centrifuged at 2500 rpm for 10 min. The supernatant was discarded and only the erythrocytes were collected. The erythrocytes were further washed three times with PBS (pH 7.4). A 5% (v/v) suspension of erythrocytes in PBS was prepared; 0.95 ml of this erythrocyte solution was placed in a 1.5 ml centrifuge tube and 0.05 ml of sample (0.5 mg dissolved in 1 ml of 0.5 % DMSO) was added to it. The tubes were then incubated for 1 hr at 37°C. Triton X-100 (0.2 %) and PBS were taken as the positive and negative controls, respectively, for comparison. After incubation, the tubes were subjected to centrifugation at 2500 rpm for 10 min. Then, 0.2 ml of the supernatant was added to 96-well plate and

finally absorbance was taken at 570 nm in a UV–visible spectrophotometer (Shimadzu UV-2550 UV–visible spectrophotometer).

Hemolysis % = [(Sample O.D – Negative control O.D)/ (Positive control O.D – Negative control O.D] X 100 **(Eqn. 4.4)**

4.4.8 Loading of vitamin B_{12}

The method of soaking or equilibration was employed for vitamin B_{12} loading. In this method the amount of buffer necessary for complete swelling of the nanocomposite hydrogel was determined.[22] Dry hydrogel was placed in the drug solution at a concentration of 0.125 wt%, prepared in the buffer solution of pH 7.0 and left until all the drug solution was sucked up. Then the completely swollen hydrogel loaded with the vitamin B_{12} was placed in an oven at 30°C for drying overnight.

4.4.9 In vitro drug release studies

The dried vitamin B_{12} loaded hydrogel was immersed into 30ml solution of different pH, namely, 1.2 and 7.4. At scheduled time intervals, 5ml solution was withdrawn and assayed spectrophotometrically at 362 nm by using a UV-visible spectrophotometer (UV-2001Hitachi, Japan) for the determination of the cumulative amount of drug release. To maintain a constant volume, 5 ml of distilled water and the solution having same pH was returned to the container. The amount of vitamin B_{12} released from the nanocomposite hydrogel was calculated from a calculated from a previously calibrated standard curve.[23]

4.5 Results and discussion

4.5.1 FTIR analysis

To investigate the formation of CMC-*g*-PAAc/OMMT nanocomposite, FTIR spectra of OMMT nanoclay, CMC-*g*-PAAc copolymer and CMC-*g*-PAAc/OMMT nanocomposite hydrogels are shown in the **Fig 4.2**. In the FTIR spectrum of OMMT, a broad band centered near 3400 cm^{-1} is due to the –OH stretching mode of the interlayer water. The overlaid absorption peak in the region of 1637 cm^{-1} is assigned to the –OH bending mode of adsorbed water. The characteristic peak at 1108 cm^{-1} is due to the Si–O–Si stretching and out of plane Si–O–Si stretching mode for montmorillonite. The band in

the region of 830 cm^{-1} is due to the Si–O–Al stretching mode for montmorillonite. The FTIR peak at 522 cm^{-1} is assigned to the Si–O–Al bending vibration **(Fig 4.2a)**.

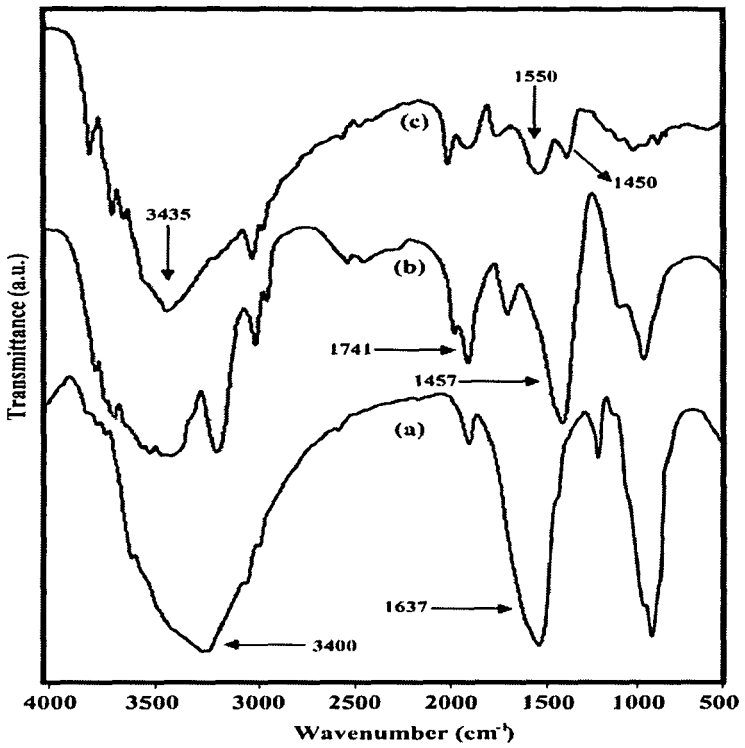

Fig 4.2 FTIR spectra of (a) Pure OMMT nanoclay, (b) CMC-*g*-PAAc copolymer and (c) CMC-*g*-PAAc/OMMT nanocomposite hydrogels.

Also, the FTIR spectrum of CMC-*g*-PAAc copolymer **(Fig 4.2b)** shows characteristics peaks at 1741 cm^{-1} due to the presence of C=O stretching vibration and the peak observed at 613 cm^{-1} is due to the -OH out of plane vibration of the carboxylic groups of PAAc, which confirms the grafting reaction. The characteristic peaks at 3552 cm^{-1} and 3431 cm^{-1} are due to -OH stretching vibration of CMC and PAAc, respectively, which also confirms the grafting of PAAc onto CMC backbone. Other characteristics peaks at 1657 and 1457 cm^{-1} are assigned to the asymmetrical and symmetrical stretching of $-COO^-$ groups.

In the FTIR spectrum of nanocomposite hydrogel, it has been observed that the spectrum of CMC-*g*-PAAc/OMMT nanocomposite hydrogel shows variations in intensity and shifting of peak from 3552 to 3435.8 cm^{-1} appear due to -OH stretching vibration of

CMC. The intensities of peaks due to Si–O and Al–O of MMT are reduced as shown in **Fig 4.2c**. It can be explained that –OH of MMT could react with acrylic monomer and MMT particles chemically bond with the polymer chains to form the CMC/polymer/OMMT network.[24] The very intense characteristic band at 1550 cm^{-1} is due to C=O asymmetric stretching in carboxylate anion that is reconfirmed by the peak at 1450 cm^{-1} which is related to the symmetric stretching mode of the carboxylate anion.

4.5.2 XRD analysis

XRD experiments were run to gather information on the structure of CMC-*g*-PAAc/OMMT nanocomposite hydrogel. Pure OMMT **(Fig 4.3)** displays a diffraction peak at 6.24°, corresponding to a d-spacing of 14.12 Å, but the presence of 4.0 wt% of the mineral clay (OMMT) in the polymer matrix resulted in a shift of this diffraction peak towards smaller angle 2θ= 4.69° corresponding to a d-spacing of 18.6 Å. This increase in d-spacing indicates the increasing of layers spacing due to the intercalation or exfoliation of organophilic nanoclay into the CMC-*g*-PAAc copolymer matrix.

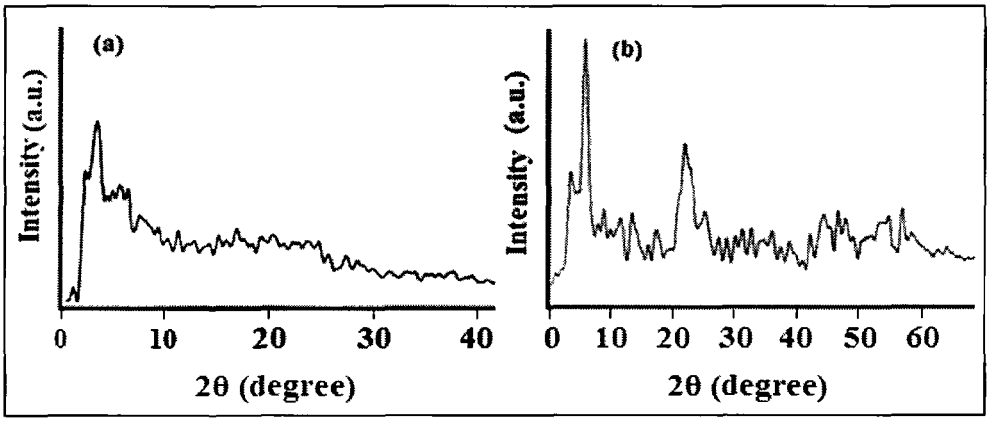

Fig 4.3 XRD patterns of (a) Pure OMMT nanoclay and (b) CMC-*g*-PAAc/OMMT nanocomposite hydrogels (10 wt% OMMT nanoclay).

4.5.3 SEM analysis

The morphological images of the copolymer hydrogel and OMMT nanoclay incorporated hydrogels were studied by SEM and are shown in the **Fig 4.4**. These micrographs indicate the change in the surface morphology of the prepared hydrogels

after the incorporation of nanoclay. A rough surface morphology is observed and some pores and gaps can be observed in the micrograph of OMMT nanoclay incorporated hydrogel. This observation implies that incorporating OMMT nanoclay is favourable to improve the surface structure of the hydrogel

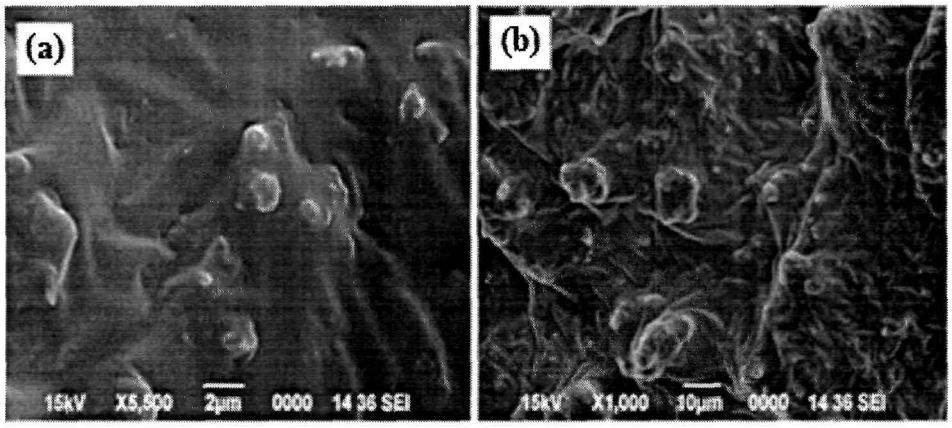

Fig 4.4 SEM images of (a) CMC-*g*-PAAc copolymer and (b) CMC-*g*-PAAc/OMMT nanocomposite hydrogels (10 wt% OMMT nanoclay).

4.5.4 Mechanical properties

Dynamic mechanical analysis was performed on the nanocomposite hydrogel to provide quantitative information on the viscoelastic and rheological properties of the hydrogel by measuring the mechanical response of the samples as they are deformed. **Fig 4.5** depicts the isothermal DMA-response of the nanocomposite hydrogels as a function of frequency in terms of storage modulus (G') and loss modulus (G''). The elastic component (G') is related with the stiffness of the material, while G'' (the viscous component) is associated with the dissipation of energy, as heat, due to internal friction at the molecular level.

It was observed, for all the compositions, that the storage (G') tends to increase with increasing frequency. It was also observed that the elastic modulus increased significantly with the increase amount of nanoclay content, indicating that the nanoclay (OMMT) acts as additional crosslinking agent and improves the stiffness of the nanocomposite hydrogels. Lima et al. developed stimuli-responsive chitosan-starch injectable hydrogels combined with encapsulated adipose-derived stromal cells with better mechanical

properties. They found that for all the compositions, the storage modulus (G') tends to increase with increasing frequency.[25]

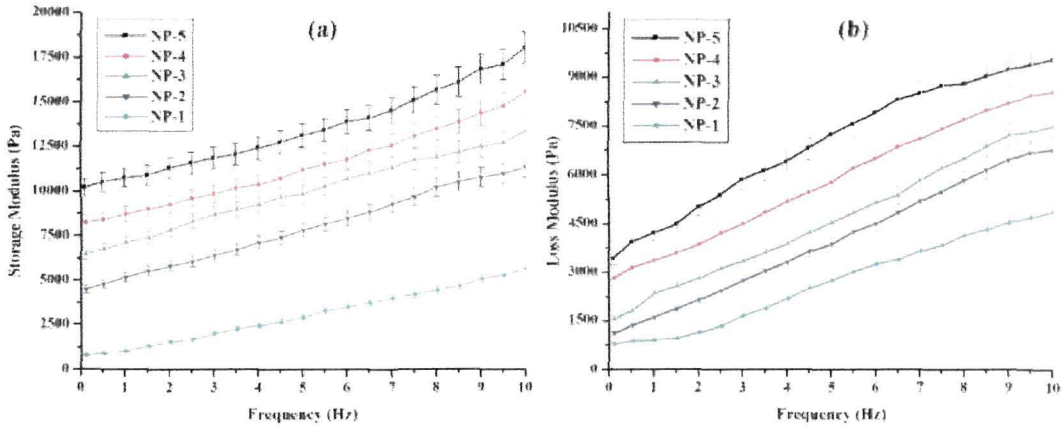

Fig 4.5 Dynamic mechanical analysis of CMC-*g*-PAAc/OMMT nanocomposite hydrogels as a function of frequency: (a) Storage Modulus (*G'*) and (b) Loss Modulus (*G''*) with OMMT nanoclay content from 0-20 wt%.

The loss modulus was also dependent on the cross-linking density and in the whole range of deformation the loss moduli was also increased with the increasing nanoclay content but lower than the storage modulus as the elastic properties dominate. The maximum G' of the nanocomposite hydrogel reached 18, 020 Pa at γ = 1%, ω = 10 Hz and 20 wt% OMMT nanoclay and the maximum value of G'' was 9,566 Pa at γ = 1%, ω = 10 Hz and 20 wt% OMMT nanoclay content, which was remarkably lower than the value for G'. However, larger values of G' and G'' were observed for the clay incorporated hydrogel indicating the improved mechanical properties. The values indicate the formation of a strong nanocomposite hydrogel.

4.5.5 Swelling properties of the hydrogels

4.5.5.1 Effects of initiator content

It was observed that the swelling behavior increased initially with the increase in initiator (KPS) content from 0.1 wt% to 0.5 wt% but tends to decrease with further increase in KPS content. Because, with increase in KPS content, the 3D network of the hydrogel form effectively due to an increase in the number of radicals produced. So, the

swelling capacity increases. **Fig 4.6a** depicts the effect of initiator content on swelling behavior of CMC-*g*-PAAc/OMMT nanocomposite hydrogels.

4.5.5.2 Effects of crosslinker content

The swelling behaviors of nanocomposite hydrogel with 0.05, 0.1, 0.15, 0.2 and 0.25 % crosslinker content (MBA) are shown in **Fig 4.6b**. It was observed that higher crosslinker content resulted in the generation of more crosslink points, which, in turn, caused the formation of an additional network and decreased the available free volume within the nanocomposite hydrogel. So, it can be observed that there is a decrease in swelling percentage with 0.05-0.15 wt% of methylene bis-acrylamide.

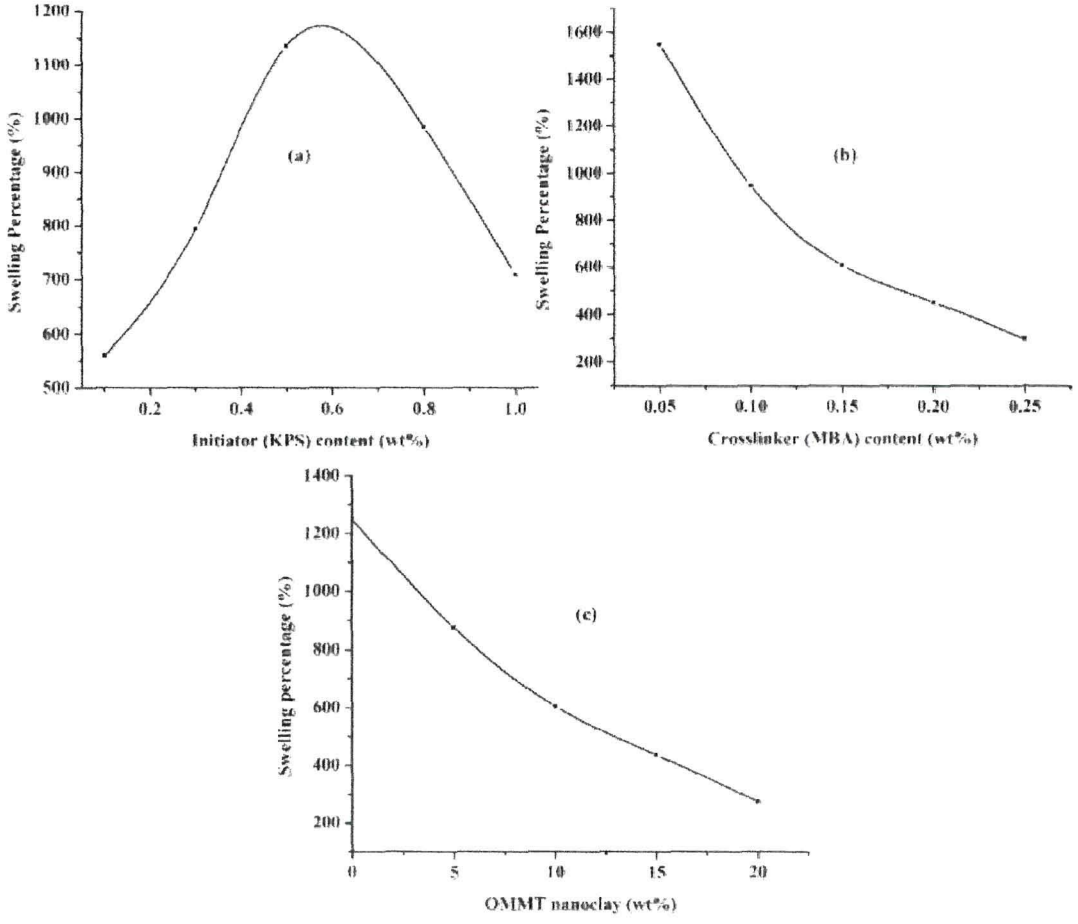

Fig 4.6 Influence of preparation conditions on the swelling behaviours of the nanocomposite hydrogels: (a) KPS content, (b) MBA content and (c) OMMT-nanoclay content.

4.5.5.3 Effects of nanoclay content

The water absorbency of the nanocomposite hydrogels was found to follow a similar trend as in case of crosslinker, i.e. swelling percentage decreased with the increase of clay content. It may be due to the fact that, inorganic clay mineral particle in network acted as an additional network point. The crosslinking density of composite increased with the increase of OMMT content, which resulted in a decrease in water absorbency. The influence of OMMT nanoclay content on the swelling behavior of CMC-*g*-PAAc/OMMT nanocomposite hydrogels is shown in the **Fig 4.6c.**

4.5.6 Determination of Gel fraction

A typical dependency of gel fraction to the quantity of clay incorporated into hydrogels is given in **Table 4.3**. It was observed that the gel fraction of the prepared nanocomposite hydrogels was gradually increased with increasing clay content. The gel fraction data reveal that the presence of clay within the three dimensional network of hydrogel causes an increase in crosslinking density and creates more entangled structure. As the organo-modified MMT nanoclay was added to the CMC-*g*-PAAc hydrogel, strong interactions are developed between the functional groups of the nanoclay and the polymer matrix which may cause an increase in the gel fraction.[26]

4.5.7 Blood compatibility studies

Continuous efforts have been made to design novel biomaterials with superior blood compatibility by various research groups. Biomedical applications such as drug delivery, tissue engineering are the well known examples of the use of hydrogels which have been extensively reported.[27] Since these applications involve use of humans or other animals, it is important to study their biocompatibility with blood. The in vitro blood compatibility studies were carried out for the prepared nanocomposites hydrogels by using hemolysis tests as described in section 4.4.7. The hemolysis test was performed both for the native hydrogel and OMMT nanoclay incorporated nanocomposite hydrogel with different concentrations. Significantly less hemolysis activity was found for the clay incorporated hydrogel (10 wt%). For all samples, in contact with blood showed a mean hemolysis value

less than 0.5 %.The test showed very low hemolysis activity and the data obtained are at the permissible limit as shown in the **Fig 4.7**. Photographs showing precipitated RBCs at the end of the hemolysis experiment are also given.

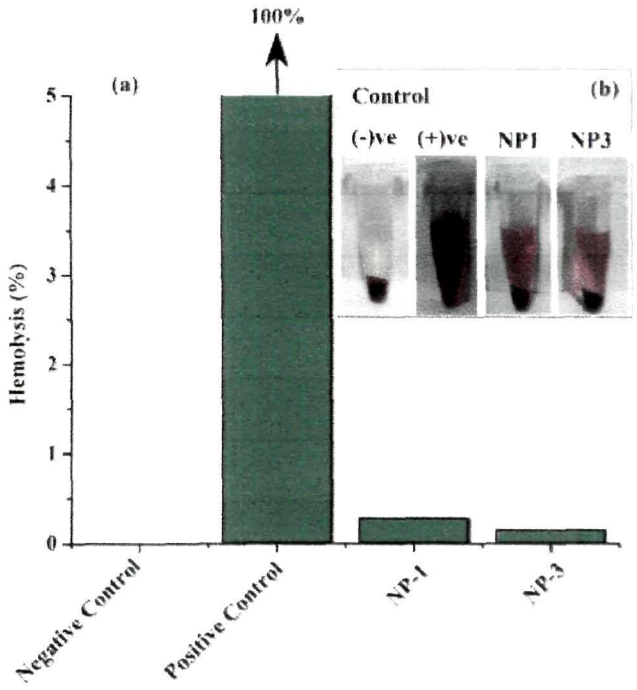

Fig 4.7 Hemolysis results: (a) Hemolysis percentage of the nanocomposite hydrogels without nanoclay (NP-1) and with nanoclay (NP-3, 10 wt%), (b) Photographs of RBCs treated with different samples (NP-1 and NP-3).

4.5.8 In vitro release of vitamin B_{12} from CMC-g-PAAc/OMMT nanocomposite hydrogel

4.5.8.1 Effects of pH

Fig 4.8a shows the release profile of vitamin B_{12} from sample MP-4 at various time intervals in solutions of pH 1.2 and 7.4 at room temperature. It was found that the cumulative release (%) of vitamin B_{12} from CMC-*g*-PAAc/OMMT nanocomposite hydrogel was pH dependent. At pH 1.2 (below the pKa of AAc), the number of negative charges were very low. So, the carboxylic acid groups of the acrylate structure were hardly ionized for which a poor swelling behavior is observed. With diminishing acidity of the media (higher pH), ionization of the carboxylic acid groups occurs, resulting in

both electrostatic repulsion between the carboxylate ($-COO^-$) groups as well as expansion of the space network thereby improving the swelling behavior.[28] As swelling behavior of the hydrogel is the main factor governing the controlled release of the drug, release of vitamin B_{12} increased as the pH of the medium was increased from 1.2 to 7.4.

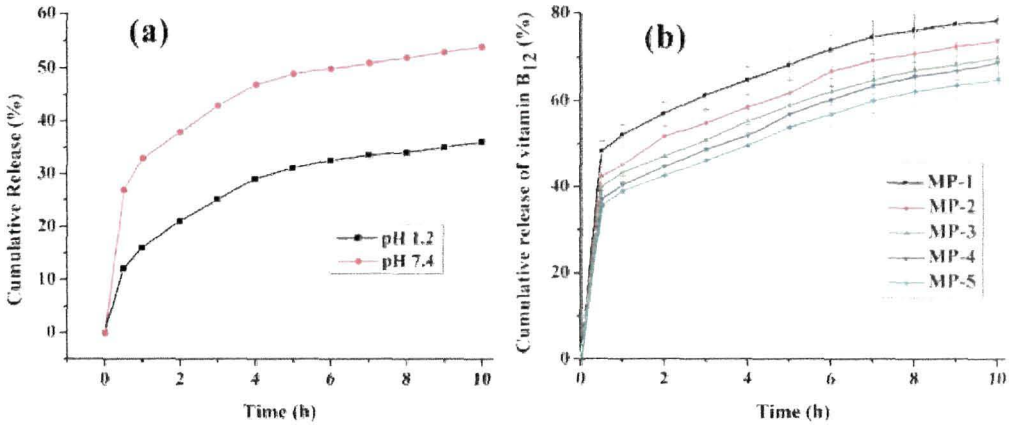

Fig 4.8 The vitamin B_{12} release profile from the CMC-*g*-PAAc/OMMT nanocomposite hydrogels: (a) With different pH values at pH 1.2 and 7.4 (MP-4), (b) With different crosslinker content (0.05-0.25 wt%).

There was a burst release initially for the first hour both in acidic and basic medium, followed by an almost constant release of vitamin B_{12} from the nanocomposite hydrogel for 10 hrs. Similar release behavior was observed by Wang et al. while performed the pH-dependent release of vitamin B_{12} and paclitaxel from poly(MPEG-PLA-*co*-IA-MEGMA) hydrogels. They found that the release behavior has apparent pH responsiveness and release rate was increased as the pH of the release medium was increased from 1.2 to 6.8.[29]

4.5.8.2 Effects of crosslinker content (MBA)

Fig 4.8b depicts the effect of crosslinker content on the release profile of vitamin B_{12}. The effect of MBA content on vitamin B_{12} release was conducted in deionized water at room temperature. Here, cumulative release was inversely proportional to MBA content in CMC-*g*-PAAc/OMMT nanocomposite hydrogels. The cumulative drug release reached about 76.2, 72.4, 68.9, 62.5 and 57.2 % after 10 hrs release, as MBA was fixed at 0.05, 0.1, 0.15, 0.2 and 0.25 % respectively. Higher the content of MBA, the lower is the

swelling ability of nanocomposite hydrogels resulting lower release amount. The network space for vitamin B_{12} release got small at the higher MBA content, which further hindered the effective diffusion of vitamin B_{12} from the nanocomposite hydrogels. As a result, the rate and the cumulative vitamin B_{12} release were subsequently decreased.

4.5.9 Determination of release kinetics of vitamin B_{12}

In order to study vitamin B_{12} transport mechanism from the nanocomposite hydrogels with different crosslinker content, the data was modeled by the Ritger–Peppas equation[30]-

$$M_t/M_\alpha = kt^n \qquad \textbf{(Eqn. 4.5)}$$

Where, M_t/M_α is the fractional vitamin B_{12} release, *'k'* is a kinetic constant and *'n'* is the diffusional exponent which be related to the drug transport mechanism. For a thin hydrogel, when $n = 0.5$, the drug release mechanism is Fickian diffusion. When $n = 1$, Case II transport occurs, leading to zero-order release. When the value of n is between 0.5 and 1, anomalous transport is observed. The values of *'n'* were found to be increased from 0.63 to 0.87 with increasing crosslinking agent as shown in the **Table 4.2**.These results indicate that neither pure Fickian diffusion nor pure polymer chain relaxation was the predominant drug transport mechanism, but anomalous drug transport was observed. So, release of vitamin B_{12} was controlled by diffusion and relaxation of the nanocomposite hydrogels.

4.6 Conclusion

- Nanocomposite hydrogels based on CMC, partially neutralized acrylic acid and layered organically modified OMMT clay were prepared by free radical graft polymerization reaction.
- X-ray diffraction analysis showed that the nanocomposite forms a partially exfoliated or intercalated structure. Also, SEM studies demonstrated an improvement of surface properties of the nanocomposite as compared to the composite.

- The evaluation of the dynamic mechanical analysis of the nanocomposite hydrogels showed an increase in the storage modulus within increasing frequency and OMMT nanoclay content, clearly demonstrating a good mechanical behavior.
- The swelling properties of the nanocomposite hydrogels were found to be dependent on initiator (KPS), crosslinker (MBA) and nanoclay (OMMT) content.
- Blood compatibility of the prepared hydrogels was improved after the incorporation of nanoclay as confirmed by *in vitro* experiments of percentage hemolysis.
- The vitamin B_{12} release behavior was found to be greater in basic medium (pH 7.4) than in the acidic medium (pH 1.2).
- Kinetic study of release behavior showed increase in 'n' value from 0.63 to 0.87 exhibiting a non-Fickian transport mechanism with increase in crosslinker content.
- The results obtained in this work lead us to the conclusion that CMC-*g*-PAAc/OMMT nanocomposite hydrogels can be a promising platform for the development of pH-responsive drug delivery systems.

References

1. Ravi, N., et al. *J. Polym. Sci. Part B* **40** (23), 2677-2684, 2002.
2. Kang, H.M., et al. *Carbohydr. Res.* **341** (17), 2851-2857, 2006.
3. Lin, Y.W. *Carbohydr. Res.* **342** (1), 87-95, 2007.
4. Cai, W.S., & Gupta, R.B. *J. Appl. Polym. Sci.* **83** (1), 169-178, 2002.
5. Kim, S.J., et al. *J. Appl. Polym. Sci.* **83** (1), 169-178, 2002.
6. Engin, K., et al. *Int. J. Hyperthermia* **11** (2), 211-216, 1995.
7. Kurkuri, M.D., & Aminabhavi, T.M. *J. Appl. Polym. Sci.* **91** (6), 4091-4097, 2004.
8. Amiji, M.M. *Biomaterials* **16** (8), 593-599, 1995.
9. Changa, J.H., et al. *Polymer* **44** (13), 3715-3719, 2003.
10. Mansoori, Y., et al. *Eur. Polym. J.* **46** (9), 1844–1853, 2010.
11. Theng, B.K.G. *Formation and properties of clay–polymer complexes*, Elsevier, Amsterdam, 1979.
12. Ogata, N., et al. *J. Appl. Polym. Sci.* **66** (3), 573-581, 1997.
13. Zhang, Z., et al. *Appl. Clay Sci.* **50** (4), 576-581, 2010.
14. Miki, M., et al. *Arch. Biochem. Biophys.* **258** (1), 373-377, 1987.
15. Crini, G. *Prog. Polym. Sci.* **30** (1), 38-70, 2005.
16. Sadeghi, M., & Yarahmadi, M. *Afr. J. Biotechnol.* **10** (56), 12085-12093, 2011.
17. Wang, M., & Wang, L. *Water Sci. Eng.* **6** (3), 272-282, 2013.
18. Irani, M., et al. *Polym. Test.* **32** (3), 502–512, 2013.
19. Samakande, A., et al. *Polymer* **48** (6), 1490-1494, 2007.

20. Kokabi, M., et al. *Eur. Polym. J.* **43** (3), 773-781, 2007.

21. Purkayastha, M.D., et al. *J. Agric. Food Chem.* **61** (45), 10746-10756, 2013.

22. Bajpai, S.K., et al. *Iran. Polym. J.* **16** (8), 521-527, 2007.

23. van Dijkhuizen-Radersma, R., et al. *Biomaterials* **23** (6), 1527-1536, 2002.

24. Boruah, M., et al. *Polym. Compos.* DOI 10.1002/pc.22909, 2014.

25. Lima, H., et al. *Soft Matter* **6** (20), 5184–5195, 2010.

26. Kurecic, M. & Smole, M.S. *Polymer Nanocomposite Hydrogels for Water Purification, Nanocomposites - New Trends and Developments*, F. Ebrahimi, ed., InTech Europe, Croatia, 2012, 161-185.

27. Lin, C.H., et al. *Colloid Surf. B.* **70** (1), 87-95, 2009.

28. Wang, L., et al. *Colloid Surf. A, Physicochem. Eng. Aspects* **322** (1-3), 47-51, 2008.

29. Wang, R., et al. *RSC Adv.* **2** (20), 7772-7780, 2012.

30. Ritger, P.L., & Peppas, N.A. *J. Control. Release* **5** (1), 23-36, 1987.

CHAPTER 5

Electric field assisted drug release from pH and electro-responsive gelatin-g-poly(acrylic acid)/MWCNTs nanocomposite hydrogels.

GRAPHICAL ABSTRACT

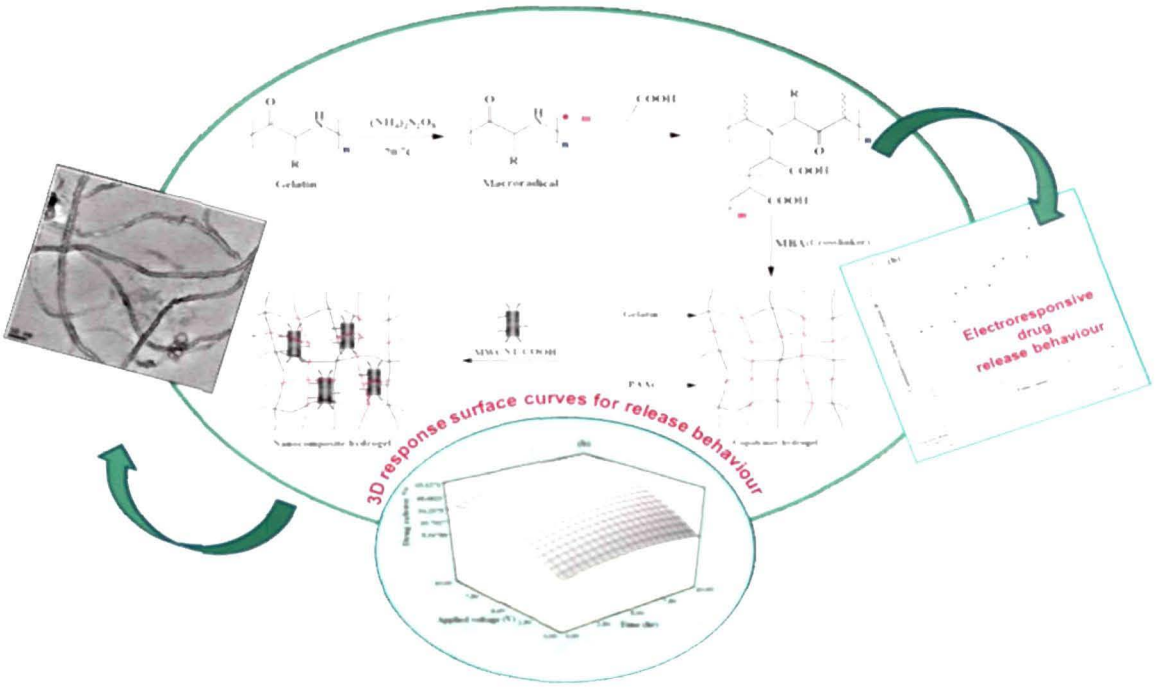

5.1 Introduction

In recent times, stimuli-responsive polymeric hydrogels constitute a new generation of biomaterials for a wide range of applications such as drug delivery, tissue engineering, bioseparation, sensors, actuators etc [1-3] Despite many advantages of using conventional hydrogels, their applications are often limited due to their poor mechanical and some restricted response properties [4] So, attention has been given to improve the properties of a hydrogel such as mechanical strength, thermal properties, response to a stimuli etc In the current scenario of drug delivery technologies, hydrogels have emerged an irreplaceable space because of their special three dimensional network structure which can effectively provide a matrix for the entrapment of drugs [5]

It is obvious that the precise controls over the drug quantity and the release rate are required in order to optimize the drug release Now- a -days, pulsatile drug release devices are extensively developed which releases drug at a predetermined time or in pulses of a predetermined sequence These systems have been shown to alter their rate of drug delivery in response to various stimuli [6] Therefore, stimuli-responsive polymeric hydrogels have been profoundly employed as intelligent drug delivery systems Amongst various stimuli-responsive drug delivery systems, electro-responsive hydrogels which carry free cations or anions are fascinating materials for the design of electrically modulated drug-delivery systems [7] The advantages of an electric field as an external stimulus are accessibility of equipment, which imparts precise control with respect to the magnitude of the current, duration of electric pulses, interval between pulses[8] etc Electro-responsive behavior of the hydrogels can be significantly improved by the successful incorporation of different conducting polymers such as polyaniline,[9] polypyrrol etc or different carbon conducting fillers such as graphite,[10, 11] carbon fibers,[12] carbon black[13] and carbon nanotubes[14] into the hydrogel matrix

Both single-walled (SWCNT) and multi-wall (MWCNT) carbon nanotubes are promising nanomaterials with great potential in the field of nanomedicine for both therapeutic and diagnostic applications [15] They have also been proved to be advanced multi-

functional fillers in polymer-based nanocomposites [16] But, incorporation of CNTs into different polymeric systems becomes a technical challenge due to their poor dispersibility in water or organic solvents [17,18] So, this problem has been removed by chemical functionalization, in which some strong oxidants are used to generate carboxyl group on the surface of CNTs [19] Moreover, it has been already reported that the biocompatibility of carbon nanotubes can be enhanced by the surface functionalization and introduction of hydrophilic moieties to avoid unwanted cytotoxic responses and risks for carcinogenesis [20] Gelatin is a low cost material and has been extensively studied to be used as a biomaterial like artificial skin, bone grafts, and scaffolds for tissue engineering[21-24] etc Its physicochemical properties can be suitably modulated by developing composites or nanocomposites through the introduction of some reinforcing fillers into its structure [25]

Various approaches have been demonstrated in the literature describing the preparation of electro-responsive drug delivery systems using hydrogels Kulkarni et al developed polyacrylamide-g-alginate based electrically responsive hydrogel for drug delivery application A pulsatile pattern of drug permeation was observed as electric stimulus was switched on and off [26] Banga et al synthesized polyacrylamide hydrogels and demonstrated the feasibility of the prepared hydrogels in iontophoretic release and transdermal delivery of three model peptides, insulin, calcitonin and vasopressin under an applied electric field It was observed that the release of drug from a hydrogel matrix under action of electric field strength was more than the release in the absence of electric field and the release can be precisely controlled [27] Kim et al investigated the electrically modulated delivery of ionic drug cefazoline from electro-active Poly(vinyl alcohol)/Poly(acrylic Acid) IPN hydrogels The rapid release behaviors of cefazoline were observed when an electric stimulus was at "ON" state, whereas they showed relatively slow release during the "OFF" state [28] Tanaka et al demonstrated that the partially hydrolyzed polyacrylamide gel undergoes phase transition upon application of an electric field, and collapsed if the gel was placed in a solvent such as 50% acetone-water binary mixture [29]

Modern optimization techniques using experimental designs are important assistance to the formulator, as they help in developing the best possible formulation under

a given set of conditions, consequently saving considerable time, money and developmental effort.[30,31] Moreover, these systematic techniques are known to provide a depth of understanding and ability to explore and defend the ranges for varied formulation and processing factors. In this regard, Central composite design (CCD) has been frequently employed for the optimization of controlled drug delivery systems.[32] The advantages of experimental design method over classical experimental approach are, the reduction in the number of trials, ability to cover a large number of factors, the detection of interactions between factors, detection of optimum reaction condition, a higher precision of the response data and the empirical modeling of the data.[33] Statistical methods, such as response surface methodology are used in developing and optimizing polymeric systems for a wide range of applications.[34] For example, Li et al. performed the optimization of sustained release matrix tablet of metoprolol succinate using central composite design. After investigating the effects of various parameters on drug release, a 2-factor, 5-level central composite design was employed. Response surfaces were also established to obtain the matrix ranges and the main factors affecting four responses. They predicted that this matrix combination can be used as a good alternative to the commercially pellet technology, which was complicated, time-consuming and energy-intensive.[35]

Observing the significant applications of electro-responsive nanocomposite hydrogel, the present chapter involves the development of a pH and electro-responsive nanocomposite hydrogel based on gelatin-*g*-poly(acrylic acid) and acid functionalized multiwall-carbon nanotubes. Physical characteristics such as molecular structure and surface morphology of the prepared hydrogels were investigated thoroughly. We examined the release behavior of vitamin B_{12} at different applied voltages and ionic strength of the release media. Also, the effect of time, MWCNT-COOH content and applied voltage on electro-responsive drug release behavior was studied by response surface analysis. Vitamin B_{12} is a water-soluble vitamin with a key role in the normal functioning of the nervous system and for the formation of blood.[36] Therefore, vitamin B_{12} is chosen as a model drug.

5.2 Experimental

5.2.1 Materials

Acrylic acid monomer (Aldrich) was distilled under reduced pressure prior to use. Gelatin A (300 Bloom), ammonium persulfate (initiator), methylene bis-acrylamide (MBA) as a crosslinking agent and N, N, N', N'- tetramethylethylene diamine were supplied by Aldrich (A.R. grade). Multiwall carbon nanotubes (MWCNTs) were supplied from Shenzhen Nanotech Port Co., Ltd., China. Nitric acid, sodium hydroxide and ethanol (A. R grade) were purchased from Merck, Mumbai. Vitamin B_{12} ($C_{63}H_{88}CoN_{14}O_{14}P$) was purchased from Merck, Mumbai (M.W= 1355.4 g/mol).

5.3 Preparation of gelatin-*g*-poly(acrylic acid)/MWCNTs nanocomposite hydrogel

5.3.1 Acid treatment of MWCNT

Functionalization of CNTs with different chemical groups is generally used to enhance their dispersibility in water and the mostly used technique for this purpose is the oxidization with strong oxidants to generate carboxyl group on the surface of CNTs. In this case, the carboxylic acid functionalized MWCNTs were prepared according to the earlier described method.[37,38] 60 mg of MWCNTs were added to a round-bottom flask containing 50 ml of 60% HNO_3 aqueous solution. The mixture was refluxed for 6 hrs and then cooled to room temperature. The mixture was diluted with 500 ml of deionized water and then collected by low speed centrifugation. The obtained product was washed with deionized water until the pH of the filtrate reached 7 and was dried under vacuum for 24 hrs at 80°C.

5.3.2 Preparation of Gelatin-*g*-PAAc/MWCNTs nanocomposite hydrogel

Gelatin-*g*-poly(acrylic acid) /MWCNT-COOH nanocomposite hydrogels were prepared by free radical polymerization in distilled water. 2 g of gelatin was dissolved in 30 ml of distilled water at 60°C and 1.5 ml of partially neutralized (60%) acrylic acid

monomer was added to this solution. Also, MWCNT-COOH (0.1-0.6 wt%) was added to gelatin-acrylic acid mixture and dispersed under the ultrasonic vibration for 30 min. Subsequently, methylene bis-acrylamide (0.05-0.25 wt%), ammonium persulfate (1.0 wt%) and TEMED (0.05 ml) were added to the mixture under continuous stirring. Nitrogen was used to remove dissolved oxygen from the reactive solution. The reactive solution was first prepolymerizd at 60°C for 1 hr under stirring, and then poured into a petri dish quickly. The post polymerization was carried out at 70°C for 3 hrs. When the reaction was completed, the nanocomposite hydrogel was cut into (3×3 cm) blocks and immersed in repeatedly changed deionized water for 72 hrs to remove the residual monomers. **Tables 5.1-5.2** outline the feed compositions of subsequently prepared hydrogels. Also, the preparation of nanocomposite hydrogel is shown schematically in **Fig 5.1.**

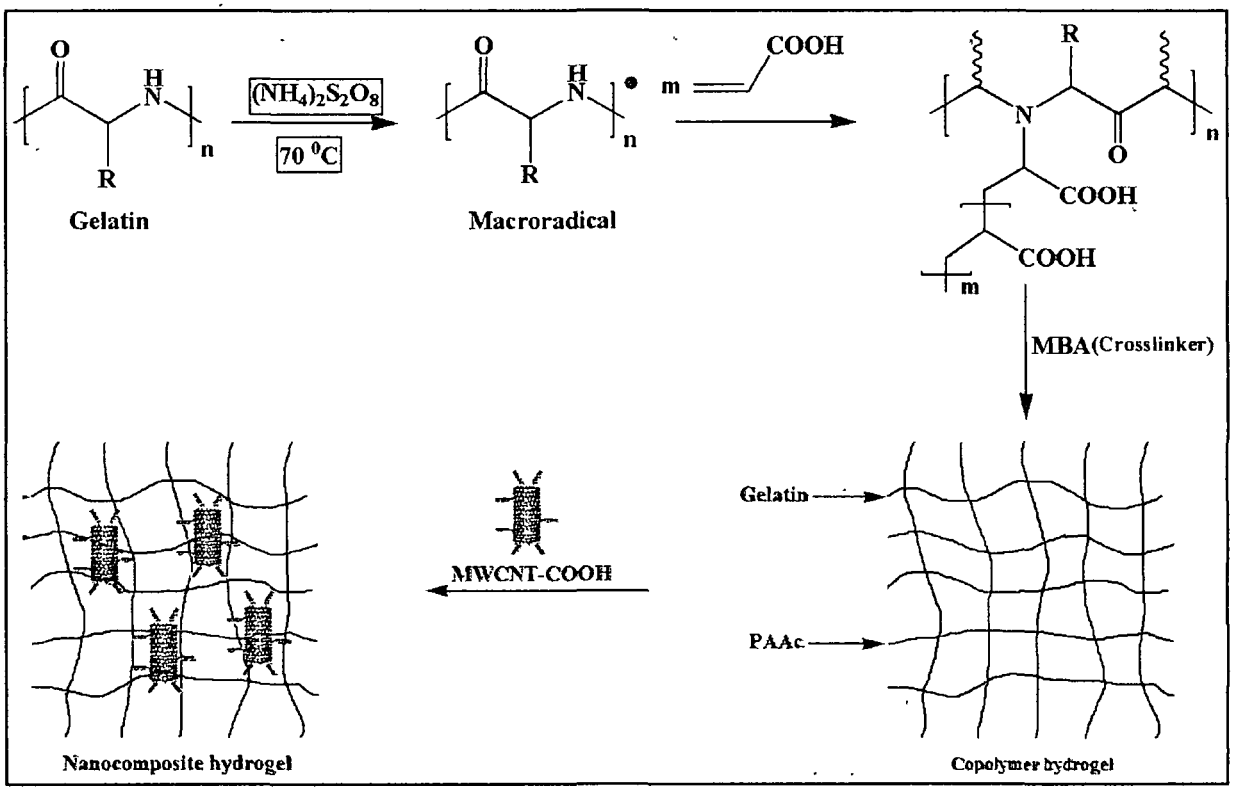

Fig 5.1 Schematic representation for the formation of Gelatin-g-PAAc/MWCNT-COOH nanocomposite hydrogel.

Table 5.1 Recipe in the preparation of Gelatin-*g*-PAAc/MWCNT-COOH nanocomposite hydrogel with different crosslinker (MBA) content:

Recipe	GM-1	GM-2	GM-3	GM-4	GM-5
Gelatin (g)	2	2	2	2	2
Acrylic acid (ml)	1.5	1.5	1.5	1.5	1.5
Methylene bis-acrylamide (wt%)	0.05	0.1	0.15	0.2	0.25
Gel fraction determined (%)	54	62	74	82	91
Ionic Conductivity (S/cm $\times 10^{-2}$)	2 50	1.94	1.72	1.58	1.37

Tetramethylethylene diamine (ml) = 0.05 ml, MWCNT-COOH (wt%) = 0 4 and ammonium persulphate (wt%) = 0.1.

Table 5.2 Recipe in the preparation of Gelatin-*g*-PAAc/MWCNT-COOH nanocomposite hydrogel with different MWCNT-COOH content:

Recipe	GA	GA-1	GA-2	GA-3	GA-4	GA-5	GA-6
Gelatin (g)	2	2	2	2	2	2	2
Acrylic acid (ml)	1.5	1.5	1.5	1.5	1.5	1 5	1.5
MWCNT (wt%)	0	0.1	0.2	0.3	0.4	0.5	0.6
Ionic Conductivity (S/cm $\times 10^{-2}$)	0.92	1.65	2.2	2.85	3.41	3.92	4.52

Tetramethylethylene diamine (ml) = 0.05ml, methylene bis-acrylamide (wt%) = 0.15 and ammonium persulphate (wt%) = 0.1.

5.4 Characterization

5.4.1 Fourier transform infrared spectrometer (FTIR)

To gain insights into the structural information of prepared hydrogels, the IR spectra of the hydrogels were recorded with a Nicolet Impact-410 IR spectrometer (USA) in KBr medium at room temperature in the region 4000-450 cm^{-1}.

5.4.2 Powder X-ray diffractometer (XRD)

Powder X-Ray diffraction (XRD) data were collected on a Rigaku Miniflex X-ray diffractometer (Tokyo, Japan) with Cu Kα radiation (λ=0.15418 Å) at 30 kV and 15 mA with a scanning rate of $0.05^{\circ}s^{-1}$ in a 2θ ranges from 20°-80°.

5.4.3 Morphological Analysis

The surface morphology of the composites was observed using a scanning electron microscope (SEM) (Model- JSM-6390LV, JEOL, Japan). The surface of the sample was platinum coated before SEM analysis. Further morphological analysis was done by Transmission electron microscope (JEM 2100) with an acceleration voltage of 200 kv.

5.4.4 Swelling properties

To measure the degree of swelling the hydrogels, dried samples were placed in buffer media of different pH values at room temperature until the hydrated gels reached a stable weight. The swelling behavior under an applied electric field was determined by applying different electric potentials to the nanocomposite hydrogel in distilled water. The water absorbed on the surface of the hydrogels was removed using filter paper and the weight noted.

$$Swelling\ \% = W_s - W_{dry}/W_{dry} \times 100 \qquad \textbf{(Eqn. 5.1)}$$

where, 'W_s' is the weight of the hydrogel in swollen state and 'W_{dry}' is that of the hydrogel in dry state.

5.4.5 Gel fraction

The weight ratio of the dried hydrogels in rinsed and unrinsed conditions can be assumed as an index of degree of crosslinking or gel fraction. The pieces of hydrogel samples (3×3 cm) were dried for 6 hrs at 50°C under vacuum. Then the sample (3×3 cm) was immersed into excess of double distilled water for 4 days to rinse away unreacted parts. The gels were dried again at 50°C under vacuum. The gel fraction percentage was calculated by the following equation[39]:

$$Gel\ fraction\ \% = W_f/W_i \times 100 \qquad \textbf{(Eqn. 5.2)}$$

where, W_i = Initial weight before rinse and W_f = Final weight after rinse.

5.4.6 Ionic conductivity

Impedance spectroscopy was used to assess the ionic conductivity by using a two electrode cell and an impedance analyzer (HIOKI IM 3570). The impedance spectrum was measured in the frequency range 100 Hz to 1 MHz with potential amplitude of 10 mV at room temperature. The ionic conductivity was calculated using the following equation-

$$\delta = l/R \times A \qquad \textbf{(Eqn. 5.3)}$$

where, δ is the ionic conductivity of the nanocomposite hydrogel ($S.cm^{-1}$), l is the thickness of the film (cm), R is the film resistance (Ω) and A is the surface area of the electrodes (cm^2) prior to the measurement, the hydrogel films (2.5 cm×2.5 cm) were immersed in distilled water at room temperature for 24 hrs and the surface water was gently removed before the film were positioned between the electrodes in the measurement cell.

5.4.7 Blood compatibility by hemolytic activity assay

The hemolytic test was performed following the protocol of Das Purkayastha, M. et al, with slight modification.[40] Briefly, fresh goat blood from a slaughterhouse was collected in a centrifuge tube containing anticoagulant, trisodium citrate (3.2%), and was centrifuged at 2500 rpm for 10 min. The supernatant was discarded, and only the erythrocytes were collected. The erythrocytes were further washed three times with PBS (pH 7.4). A 5% (v/v) suspension of erythrocytes in PBS was prepared; 0.95 ml of this erythrocyte solution was placed in a 1.5 ml centrifuge tube and 0.05 ml of sample (0.5 mg dissolved in 1 ml of 0.5% DMSO) was added to it. The tubes were then incubated for 1 hr at 37°C. Triton X-100 (0.2 %) and PBS were taken as the positive and negative controls, respectively, for comparison. After incubation, the tubes were subjected to centrifugation at 2500 rpm for 10 min. Then, 0.2 ml of the supernatant was added to 96-well plate, and finally absorbance was taken at 570 nm in a UV–visible spectrophotometer (Shimadzu UV-2550 UV–visible spectrophotometer).

$$\textit{Hemolysis \%} = [(\textit{Sample O.D} - \textit{Negative control O.D})/(\textit{Positive control O.D} - \textit{Negative control O.D}] \times 100 \qquad \textbf{(Eqn. 5.4)}$$

5.4.8 Loading of vitamin B_{12}

The method of soaking or equilibration was employed for vitamin B_{12} loading In this method, the amount of buffer necessary for complete swelling of the nanocomposite hydrogel was determined [41] Dry hydrogel was placed in the drug solution at a concentration of 0 125 wt%, prepared in the buffer solution of pH 7 0 and left until all the drug solution was sucked up Then the completely swollen hydrogel loaded with the vitamin B_{12} was placed in an oven at 30°C for drying overnight

5.4.9 Drug release experiment under electric field

To investigate the release behavior of vitamin B_{12} under electric stimulus, drug loaded hydrogels were placed in the middle of two carbon electrodes in a desired release medium as shown in the **Fig 5.2.** Then, the amount of drug released into the respective medium was monitored by varying factors such as ionic strength of the release medium and the MWCNT-COOH content in the nanocomposite hydrogel The pulsatile release of vitamin B_{12} under the applied electric field was also determined by applying pulses of electric current at 5 V, 30 min 'ON' and 30 min 'OFF'

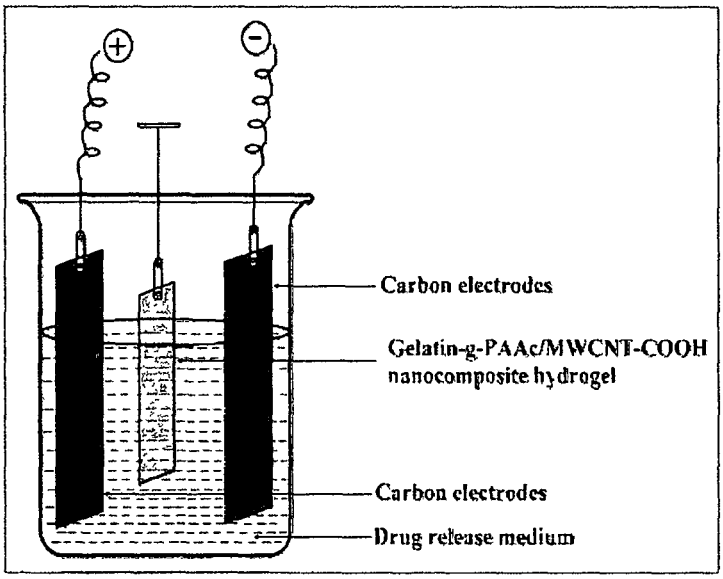

Fig 5.2 Apparatus for electro-responsive drug delivery

At scheduled time intervals, 5 ml solution was withdrawn and assayed spectrophotometrically by using a UV-visible spectrophotometer (UV-2001Hitachi, Japan) for the determination of the cumulative amount of drug release from the absorbance at 362 nm. To maintain a constant volume, 5 ml of the same solution was returned to the container. The amount of vitamin B_{12} released from the nanocomposite hydrogel was calculated from a calculated from a previously calibrated standard curve.[42]

5.4.10 Experimental Design

Central composite design (face-centered) was used in this study and 2 factors were evaluated, each at 3 levels; experimental trials were performed at all 13 possible combinations to investigate influence of the parameters such as time, MWCNT-COOH content and applied voltage on release behaviour of the drug. Two central composite designs (with electric field and without electric field) were constructed to study the effect of two different factors in each study on drug release behavior. In each case, the two factors, X_1 (time) and X_2 (MWCNT-COOH content); X_1(time) and X_2 (applied voltage) were varied as required by the experimental design and the factor levels were suitably coded **(Table 5.3-5.4)**.

Suppose, we code the levels in standardized units so that the values taken by each of the two variables X_1 and X_2 are -1, 0 and +1.Coded values were obtained by the following formula[43]:

$$Z = (X-X_o)/\Delta X \qquad \textbf{(Eqn. 5.5)}$$

Where, Z is the coded values, X is the corresponding natural value, X_o is the natural value in the center of the domain and ΔX is the increment of X corresponding to one unit of Z.

Table 5.3 Central composition design conditions (without electric field):

Run	Coded factor levels	
	X_1	X_2
1	1	1
2	0	1
3	0	0
4	0	0
5	0	0
6	0	0
7	-1	1
8	1	-1
9	0	-1
10	-1	0
11	-1	-1
12	0	0
13	0	0

Translation of coded levels in actual units			
Coded level	*-1*	*0*	*+1*
X_1: Time (hr)	0	5	10
X_2: MWCNT-COOH (wt%)	0.2	0.4	0.6

Table 5.4 Central composition design conditions (with electric field):

Run	Coded factor levels	
	X_1	X_2
1	1	0
2	1	-1
3	-1	-1
4	1	1
5	0	1
6	-1	1
7	-1	0
8	0	-1
9	0	0
10	0	0
11	0	0
12	0	0
13	0	0

Translation of coded levels in actual units

Coded level	*-1*	*0*	*+1*
X_1: Time (hr)	0	5	10
X_2: Applied voltage (V)	0	5	10

Again, data were analyzed by multiple regressions to fit the following second order equation:

$$Y = B_o + \sum_{i=1}^{k} B_i X_i + \sum_{i=1}^{k} B_{ij} X_i X_j \qquad \textbf{(Eqn. 5.6)}$$

where, Y = predicted response.

The resulting data were fitted into Design Expert Software (Version 6.0.10 Stat-Ease, USA) and the developed models were adopted for the multiple correlation coefficient (R^2), the adjusted multiple correlation coefficient (adjusted R^2) and corresponding 'P' value provided by analysis of variance (ANOVA). The greater values of R^2 and adjusted R^2 are preferable and it was considered significant when the corresponding 'P' value was less than 0.05. The data were also subjected to 3D response surface methodology to determine the influence of each factor on electro-responsive release behaviour of vitamin B_{12}. Effectiveness of the model is evaluated based on the calculated coefficient of determination (R^2) by the program.

5.5 Results and discussion

5.5.1 FTIR analysis

FTIR spectra of pristine MWCNT, acid functionalized MWCNT, gelatin-*g*-PAAc copolymer and gelatin-*g*-PAAc/MWCNT-COOH nanocomposite hydrogels are shown in the **Fig 5.3.** The characteristic bands due to generated polar functional groups on the MWCNT are observed in the FTIR spectrum of the MWCNTs after chemical oxidation in HNO_3 acid. The FTIR spectrum of MWCNT-COOH shows absorption peak at 2910 cm^{-1} corresponding to the C-H symmetric stretching vibration. Also, the appearance of peak at 1531 cm^{-1} confirms the existence of carbon double bonding (C=C), which again reveals the integrity of hexagonal structure on the pristine MWCNT.[44] Appearance of peak at 1731 cm^{-1} assigns carbonyl (C=O) stretching vibration of carboxyl groups which is not present in pristine MWCNTs. It confirms the carboxylation on the surfaces of functionalized MWCNTs **(Fig 5.3a).**

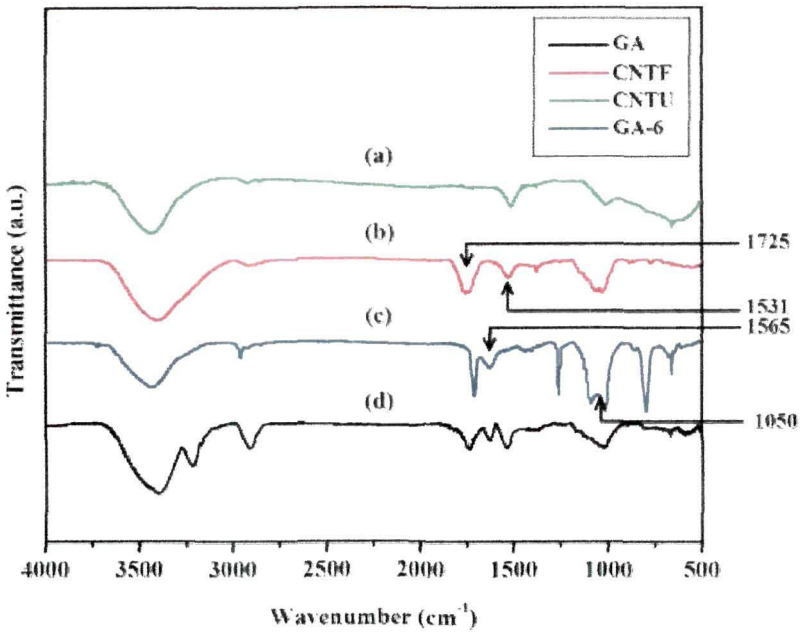

Fig 5.3 FTIR spectra of (a) MWCNT-pristine, (b) MWCNT-COOH, (c) gelatin-*g*-PAAc/MWCNT-COOH nanocomposite hydrogels and (d) gelatin-*g*-PAAc hydrogel.

FTIR spectrum of gelatin-*g*-PAAc shows absorption peaks at 3391 cm^{-1} and 2950 cm^{-1} which are attributed to the N-H stretching vibration and C-H stretching vibration in $-CH_3$ group. The peaks at 1630 cm^{-1} and 1520 cm^{-1} are due to the amide I (C=O stretching vibration) and amide II (-NH bending vibration) respectively. The absorption peak at 1126 cm^{-1} is due to the C-N stretching vibration of amide III. Also, the characteristic peaks at 3450 cm^{-1}, 1735 cm^{-1} and 613 cm^{-1} are due to the -OH stretching vibration of PAAc, C=O stretching vibration and the -OH out of plane vibration of the carboxylic groups of PAAc, which confirms the grafting reaction. **Fig 5.3c** represents the FTIR spectrum of gelatin-*g*-PAAc/MWCNT-COOH nanocomposite hydrogel which shows characteristics peaks of MWCNT–COOH at 1565 cm^{-1} which is ascribed to the C=C bonding that forms the framework of the carbon nanotube sidewall. The peak at 1050 cm^{-1} indicates the presence of –COOH groups of carboxylated MWCNT and the peaks present in 500-1000 cm^{-1} range indicates the presence of hexagonal carbon atom. Presence of all these characteristics peaks indicates the incorporation of MWCNT–COOH into the gelatin-*g*-PAAc hydrogel matrix.

5.5.2 XRD analysis

The diffraction peaks with 2θ values of 25.54° and 45.70° are found for pristine MWCNTs and the diffraction peaks at 26.08° and 43.08° are attributed to the graphite structure (002) and (100) planes of the MWCNT-COOH as shown in the **Fig 5.4**. The shifting of characteristic peak position in the XRD pattern of MWCNT-COOH shows the perfect modification of pristine MWCNTs. There is no drastic change in the position of characteristic peaks of pristine MWCNTs and MWCNT-COOH was observed, which suggest that MWCNTs are well retained their original structure even after functionalization.[45]

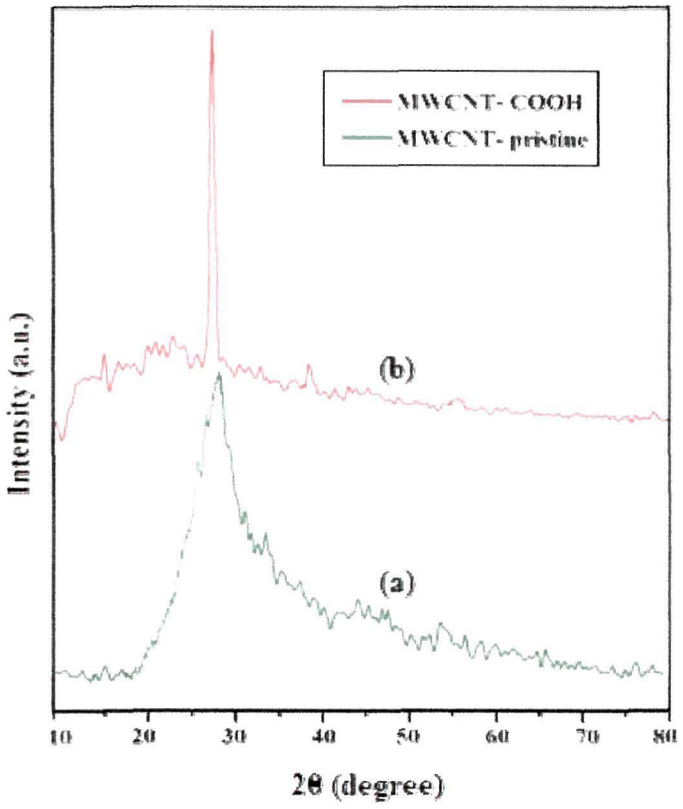

Fig 5.4 XRD patterns of (a) MWCNT-pristine and (b) MWCNT-COOH.

Fig 5.5 depicts the XRD patterns of gelatin-*g*-PAAc copolymer hydrogel and gelatin-*g*-PAAc/MWCNT-COOH nanocomposite hydrogels respectively. The XRD pattern of gelatin-*g*-PAAc doesn't possess any characteristics peaks, but some minor peaks

were observed around 21 and 22°, which could be attributed to minor crystallites of grafted polyacrylic acid chains. On the other hand, the XRD pattern of gelatin-*g*-PAAc/MWCNT-COOH shows the characteristics peaks of MWCNT-COOH with low intensity which confirms the incorporation of acid functionalized multiwall carbon nanotubes into the Gelatin-*g*-PAAc hydrogels.

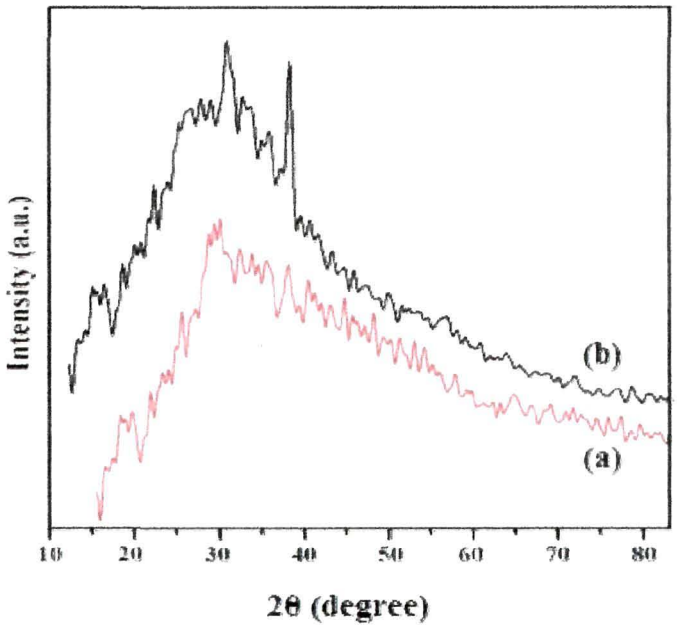

Fig 5.5 XRD patterns of (a) gelatin-*g*-PAAc hydrogel and (b) gelatin-*g*-PAAc/MWCNT-COOH nanocomposite hydrogels.

5.5.3 Morphological analysis

The morphological images of the copolymer hydrogel and MWCNT-COOH incorporated hydrogels were studied by SEM and are shown in **Fig 5.6.** SEM micrographs indicate the change in the surface morphology of the prepared hydrogels after the incorporation of MWCNT-COOH. A rough surface morphology is observed and some pores can be observed in the micrograph of gelatin-*g*-PAAc hydrogel. But, comparatively a smooth surface was observed after the impregnation of MWCNT-COOH into the hydrogel. This observation implies that MWCNT-COOH is uniformly dispersed within the hydrogel. Also, scanning electron microscopy was used to investigate possible MWCNTs fragmentation occurred during treatment. SEM images of MWCNT-COOH and pristine

MWCNT are also shown in **Fig 5.6.** From both the micrographs, a significant difference was observed. A sharp surface was observed for the functionalized MWCNT, which was apparently smooth in case of pristine MWCNT. Also, the transparency of nanotubes has been decreased after the functionalization as compared to the pristine MWCNTs which possibly related the introducing of functional groups.[46,47]

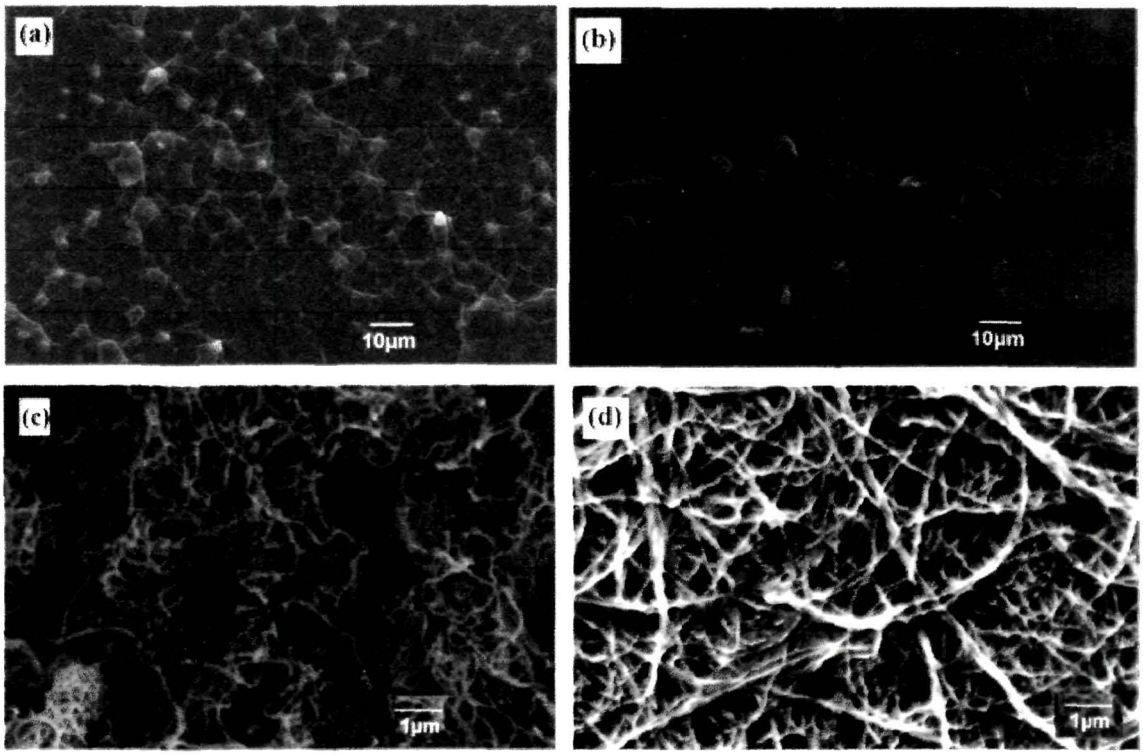

Fig 5.6 SEM images of (a) gelatin-*g*-PAAc hydrogel, (b) gelatin-*g*-PAAc/MWCNT-COOH nanocomposite hydrogels, (c) MWCNT-pristine and (d) MWCNT-COOH.

The stable and uniform dispersion of the MWCNT-COOH within the gelatin-*g*-PAAc matrix is evident from the TEM study. The TEM image (**Fig. 5.6a**) shows that the MWCNT-COOH has an average external diameter of 20-25 nm. A representative TEM image (**Fig. 5.6b**) shows the anchoring of a gelatin-*g*-PAAc layer onto a MWCNT-COOH with a diameter of 30-35 nm. This increase in the diameter in the nanocomposite hydrogel indicates the presence of a layer of gelatin-*g*-PAAc molecules on the surface of the MWCNT-COOH.

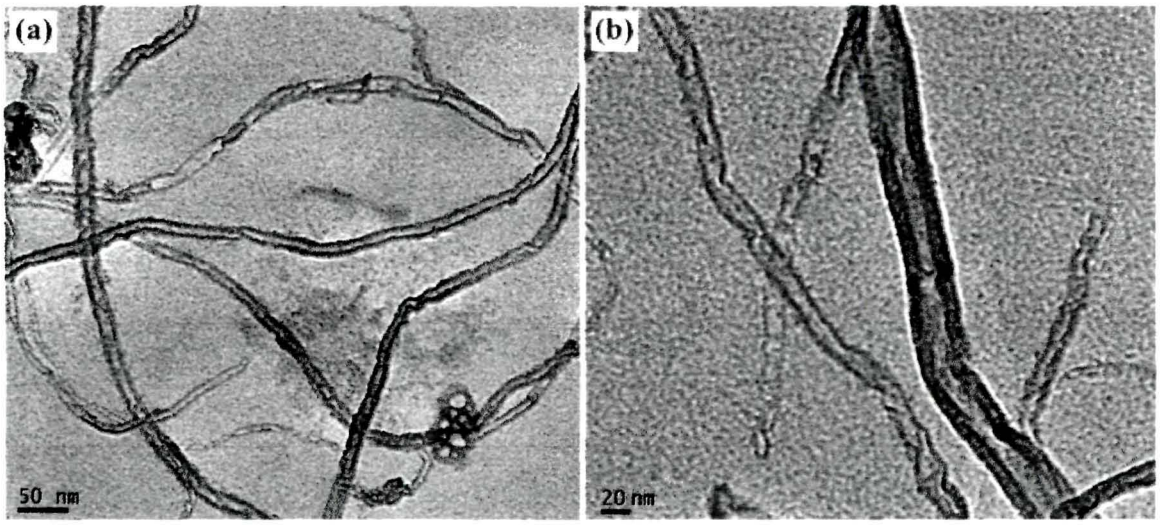

Fig 5.7 TEM images of (a) MWCNT-COOH and (b) nanocomposite hydrogel (0.3 wt% MWCNT-COOH).

5.5.4 Ionic Conductivity

Impedance spectroscopy provides a relatively straightforward and rapid technique to assess ionic conductivity. Ionic conductivities of the prepared hydrogels were determined with the variation of crosslinker (MBA) and MWCNT-COOH content in gelatin-*g*-PAAc/MWCNT-COOH nanocomposite hydrogel. It was observed that ionic conductivities decrease with an increase in crosslinker (MBA) concentration. It may be due to the decreased proton mobility resulting from increased methylene bis-acrylamide concentration. As the crosslinking density is increased, more crosslinking points will be developed forming a dense network, which will restrict the ionic mobilities of the ionic groups present in the nanocomposite hydrogel. On the other hand, the ionic conductivity was found to be increased with MWCNT-COOH content in the nanocomposite hydrogel. This may be due to the improved ionic transport in presence of MWCNT-COOH in the hydrogel.[48] Ionic conductivities values with the variation of crosslinker and MWCNT-COOH content are given in the **Table 5.1-5.2.**

5.5.5 Swelling study

5.5.5.1 Effects of pH

The hydrogels have shown tremendous promise in different biomaterial applications because of their unique water holding capacity. Hence, swelling behavior of a particular hydrogel material should be investigated in order to confirm its utility in different biomedical areas. **Fig 5.8** represents the swelling behavior of the prepared nanocomposite hydrogels with different crosslinker amount in acidic (pH=4) and basic (pH=7.4). The swelling behavior was found to be increased with an increase in pH from 4 to 7.4. The gelatin structure is ionizable because the basic dissociation constant (pK_b) of the NH_3^+ is about 6.5 and the acid dissociation constant (pK_a) of the COOH is about 4.7 in gelatin.[49]

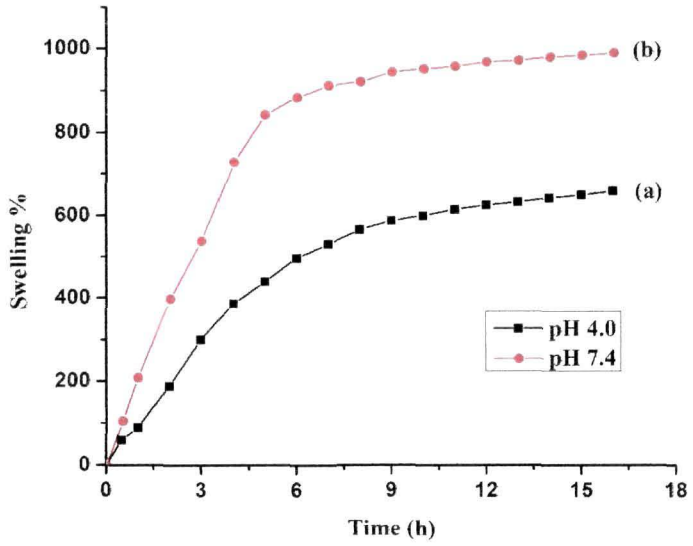

Fig 5.8 Influence of pH of the medium on the swelling behaviours of the nanocomposite hydrogels: (a) pH = 4 and (b) pH = 7.4.

So, this improved swelling behavior is due to the presence of the hydrophilic functional groups (mainly $-COO^-$) in the gelatin structure. Moreover, at higher pH, ionization of the carboxylic acid groups occurs, resulting in electrostatic repulsion between the carboxylate ($-COO^-$) groups as well as expansion of the space network thereby increasing the swelling percentage.[50]

5.5.5.2 Effect of MWCNT-COOH content

Fig 5.9a depicts the effect of MWCNT-COOH content on the swelling behavior of gelatin-*g*-PAAc hydrogels. It was observed that the extent of swelling was decreased with an increase in the concentration of MWCNT-COOH. It may be mainly due to the hydrophobic nature of MWCNT-COOH. The result is consistent with other reports in the literature.[51] Moreover, functionalized MWCNT in gelatin-*g*-PAAc may acts as like some crosslinking sites which make the diffusion of water into the hydrogel more difficult. So, interaction between MWCNT-COOH and hydrogels contributed to lower the swelling percentage of the nanocomposite hydrogels than for the native gel.

5.5.5.3 Effect of applied electric field

The response of an electro-responsive hydrogel in presence of an external electric field depends on the shape and position of the gel between the electrodes.[52] When the gel is placed at a fixed position away from the electrodes, as in our experiment, the swelling behaviour is observed. So, the swelling behavior of the nanocomposite hydrogels with various MWCNT-COOH content were measured as a function of time in distilled water under the applied electric potential of 10 V. The swelling percentage of gelatin-*g*-PAAc/MWCNT-COOH gradually increased with increasing MWCNT-COOH content **(Fig 5.9b).** MWCNT-COOH provides the efficient pathway of electric field. Therefore, MWCNTs could contribute to the increase in swelling percentage of the nanocomposites by increasing the extent of ionization of the functional groups in the nanocomposite hydrogel under electric voltage applied. This behavior is completely opposite to the swelling character under normal condition where swelling percentage decreases with increase in MWCNT-COOH content.

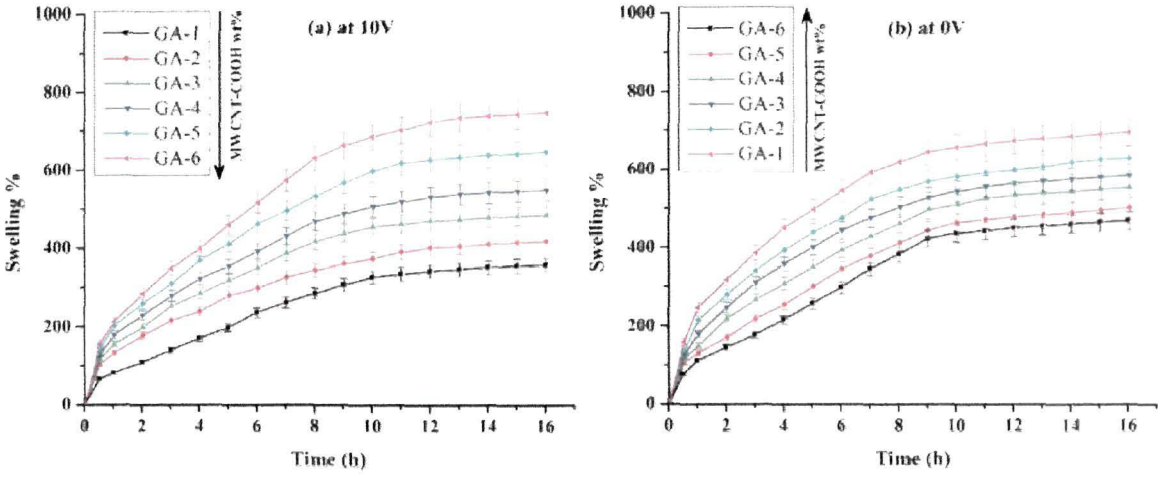

Fig 5.9 Effect of MWCNT-COOH content on the swelling behavior of gelatin-*g*-PAAc hydrogels: (a) at 0 V and (b) at 10 V.

5.5.6 Gel fraction

A typical dependency of gel fraction to the quantity of crosslinker incorporated into hydrogels is given in the **Table 5.1**. As seen, the gel fraction of samples is increased by increasing the amounts of crosslinker from 0.05% up to 0.25% by weight. The gel fraction data reveal that the increase in crosslinker amount within the three dimensional network of hydrogel causes an increase in crosslinking density, thus creates more entangled structure.

5.5.7 Blood compatibility studies

Numerous efforts have been given to design novel biomaterials with superior blood compatibility by various research groups. Hemocompatibility is a prime requirement for biomedical applications such as drug delivery, tissue engineering etc. intended for direct or indirect blood exposure. **Fig 5.10** represents the data obtained from hemolysis test as described in Section 5.4.7. The hemolysis test was performed for the nanocomposite hydrogels with 0.1 and 0.6 wt% of MWCNT-COOH content with different concentrations. For all samples, in contact with blood showed a mean hemolysis value less than 0.5 %.The test showed very low hemolysis activity and the data obtained are at the permissible limit

as shown in the **Fig 5.10a.** Photographs showing precipitated RBCs at the end of the hemolysis experiment are also given **(Fig 5.10b)**.

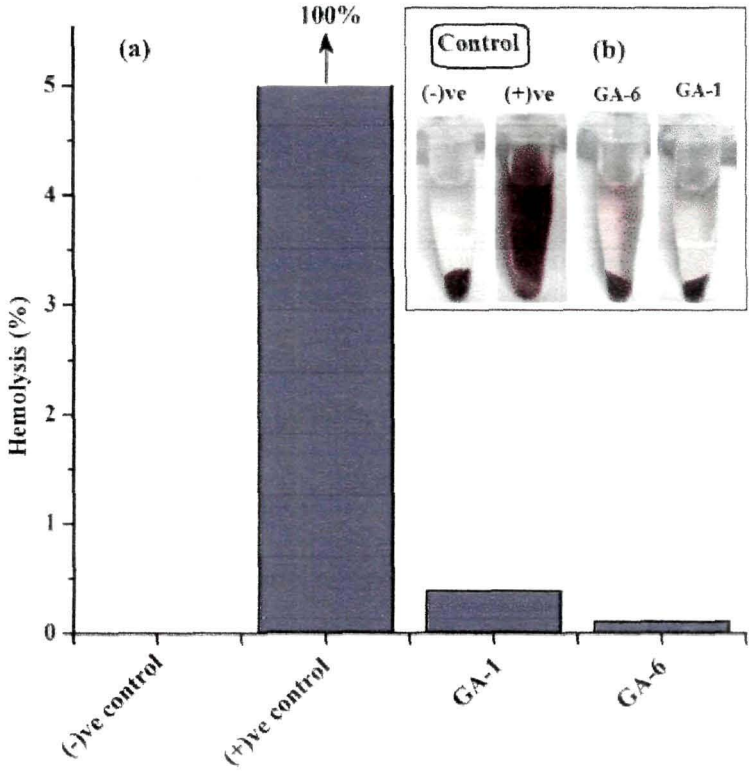

Fig 5.10 Hemolysis results: (a) Hemolysis percentage of the nanocomposite hydrogels with 0.6 wt% (GA-6) and 0.1 wt% (GA-6) MWCNT-COOH content, (b) Photographs of RBCs treated with different samples (GA-6 and GA-1).

5.5.8 Electro-responsive release behavior of vitamin B_{12} from Gelatin-g-PAAc/MWCNT-COOH nanocomposite hydrogels

5.5.8.1 Effect of applied voltage

The effect of applied electric potential on release behavior of vitamin B_{12} from gelatin-*g*-PAAc/MWCNT-COOH nanocomposite hydrogel is shown in **Fig 5.11.** It can be observed that the drug release rate was much higher under the influence of an electrical stimulus than without electric stimulus. A systematic increase in the drug release rate was observed when the applied voltage was increased from 5 V to 10 V.

According to Sawahata et al. drug transport occurs only if the applied electrical current is sufficiently high to induce dimensional changes in the hydrogel. Under higher applied voltage, the ionizable groups are more ionized which results in improved swelling behavior of the nanocomposite hydrogel. The improved swelling will enhance the release of drug from the nanocomposite hydrogel through diffusion.[53]

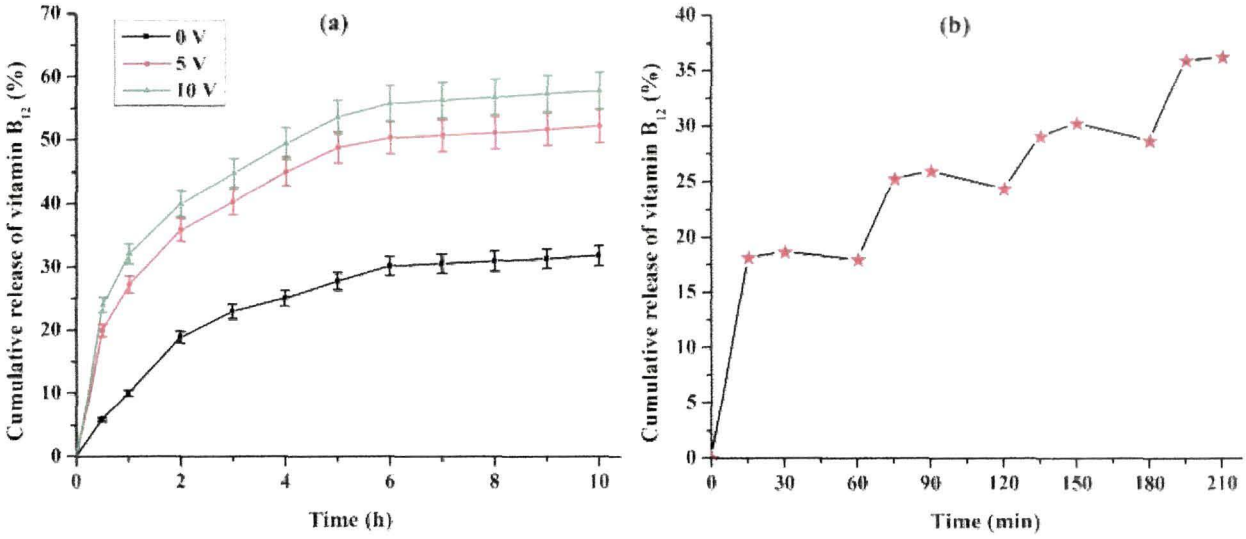

Fig 5.11 Drug release behavior of gelatin-*g*-PAAc/MWCNT-COOH nanocomposite hydrogels: (a) At different electric voltage applied: 0 V, 5 V and 10 V, (b) Drug release behavior as a function of applied voltage of 0 V and 5 V, which was altered at 30 min time intervals.

Moreover, the rapid release behaviors of vitamin B_{12} were observed when an electric stimulus was at 'ON' state, whereas they showed a relatively slow release rate during the 'OFF' state while applied electric potential was maintained at 0 and 5V alternately. The plausible reason for this switching pattern of the release of drug molecules is due to the electrically induced changes in osmotic pressure within the gel and local pH gradient attributed to water electrolysis. This could also affect the swelling behaviour of the nanocomposite hydrogel under electric field as well as release of drug from the gelatin-*g*-PAAc/MWCNT-COOH nanocomposite hydrogel. In 'OFF' stage (when no electric field), normal diffusion controlled release of drug is taking place which is quite slow.

5.5.8.2 Effect of ionic strength of the release medium

The ionic strength of the release medium exerts an influence on the release rates of drugs. In our study, the release of vitamin B_{12} was studied in media containing two different ionic strengths, 0.1 M and 0.2 M NaCl solutions. **Fig 5.12** exhibits the release behavior of the drug as a function of ionic strength and at a fixed electric potential of 10 V. It was observed that at higher ionic strengths, the drug release rate was slower with time than in the lower ionic strength media.

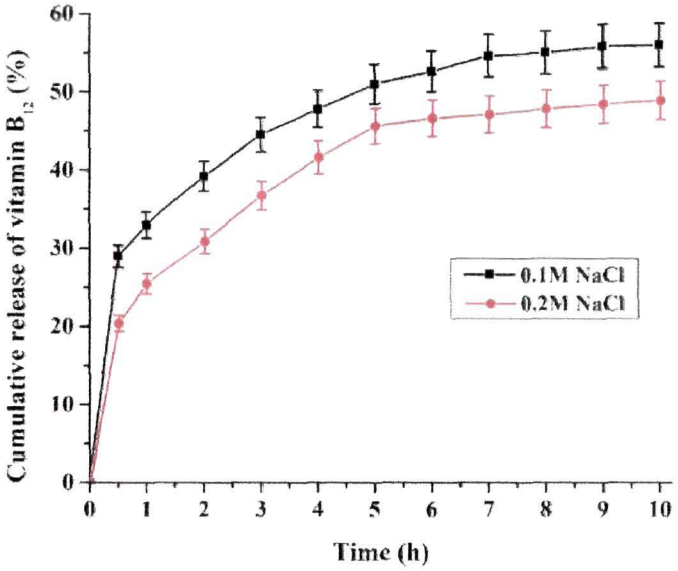

Fig 5.12 Drug release behaviour of gelatin-*g*-PAAc/MWCNT-COOH nanocomposite hydrogels depending on the ionic strength of the release medium (0.1 M and 0.2 M NaCl solution).

It may be attributed to the charge screening effect of the additional anions causing a non perfect electrostatic repulsion, which leads to a decreased osmotic pressure difference between the hydrogel network and the external solution. Thereby the shrinkage of the gel was observed instead of swelling. Moreover, the drug solubility may also decrease with increasing ionic strength of the medium, which may also affect in lowering of the drug release rate. Similar behavior was observed by Agnihotri et al. while investigated the electrically modulated release behavior of drug from sodium alginate and carbopol hydrogels. They found that the drug transport followed the switch-on and

switch-off pattern in a pulsatile manner and release rate was significantly decreased with increase in ionic strength of the release medium.[54]

5.5.8.3 Effect of MWCNT-COOH content

The release of vitamin B_{12} was found to be profoundly dependent on the MWCNT-COOH content of the nanocomposite hydrogels. It can be seen from **Fig 5.13a,** that the drug release rate was decreased as the content of MWCNT-COOH increased when no electric field was applied. On the other hand, a reverse release behavior was observed when an electric potential of 10 V was applied to the nanocomposite hydrogels. The release of vitamin B_{12} was found to be increased with increase in MWCNT-COOH content, as predicted from the swelling behavior of nanocomposites in presence of an electric field displayed in **Fig 5.13b.**

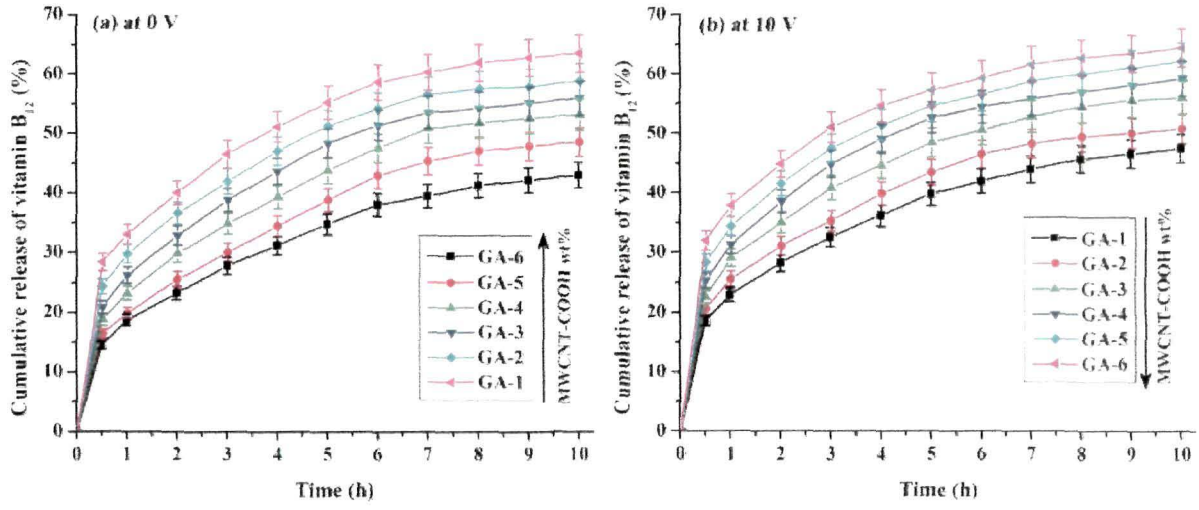

Fig 5.13 Drug release behavior of gelatin-*g*-PAAc/MWCNT-COOH nanocomposite hydrogels with various MWCNT-COOH content and at different electric voltage applied: (a) 0 V and (b) 10 V

5.5.9 *Response Surface Analysis*

The cumulative release % of vitamin B_{12} with respect to two sets of factors was regressed using the Design Expert Software. The multiple regression equation for cumulative drug release % (Y_1) with respect to time (hr) and MWCNT-COOH content:

Final Equation in Terms of Coded Factors

$$Cumulative\ drug\ release\ \%\ (Y_1) = 52.25+29.20*X_1+4.58*X_2-22.13*X_1^2-1.38*X_2^2+3.43*X_1*X_2 \quad \textbf{(Eqn. 5.7)}$$

Final Equation in Terms of Actual Factors

$$Cumulative\ drug\ release\ \%\ (Y_1) = -6.92011+13.32241*X_1+33.41236*X_2-0.88524*X_1^2-34.52586*X_2^2+3.42500*X_1*X_2 \quad \textbf{(Eqn. 5.8)}$$

The multiple regression equation for cumulative drug release % (Y_2) with respect to time (hr) and applied voltage:

Final Equation in Terms of Coded Factors

$$Cumulative\ drug\ release\ \%\ (Y_2) = 49.32+8.35*X_1+20.54*X_2-7.48*X_1^2-14.13*X_2^2+6.53*X_1*X_2 \quad \textbf{(Eqn. 5.9)}$$

Final Equation in Terms of Actual Factors

$$Cumulative\ drug\ release\ \%\ (Y_2) = -5.34788+3.35723*X_1+8.45369*X_2-0.29915*X_1^2-0.56515*X_2^2+0.26100*X_1*X_2 \quad \textbf{(Eqn. 5.10)}$$

The results are plotted in **Fig 5.14.** These results show that the electro-responsive release behaviour of the nanocomposite hydrogels was more significantly influenced by the release time and applied voltage than MWCNT-COOH content in the prepared hydrogel. It can be observed from **Table 5.5** that R^2 is high for all responses, which indicates a high degree of correlation between the experimental and predicted responses. In addition, the predicted R^2 value is in good agreement with the adjusted R^2 value, resulting in reliable models.

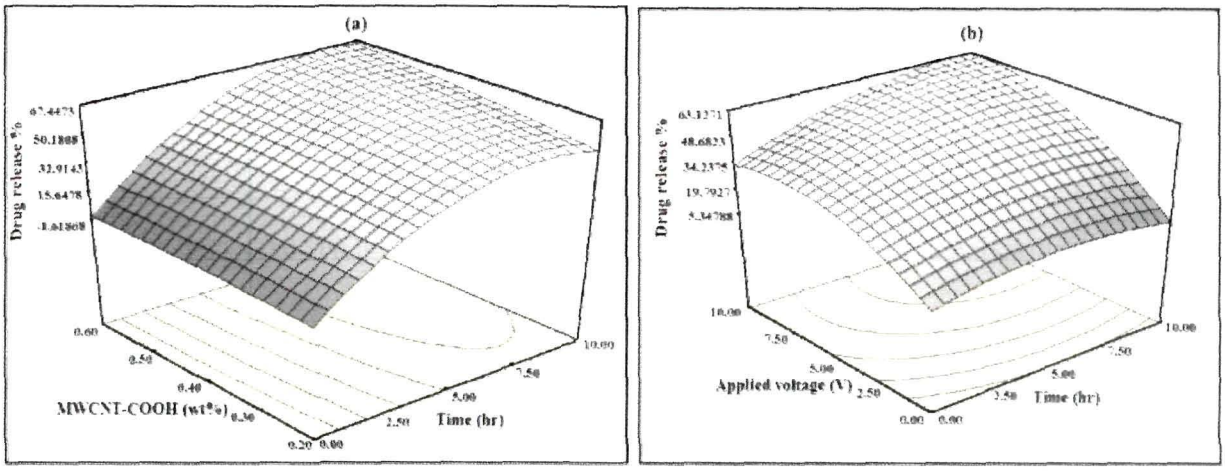

Fig 5.14 3D response surface plot of drug release behaviour of gelatin-*g*-PAAc/MWCNT-COOH nanocomposite hydrogel: (a) showing the effect of amount of MWCNT-COOH (wt%) and time (hr) on release behaviour of vitamin B_{12} and (b) showing the effect of applied voltage (V) and time (hr) on release behaviour of vitamin B_{12}.

Table 5.5 Regression statistics table:

Regression Statistics		
	Y_1	Y_2
Predicted-R	0.9742	0.6721
R -square	0.9973	0.9538
Adjusted-R	0.9954	0.9209
Standard deviation	1.64	6.29
Observations	13	13

5.6 Conclusion

- Nanocomposite hydrogels based on gelatin, partially neutralized acrylic acid and acid functionalized multiwall carbon nanotubes (MWCNT-COOH) have been developed.
- The shifting of characteristic peak position in the XRD pattern of MWCNT-COOH shows the perfect modification of pristine MWCNTs. Also, the characteristics peaks of MWCNT-COOH in the XRD pattern of gelatin-*g*-PAAc/MWCNT-COOH confirm the incorporation of acid functionalized multiwall carbon nanotubes into the Gelatin-*g*-PAAc hydrogels.
- SEM studies demonstrated the difference in surface morphology of pristine MWCNTs and after the acid functionalization of MWCNTs along with the smooth surface of the nanocomposite hydrogel, which implies the uniform dispersion of MWCNT-COOH within the nanocomposite hydrogel.
- Swelling percentage was found to be decreased with an increase in MWCNT-COOH content, when no electric field was applied; but reversed swelling behavior was observed when an external electric field (10 V) was applied.
- *In vitro* experiments of percentage hemolysis reveal that the prepared nanocomposite hydrogels possess proficient blood compatibility suitable for biomedical applications.
- The electro-responsive release behavior of vitamin B_{12} exhibited a considerable dependence on ionic strength of the medium, applied voltage and MWCNT-COOH content of the nanocomposite hydrogels.
- Drug release behavior was further investigated by response surface methodology and by applying a central composite design.
- So, the results obtained in this work lead us to the conclusion that gelatin-*g*-PAAc/MWCNT-COOH nanocomposite hydrogels can be a promising platform for the development of electro-responsive drug delivery systems.

References

1. Lutolf, M.P. & Hubbell, J.A. *Nat. Biotechnol.* **23** (1), 47-55, 2005
2. Pratt, A.B., & Weber, F.E. *Biotechnol. Bioeng.* **86** (1), 27-36, 2004.
3. Nuttelman, C.R., et al. *Matrix Biol.* **24** (30), 208-218, 2005.
4. Xiang, Y., et al. *Eur. Polym. J.* **42** (9), 2125-2132, 2006.
5. Risbud, M.V., et al. *J. Control. Rel.* **68** (1), 23-30, 2000.
6. Anal, A.K., et al. *Recent Pat. Endocr. Metab. Immune Drug Discov.* **1** (1), 83-90, 2006.
7. Qiu, Y., & Park, K. *Adv. Drug. Deliv. Rev.* **53** (3), 321-339, 2000.
8. Berner, B., & Dinh, S.M. *Electronically Controlled Drug Delivery,* CRC Press, Chicago, 1998.
9. Boruah, M., et al. *Adv. Polym. Tech.* **32 (S1),** E520–E530, 2013.
10. Chen, G., et al. *Carbon* **42** (4), 753-759, 2004.
11. Boruah, M., et al. *Polym. Compos.* **35** (1), 27-36, 2014.
12. Chen, G., et al. *Polymer* **44** (6), 1781-1784, 2003.
13. Yang, S., et al. *Carbon* **43** (4), 827-834, 2005.
14. Xiao, Y., et al. *J. Mater. Chem.* **22** (16), 8076-8082, 2012.
15. Lizundia, E., et al. *Macromol. Biosci.* **12** (7), 870-881, 2012.
16. Dubois, P., & Alexandre, M. *Adv. Eng. Mater.* **8** (3), 147-154, 2006.
17. Shiga, T. *Adv. Polym. Sci.* **134,** 131-163, 1997.

18. Teng, X.W., & Yang, H. *J. Mater. Chem.* **14** (4), 774-779, 2004.

19. O'Connell, M.J., et al. *Chem. Phys. Lett.* **342** (3-5), 265-271, 2001.

20. Coleman, J.N., et al. *Carbon* **44** (9), 1624-1652, 2006.

21. Ross-Murphy, S.B. *Polymer* **33** (12), 2622-2627,. 1992.

22. Brodsky, B., & Ramshaw, J.A.M. *Matrix. Biol.* **15** (8), 545-554, 1997.

23. Kawai, K., et al. *Biomaterials* **21** (5), 489-499. 2000.

24. Zhao, F., et al. *Biomaterials* **23** (15), 3227-3234, 2002.

25. Bigi, A., et al. *Biomaterials* **19** (7-9), 739-744, 1998.

26. Kulkarni, R.V., et al. *J. Appl. Polym. Sci.* **115** (2), 1180-1188, 2010.

27. Banga, A.K., & Chien, Y.W. *Pharm. Res.* **10** (5), 697-702, 1993.

28. Kim, S.Y., & Lee, Y.M. *J. Appl. Polym. Sci.* **74** (7), 1752-1761, 1999.

29. Tanaka, T., et al. *Science* **218** (4571), 467-469, 1982.

30. Singh, B., et al. *Crit. Rev. Ther. Drug Carrier Syst.* **22** (1), 27-106, 2005.

31. Singh, B., et al. *Crit. Rev. Ther. Drug Carrier Syst.* **22** (3), 215-294, 2005.

32. Sauzet, C., et al. *Int. J. Pharm.* **378** (1), 23-29, 2009.

33. Mutyaba, M.R., et al. Eur. *J. Pharm. Sci.* **37** (3-4), 434-441, 2009.

34. Leonardi, D., et al. *J. Pharm. Biomed. Anal.* **48** (3), 802-807, 2008.

35. Li, L., et al. *J. Pharm. Sci.* **26** (5), 929-937, 2013.

36. Boruah, M., et al. *RSC Adv.* **4** (83), 43865-43873, 2014.

37. Chen, J., et al. *Science* **282** (5386), 95-98, 1998.

38. Worsley, K.A., et al. *J. Am. Chem. Soc.* **131** (50), 18153-18158, 2009.

39. Kokabi, M., et al. *Eur. Polym. J.* **43** (3), 773-781, 2007.

40. Purkayastha, M.D., et al. *J. Agric. Food Chem.* **61** (45), 10746-10756, 2013.

41. Bajpai, S.K., et al. *Iran. Polym. J.* **16** (8), 521-527, 2007.

42. van Dijkhuizen-Radersma, R., et al. *Biomaterials* **23** (6), 1527-1536, 2002.

43. Kim, B., et al. *Macromol. Res.* **11** (4), 291-295, 2003.

44. Bhattacharyya, S., et al. *Biomacromolecules* **9** (2), 505-509, 2008

45. Neelgund, M.G., & Oki, A. *J. Nanosci. Nanotechnol.* **11** (4), 3621-3629, 2011.

46. Harris, P.J.F., et al. *Carbon nanotubes and related structures: new materials for the twenty-first century,* Cambridge University Press, United Kingdom, 1999.

47. Salvetat, J.P. *Understanding of carbon nanotubes,* Germany: Springer-Verlag Berlin, Heidelberg, 2006.

48. Veerapandian, B., et al. *Asian J. Sci. Res.* 7 (2), 256-261, 2014.

49. Pourjavadi, A., & Mahdavinia, G.R. *Turk. J. Chem.* **30** (5), 595-608, 2006.

50. Boruah, M., et al. *Polym. Compos.* DOI 10.1002/pc.22909, 2014.

51. Pourjavadi, A., & Doulabi, M. *Solid State Ionics* **257,** 32-37. 2014,

52. Murdan, S. *J. Controlled Release* **92** (1), 1-17, 2003.

53. Sawahata, K., et al. *J. Controlled Release* **14** (3), 253-262, 1990.

54. Agnihotri, S.A., et al. *J. Appl. Polym. Sci.* **96** (2), 301-311, 2005.

CHAPTER 6

Conclusion and future prospective

6.1 Conclusion

Over the past few decades, advances in hydrogel technologies have spurred development in many biomedical applications including controlled drug delivery, actuator, sensors etc. In the recent time, the field of hydrogels has moved forward at a dramatic pace. The development of suitable synthetic methods encompassing traditional chemistry to molecular biology has been used in the design of hydrogels mimicking basic processes of living systems. Stimuli-responsive hydrogels have the ability to respond towards external stimuli such as pH, temperature, ionic strength, electric field, magnetic field etc. The change in the degree of swelling may occur discontinuously at a specific value of stimulus or gradually over a (mostly small) range of stimulus values. Recently, many hydrogel based networks have been designed and tailored to meet the needs for different applications. Also, various composite and nanocomposite hydrogels have been developed to fulfill the specific requirements for specific applications.

The goal of this thesis is to develop stimuli-responsive composite and nanocomposite hydrogels for controlled drug delivery and actuator application. The influence of various parameters on swelling and bending behaviour has been determined. The mechanical properties and in vitro biocompatibility of the prepared hydrogels are also investigated.

The important findings of the thesis are summarized chapter wise below:

I. Synthesis of composite hydrogels based on poly(acrylamide-*co*-acrylic acid)/polyaniline and poly(acrylamide-*co*-acrylic acid)/graphite and study of their pH, electro-responsive behaviour and biocompatibility.

- Two sets of composite hydrogels with poly(AAm-*co*-AAc)/PANI and poly(AAm-*co*-AAc)/graphite were prepared by solution polymerization process in presence of redox initiator potassium persulfate (KPS)/TEMED and crosslinker (EGDMA).

- The swelling behaviour of both the composite hydrogels were found to be pH-responsive upon study across varying pH media. Also, the swelling is found to be highest in basic medium (pH 7.4).

- The mechanical properties of the composite hydrogels were improved with an increase in crosslinker (EGDMA) content due to the formation of a compact network structure.

- The prepared conducting composite hydrogels were found to possess gratifying conductivity which was significantly dependent on crosslinker (EGDMA) content, temperature and amount of the conducting filler.

- The hemolytic potentiality test reveals that, all the composite hydrogels are biocompatible in nature.

- Both the composite hydrogels show significant bending behaviour when exposed to an external electric field.

- The properties of composite hydrogels confirmed in this chapter indicate that the hydrogels can find possible application in artificial organ components, especially as actuator.

II. Synthesis of electric field responsive poly (vinyl alcohol)-*g*-poly(acrylic acid)/OMMT nanocomposite hydrogels and their swelling kinetics.

- Nanocomposite hydrogels based on PVA, partially neutralized acrylic acid and layered organically modified OMMT clay were prepared by free radical graft polymerization reaction and the grafting reaction of acrylic acid on PVA was confirmed by FTIR analysis.

- X-ray diffraction analysis showed that the nanocomposite forms a partially exfoliated or intercalated structure. Also, SEM studies demonstrated a finer dispersion of the clay particles in nanocomposite as compared to the composite.

- From thermogravimetric analysis, it was observed that introduction of OMMT to the polymer network results in an increase in thermal stability.

- Since, crosslinking density of composite increased with the increase of OMMT content, so there was decrease in water absorbency with an increase in OMMT content.
- Swelling kinetics of the prepared hydrogels shows that transport mode of water in the nanocomposite hydrogels exhibited Fickian diffusion which gradually changes to non-Fickian diffusion with increase in crosslinker amount.
- The nanocomposite hydrogels showed significant and quick bending towards the cathode under an applied electric field.
- The observed behaviour suggest the possible applications of PVA-*g*-PAAc/OMMT nanocomposite hydrogels as artificial muscle, sensors, switches and electric current modulated drug delivery systems etc.

III. Biocompatible carboxymethylcellulose-*g*-poly(acrylic acid)/OMMT nanocomposite hydrogel for in vitro release of vitamin B_{12}

- Nanocomposite hydrogels based on CMC, partially neutralized acrylic acid and layered organically modified OMMT clay were prepared by free radical graft polymerization reaction.
- X-ray diffraction analysis showed that the nanocomposite forms a partially exfoliated or intercalated structure. Also, SEM studies demonstrated an improvement of surface properties of the nanocomposite as compared to the composite.
- The dynamic mechanical analysis of the nanocomposite hydrogels showed an increase in the storage modulus within increasing frequency and OMMT nanoclay content, clearly demonstrating a good mechanical behavior.
- The swelling properties of the nanocomposite hydrogels were found to be dependent on initiator (KPS), crosslinker (MBA) and nanoclay (OMMT) content.
- Blood compatibility of the prepared hydrogels was improved after the incorporation of nanoclay as confirmed by *in vitro* experiments of percentage hemolysis.

- The vitamin B_{12} release behavior was found to be greater in basic medium (pH 7.4) than in the acidic medium (pH 1.2).
- Kinetic study of release behavior showed increase in 'n' value from 0.63 to 0.87 exhibiting a non-Fickian transport mechanism with increase in crosslinker content.
- The results obtained in this work lead us to the conclusion that CMC-*g*-PAAc/OMMT nanocomposite hydrogels can be a promising platform for the development of pH-responsive drug delivery systems.

IV. Electric field assisted drug release from gelatin-*g*-poly(acrylic acid)/MWCNT-COOH nanocomposite hydrogels.

- Nanocomposite hydrogels based on gelatin, partially neutralized acrylic acid and acid functionalized multiwall carbon nanotubes (MWCNT-COOH) have been developed.
- The shifting of characteristic peak position in the XRD pattern of MWCNT-COOH shows the perfect modification of pristine MWCNTs. Also, the characteristics peaks of MWCNT-COOH in the XRD pattern of Gelatin-*g*-PAAc/MWCNT-COOH confirm the incorporation of acid functionalized multiwall carbon nanotubes into the Gelatin-g-PAAc hydrogels.
- From the swelling behaviour, it was observed that the swelling percentage was more in basic medium (pH 7.4) than in acidic medium (pH 4) due to the more ionization of the carboxylic acid groups. Also, swelling percentage was found to be decreased with an increase in MWCNT-COOH content, when no electric field was applied; but reversed swelling behavior was observed when an external electric field (10V) was applied.
- *In vitro* experiments of percentage hemolysis reveal that the prepared nanocomposite hydrogels possess proficient blood compatibility suitable for biomedical applications.
- The electro-responsive release behavior of vitamin B_{12} exhibited a considerable dependence on ionic strength of the medium, applied voltage and MWCNT-COOH content of the nanocomposite hydrogels.

- Drug release behavior was further investigated by response surface methodology and by applying a central composite design.
- So, the results obtained in this work lead us to the conclusion that Gelatin-*g*-PAAc/MWCNT-COOH nanocomposite hydrogels can be a promising platform for the development of electro-responsive drug delivery systems.

6.2 Future prospects of the present investigation

- Development of hydrogels with higher mechanical, swelling and deswelling properties. This could be used in biomedical and drug delivery applications.
- To develop biomimetic hybrid hydrogels by the modification of natural polymers for higher biocompatibility.
- Development of multi-responsive hydrogels which could be used for multipurpose activity.
- Development of self-healing hydrogels.
- The use of microdevices to engineer hydrogels will continue to provide new methods for fabricating improved hydrogel based systems.

List of publications

1. **M. Boruah,** A. Kalita, B. Pokhrel, R. Boruah, S. K. Dolui. Synthesis and Characterization of pH Responsive Conductive Composites of Poly(acrylic acid-*co*-acrylamide) Impregnated with Polyaniline by Interfacial Polymerization, *Advances in polymer Technology,* 32, E520–E530, 2013.

2. **M. Boruah,** P. Phukon, B. Saikia, S. K. Dolui. Synthesis and characterization of electro-responsive hydrogels based on poly (acrylamide-*co*-acrylic acid)/Graphite suitable for biomedical applications, *Polymer Composites,* 35, 27–36, 2014.

3. **M. Boruah,** M. Mili, S. Sharma, B. Gogoi, S. K. Dolui. Synthesis and Evaluation of Swelling Kinetics of Electric Field Responsive Poly(vinyl alcohol)-*g*-polyacrylic acid/OMNT Nanocomposite Hydrogels, *Polymer Composites,* DOI 10.1002/pc.22909, 2014.

4. **M. Boruah,** P. Gogoi, A. K. Manhar, M. Khannam, M. Mandal, S. K. Dolui. Biocompatible carboxymethylcellulose-*g*-poly(acrylic acid)/OMMT nanocomposite hydrogel for in vitro release of vitamin B_{12}, *RSC Advances,* 4, 43865-43873, 2014.

5. **M. Boruah,** P. Gogoi, B. Adhikari, S. K. Dolui. Preparation and characterization of Jatropha Curcas oil based alkyd resin suitable for surface coating, *Progress in Organic Coatings,* 74, 596– 602, 2012.

6. **M. Boruah,** A. K. Manhar, S. Sharma, D. Das, P. Gogoi, M. Mandal, S. K. Dolui. Electric Field Assisted Drug Release from pH and electro-responsive Gelatin-*g*-poly(acrylic acid)/MWCNTs nanocomposite hydrogels, *RSC Advances* (communicated).

7. B. Pokhrel, I. R. Kamrupi, B. Adhikari, R. Boruah, **M. Boruah,** S. K. Dolui. Study of Optical and Photovoltaic Properties of N-Alkyl Substituted Polycarbazole Derivative and Its Copolymer with Thiophene, *Materials and Manufacturing Processes,* 27, 43–48, 2012.

8. I.R. Kamrupi, B. Pokhrel, A. Kalita, **M. Boruah,** R. Boruah, S. K. Dolui. Synthesis of Macroporous Polymer Particles by Suspension Polymerization Using Supercritical Carbon Dioxide as a Pressure-Adjustable Porogen, *Advances in Polymer Technology,* 31, 154–162 (2012).

9. A. Kalita, **M. Boruah,** D. Das, S. K. Dolui. Ethylene polymerization on polymer supported Ziegler-Natta catalyst, *Journal of Polymer Research,* 19, 9892-9897, 2012.

10. P. Gogoi, **M. Boruah,** C. Bora, S. K. Dolui. Jatropha curcas oil based alkyd/epoxy resin/expanded graphite (EG) reinforced bio-composite: Evaluation of the thermal, mechanical and flame retardancy properties, *Progress in Organic Coatings,* 77, 87–93, 2014.

11. B. Saikia, D. Das, **M. Boruah,** S. K. Dolui. Synthesis and fluorescence properties of star-shaped polymers carrying two fluorescent moieties, *Polymer International,* 63, 1047–1055, 2014.

12. B. C. Nath, B. Gogoi, **M. Boruah,** S. Sharma, M. Khannam, G. A. Ahmed, S. K. Dolui. High performance polyvinyl alcohol/multi walled carbon nanotube/polyaniline hydrogel (PVA/MWCNT/PAni) based dye sensitized solar cells, *Electrochimica Acta,* 146 106–111, 2014.

Papers presented in Academic Conferences

1. **M. Boruah** and S. K. Dolui. "Preparation of Conductive hydrogel based on poly(acrylamide-*co*-acrylic acid) and polyaniline and their actuation behaviour", 99th Indian Science Congress, KIIT University, Bhubaneswar, 3-7th Jan, 2012.

2. **M. Boruah** and S. K. Dolui. "Synthesis and Characterization of pH Responsive Conductive Composites of Poly(acrylic acid-*co*-acrylamide) Impregnated with Polyaniline by Interfacial Polymerization" National conference on Chemistry, Chemical Technology and Society, Tezpur University, 11-12th Nov, 2011.

3. **M. Boruah** and S. K. Dolui. "Electrical Actuation of electro-responsive hydrogels based on poly (acrylamide-*co*-acrylic acid)/Graphite suitable for biomedical applications" Recent Advances in Polymer Science and Technology (POLY-2012), Dept. of Chemistry, North Bengal University and Siliguri Institute of Technology, 2-4th Nov, 2012,

4. **M. Boruah,** S. K. Dolui. "Preparation and characterization of Jatropha Curcas oil based alkyd resin suitable for surface coating" UGC sponsored National Seminar on Conservation and Utilization of Resources in North-East India, Dept. of Geography, Nowgong College in collaboration with Assam Science Society, 10-11th Jan, 2011.